The Abdus Salam International Centre for Theoretical Physics

2464-9

Earthquake Tectonics and Hazards on the Continents

17 - 28 June 2013

InSAR and applications to the earthquake cycle, and use in particular earthquakes

T. J. Wright
Univ. of Leeds
UK

The Earthquake Deformation Cycle

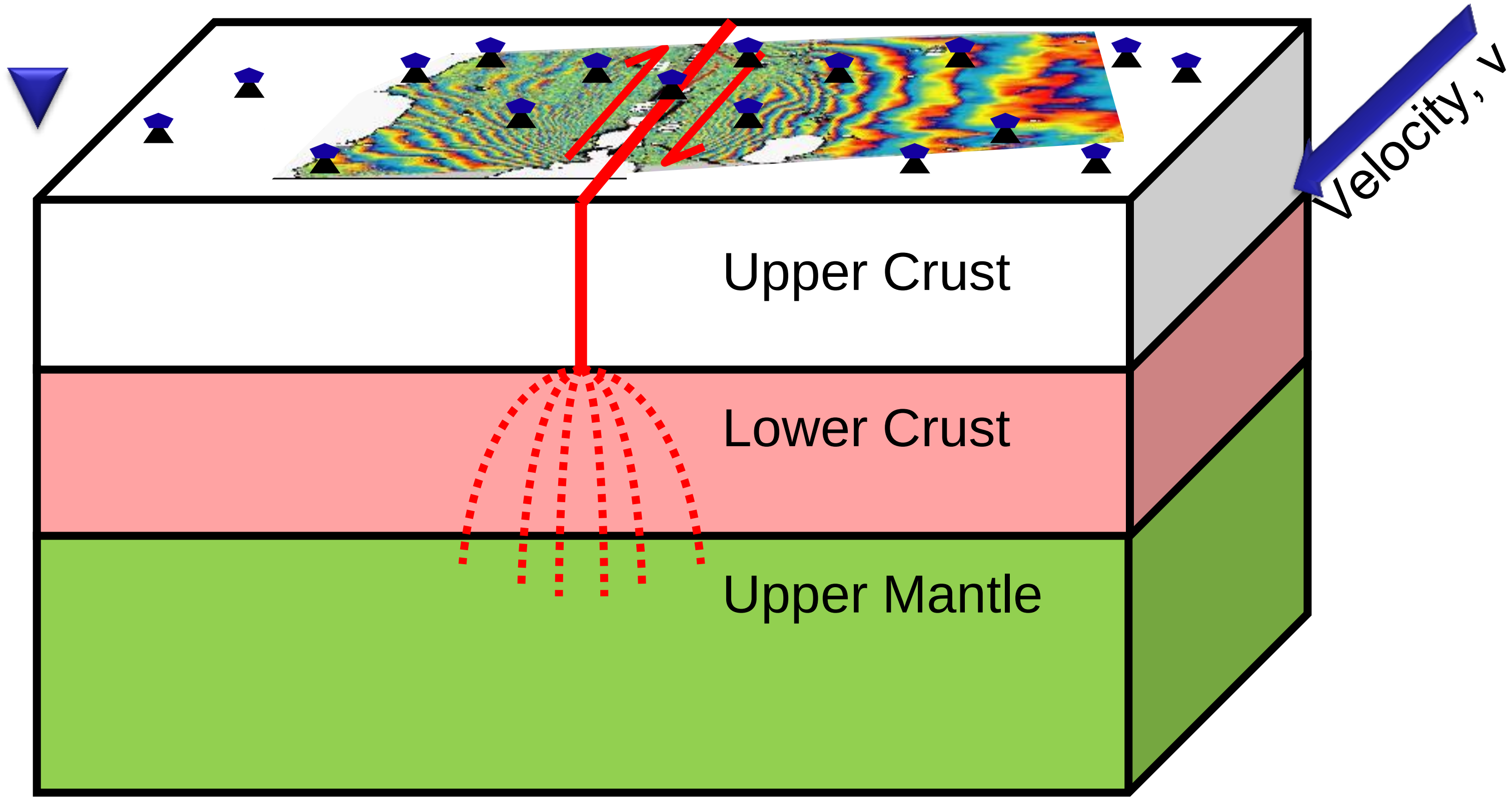

The Earthquake Deformation Cycle

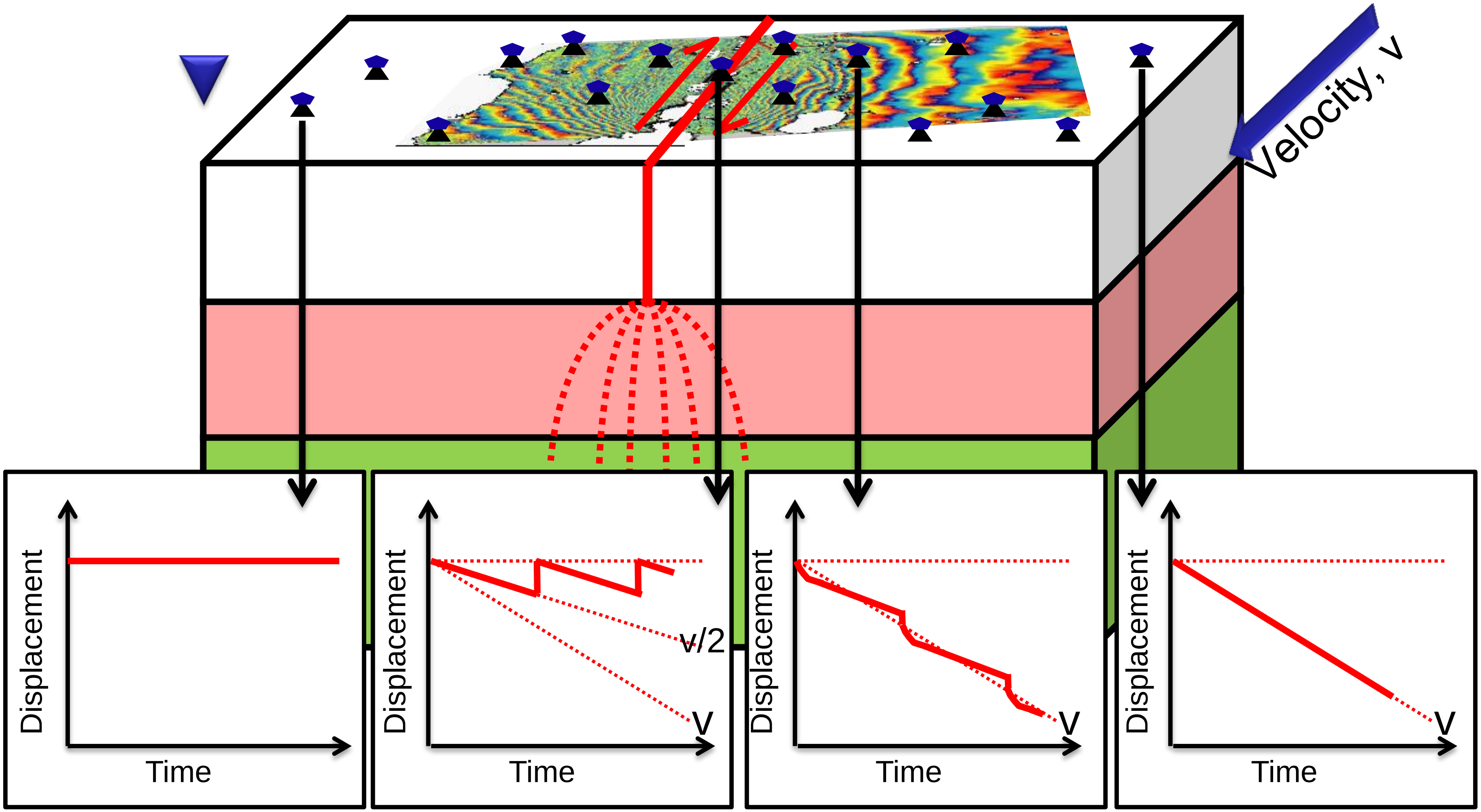

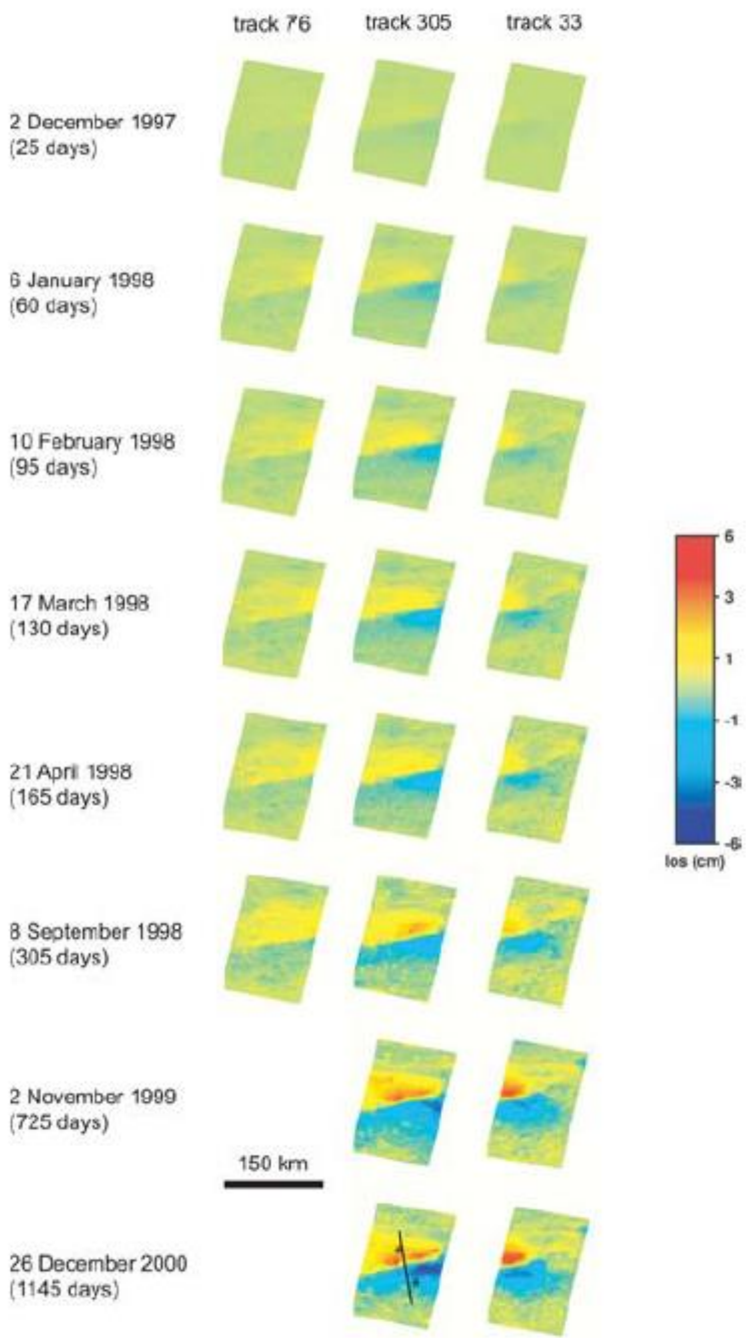

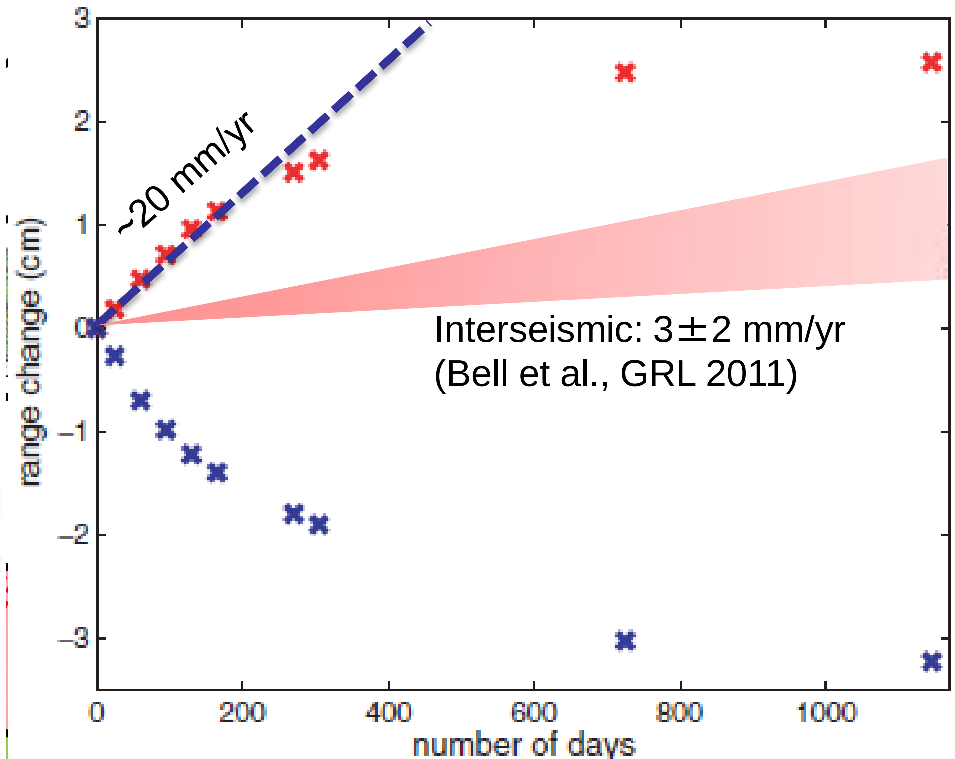

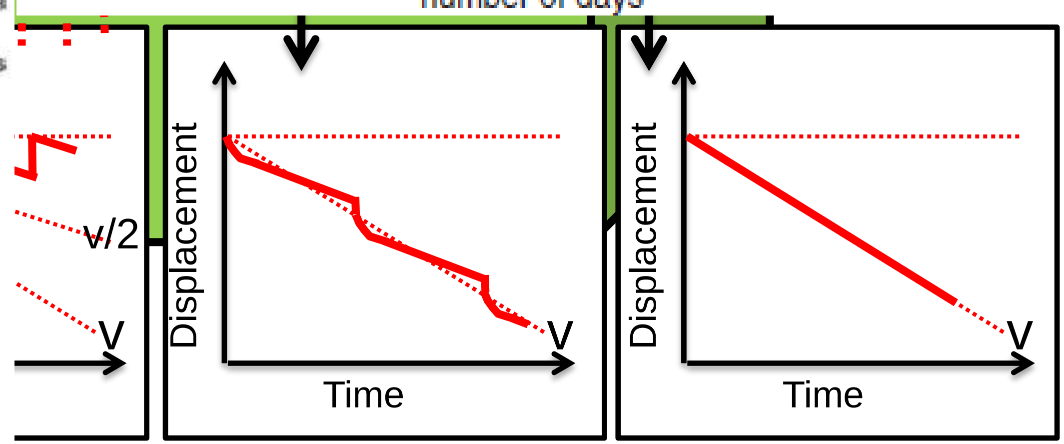

Manyi (Tibet) postseismic from Ryder et al, GJI 2007

The Earthquake Cycle

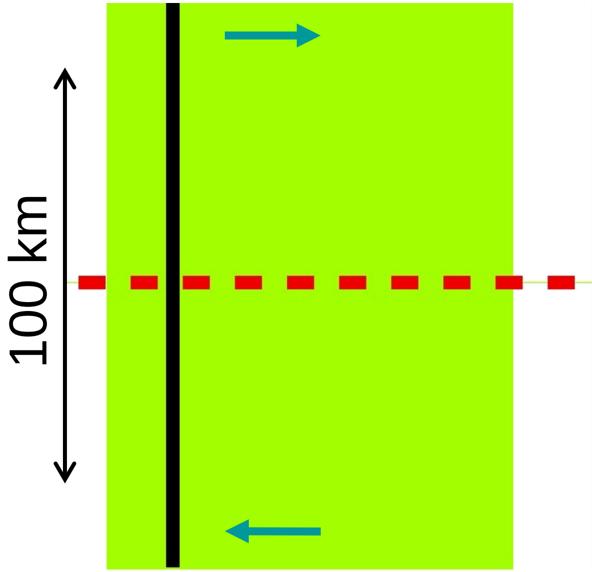

Note: Numbers vary for different faults

The Earthquake Cycle

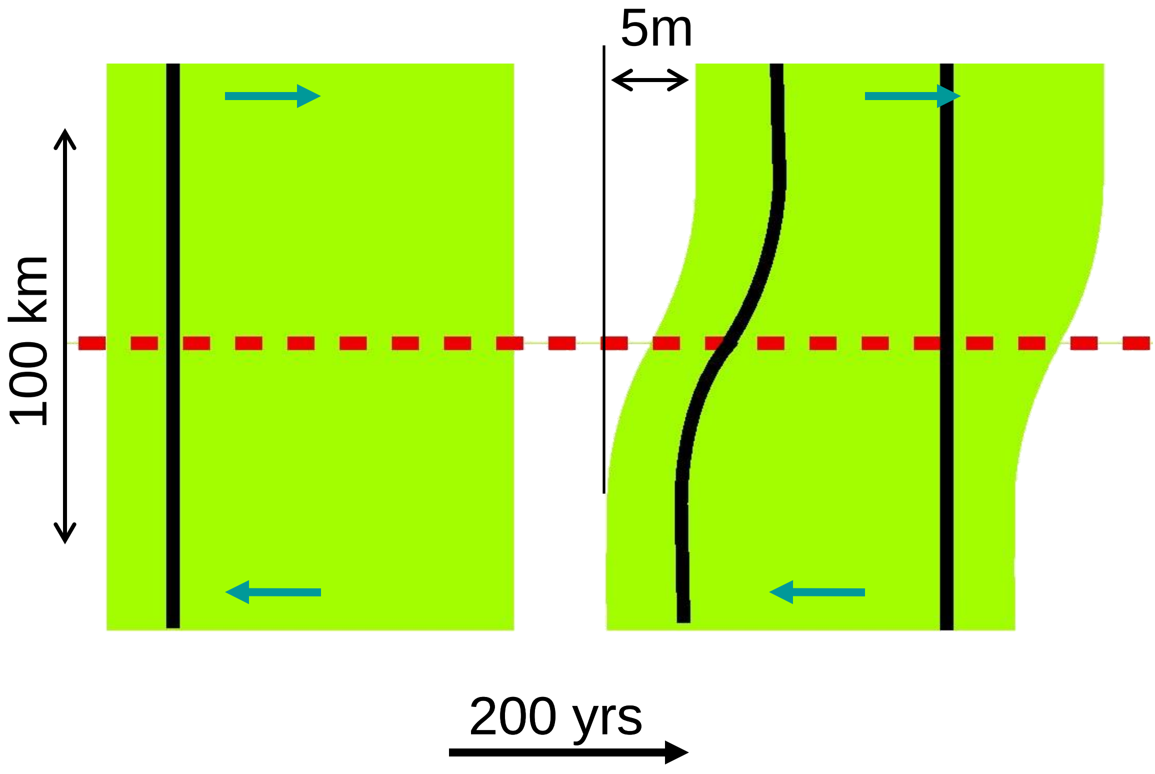

Note: Numbers vary for different faults

The Earthquake Cycle

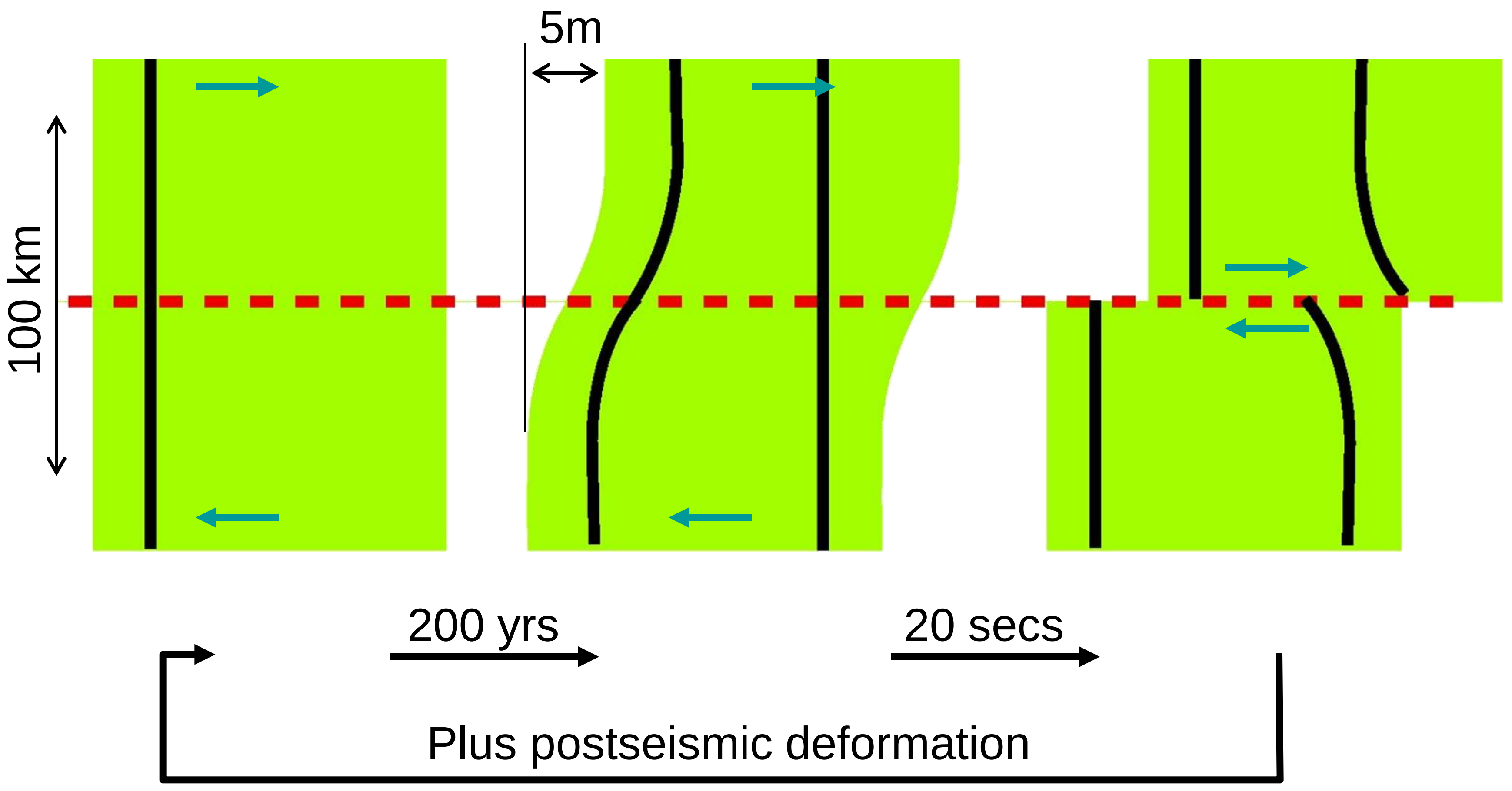

Note: Numbers vary for different faults

The Earthquake Cycle

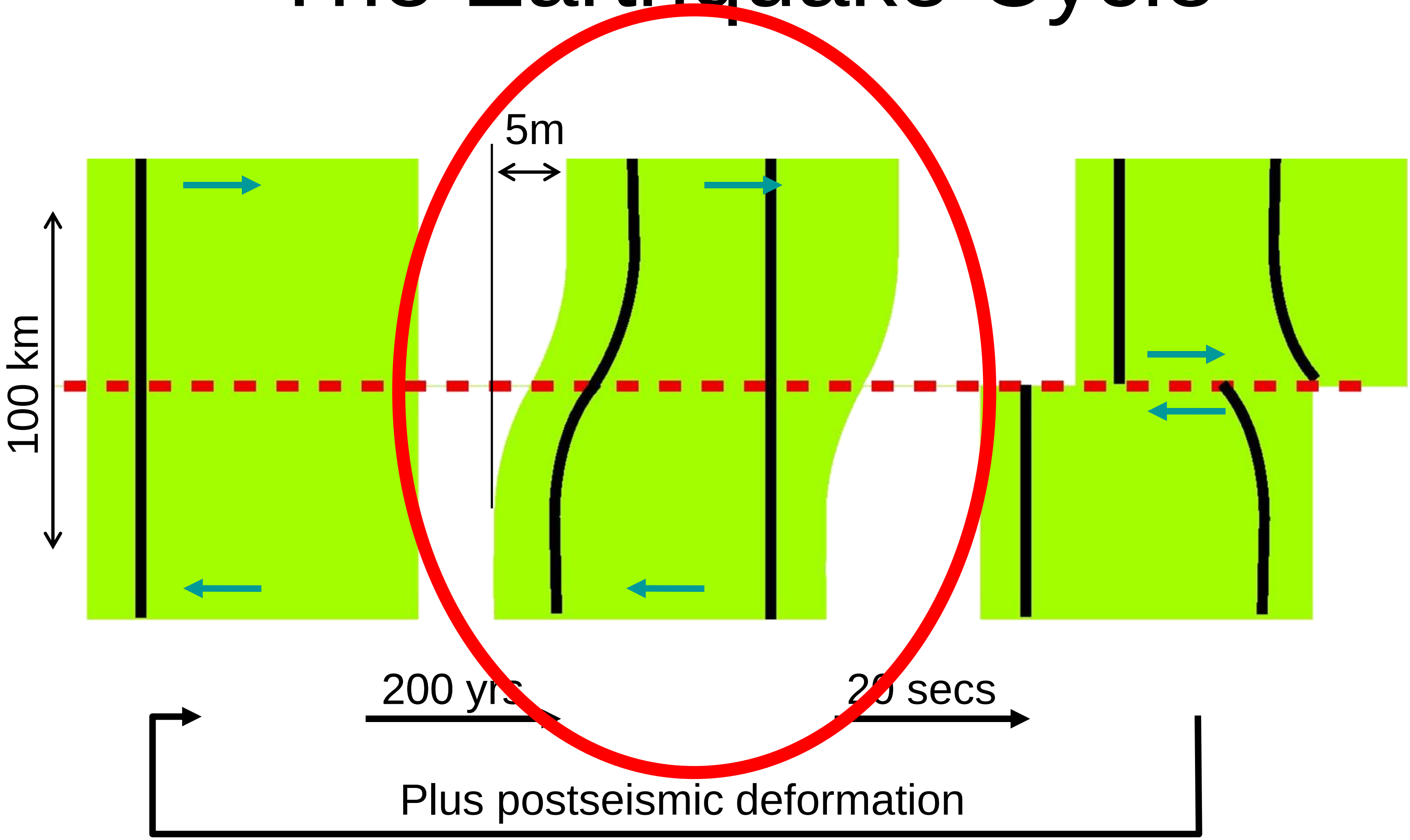

Note: Numbers vary for different faults

Interseismic Deformation

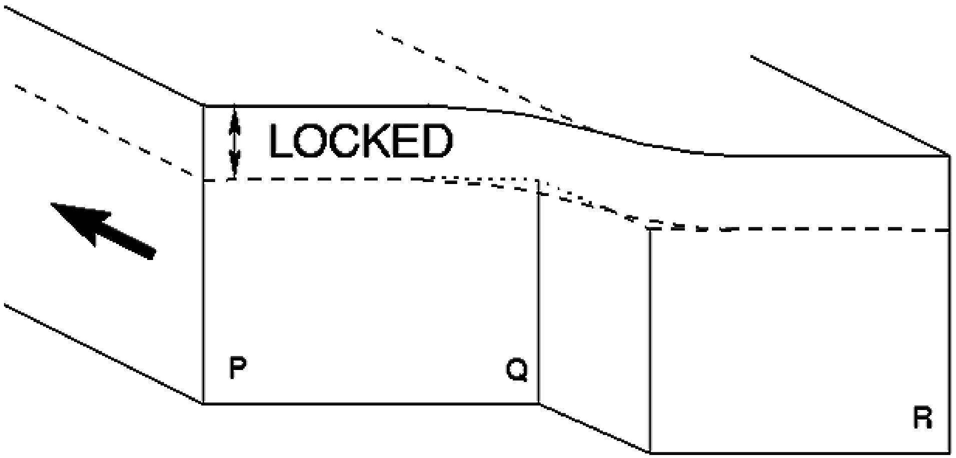

$$y = \frac{s}{\pi} \tan^{-1} \frac{x}{d}$$

Screw dislocation model, after Weertman and Weertman (1964), Savage and Burford (1973)

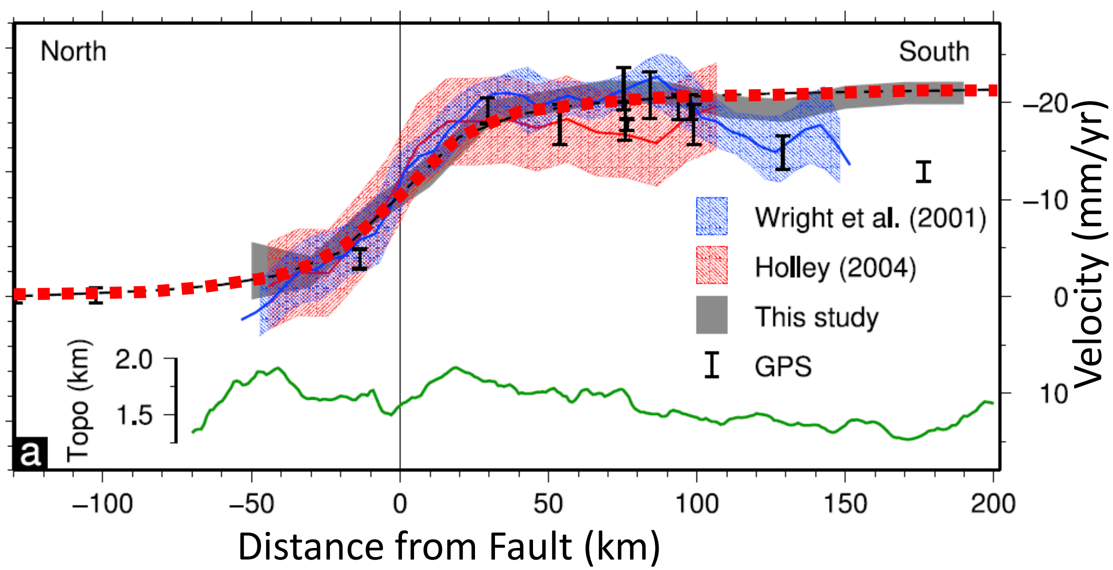

Interseismic deformation across the North Anatolian Fault, from Walters et al (GRL 2011)

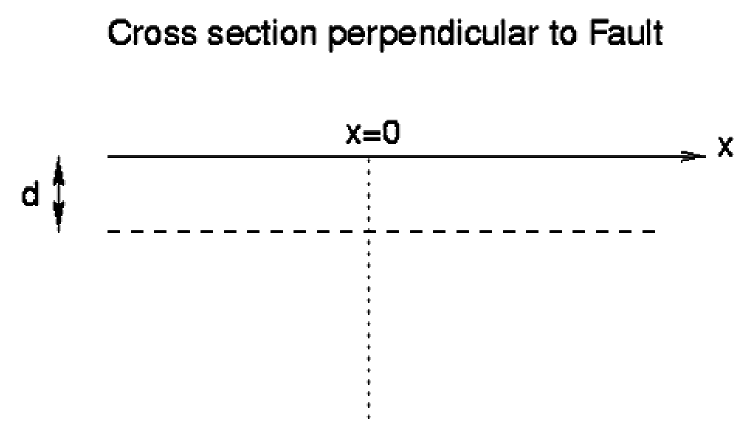

North and East Anatolian Fault (Richard Walters, PhD 2013)

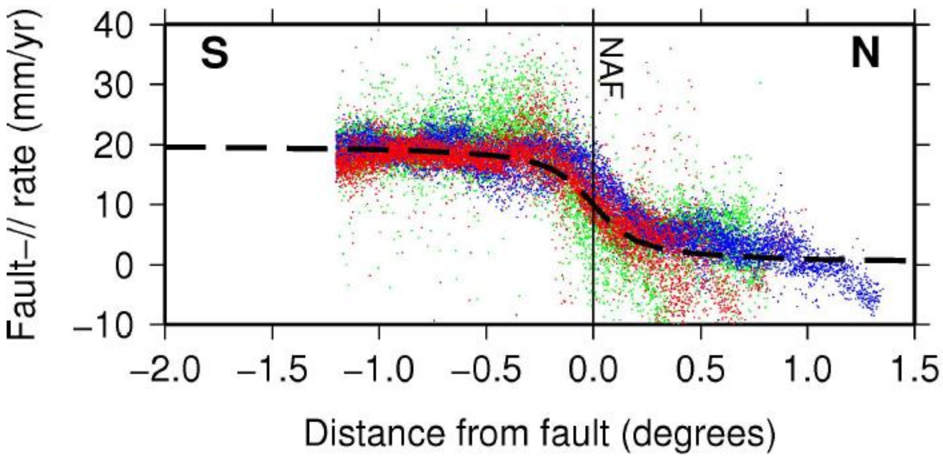

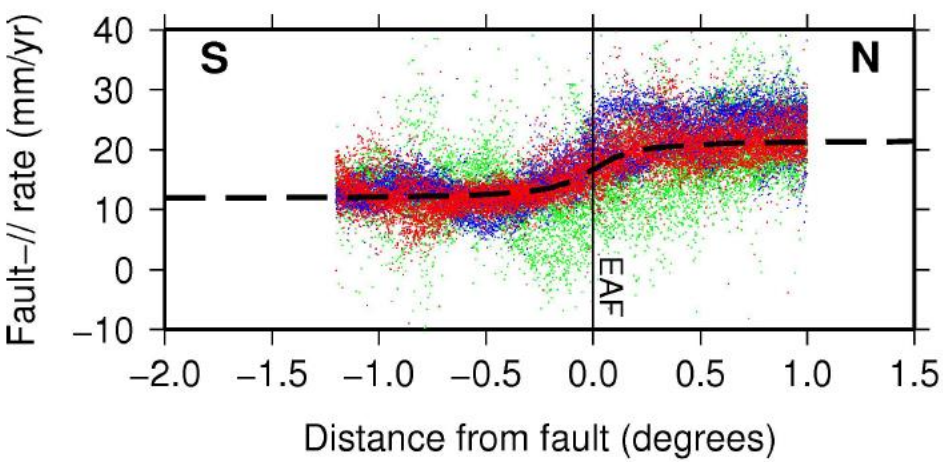

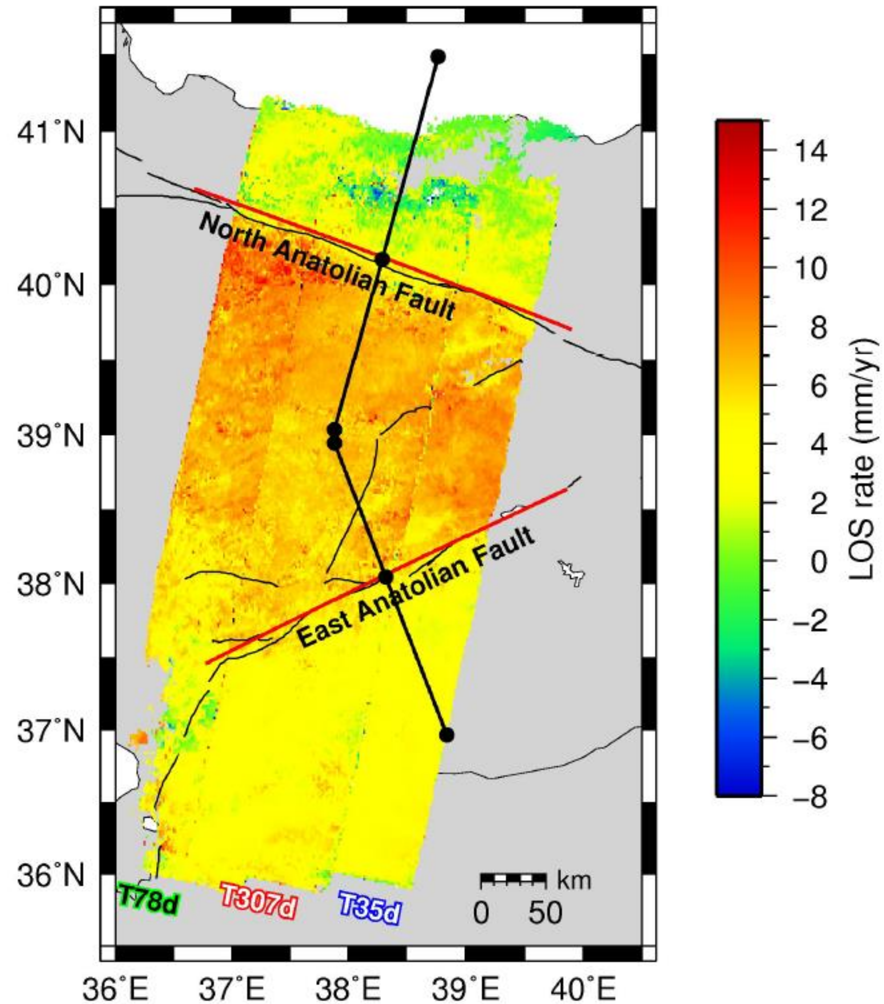

The Earthquake Deformation Cycle

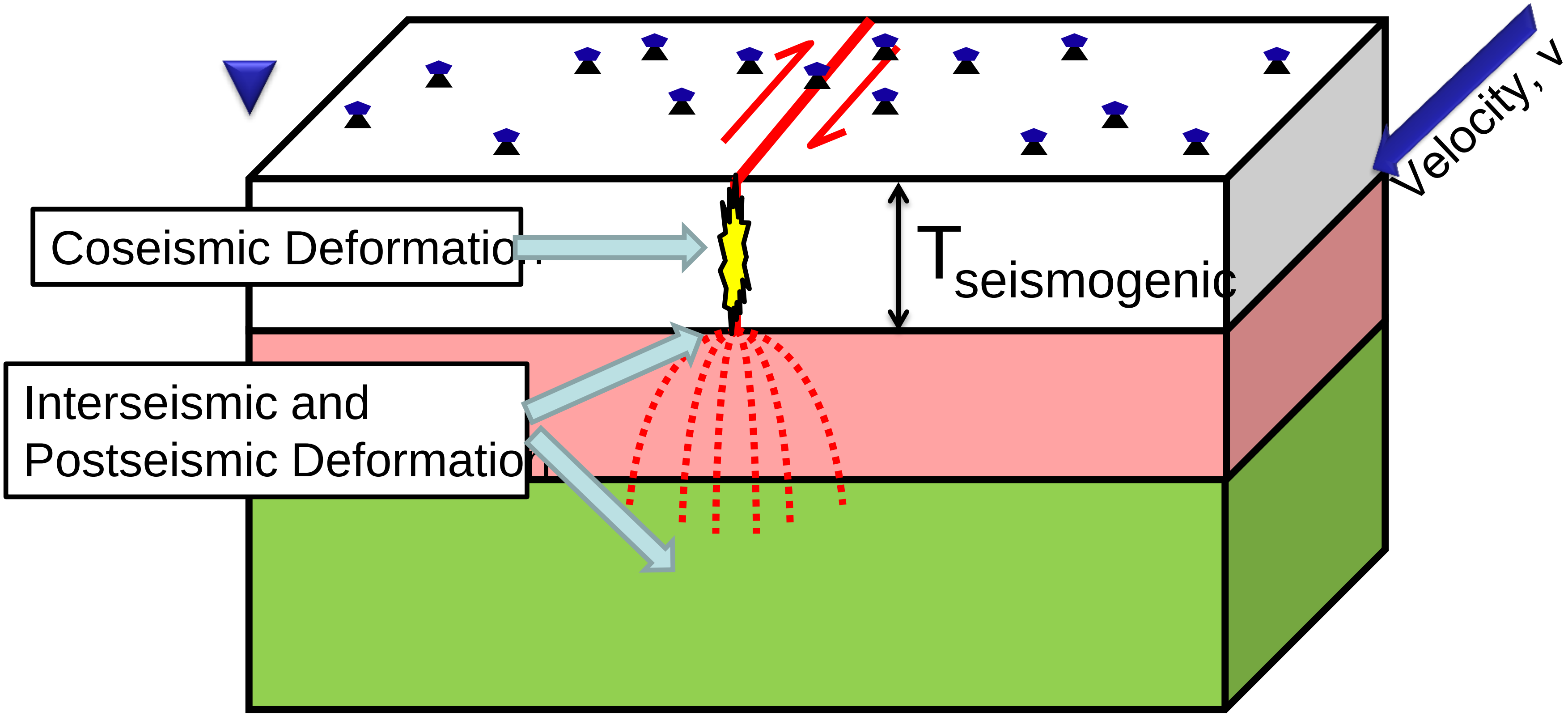

- Spatial pattern ⇨ $T_{seismogenic}$
- Time dependence ⇨ rheology

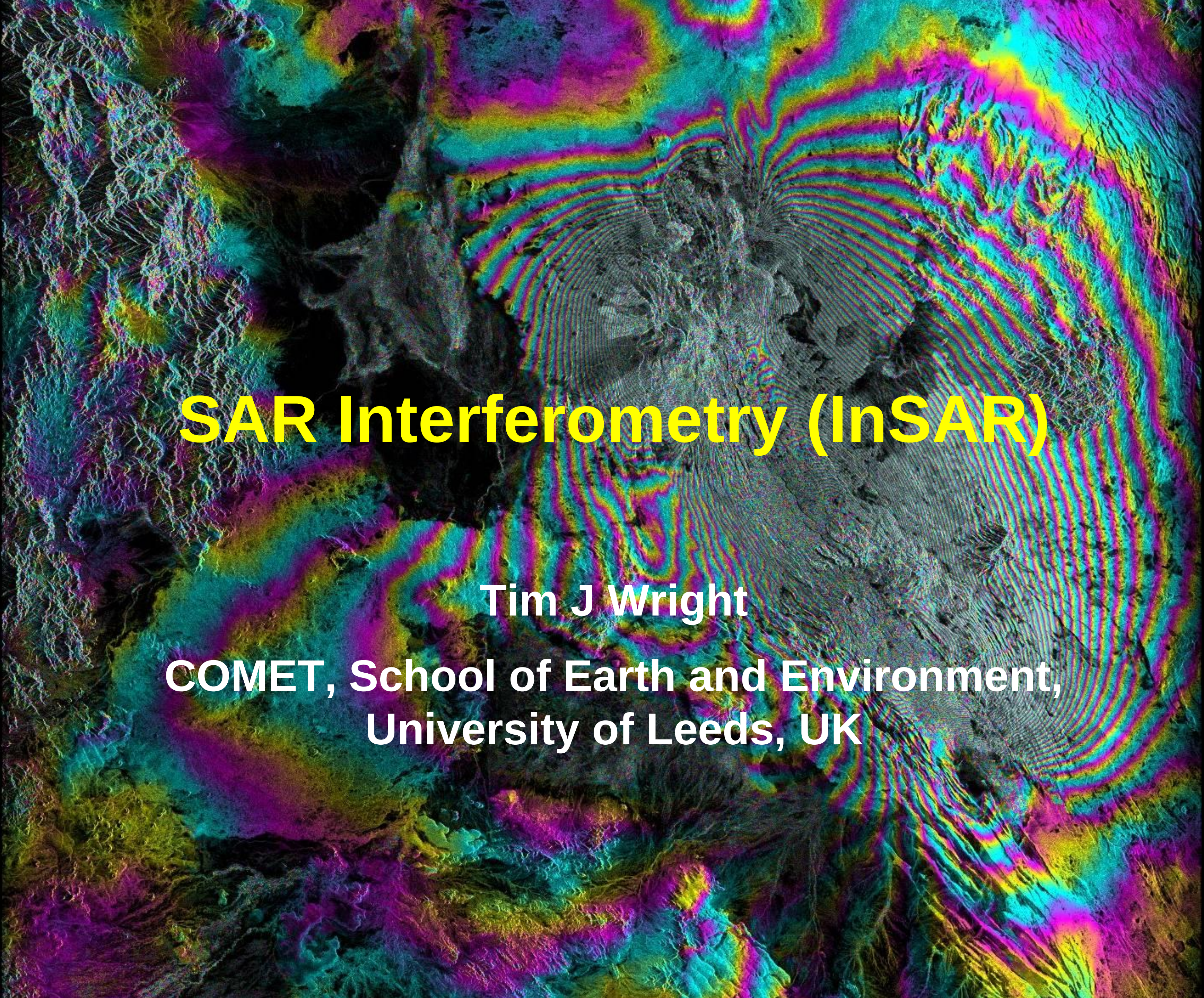

SAR Interferometry (InSAR)

Tim J Wright

COMET, School of Earth and Environment, University of Leeds, UK

Outline

PART 1: InSAR – the basics

- Synthetic Aperture Radar
- Components of interferometric phase
- Error Budget for single Interferogram

PART 2: InSAR – “advanced” methods

- Time Series Methods
- Determining 3D displacements
- Correcting Atmospheric Noise

Remote Sensing

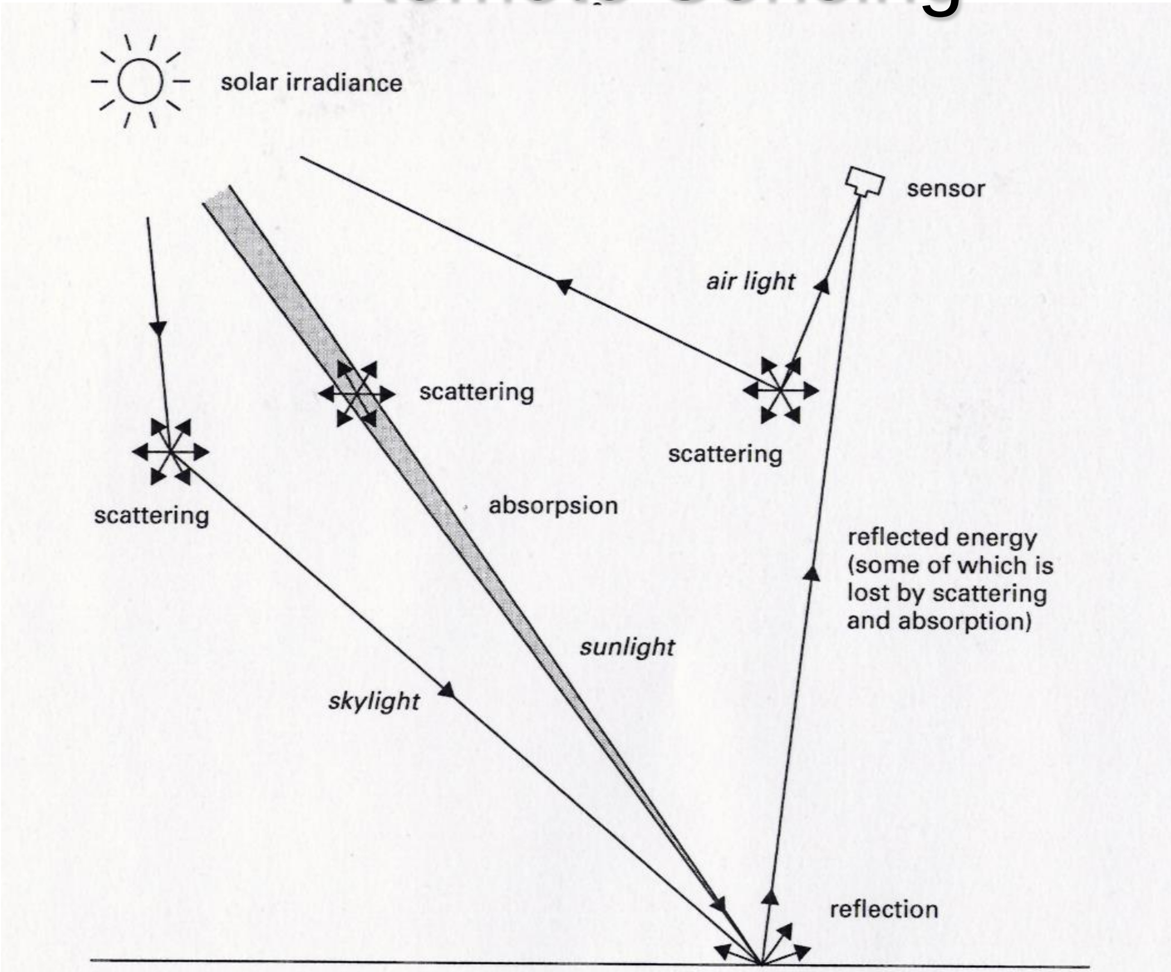

This is **passive** remote sensing where the Sun provides a natural source of illumination.

Active remote sensing involves illuminating the ground from the observing platform in some way, e.g. with radar or lasers.

The Electromagnetic Spectrum

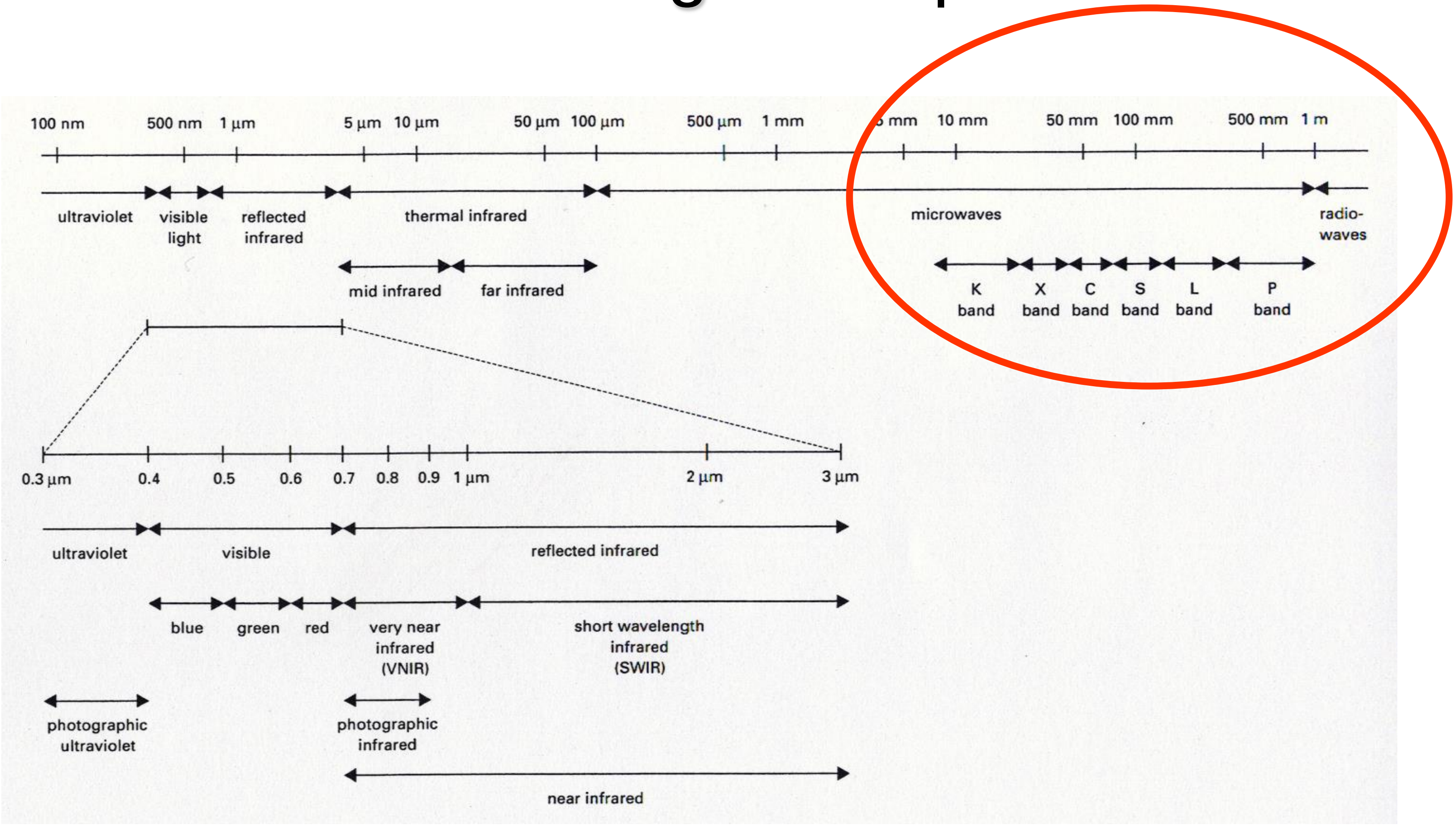

Active Remote Sensing with Microwaves

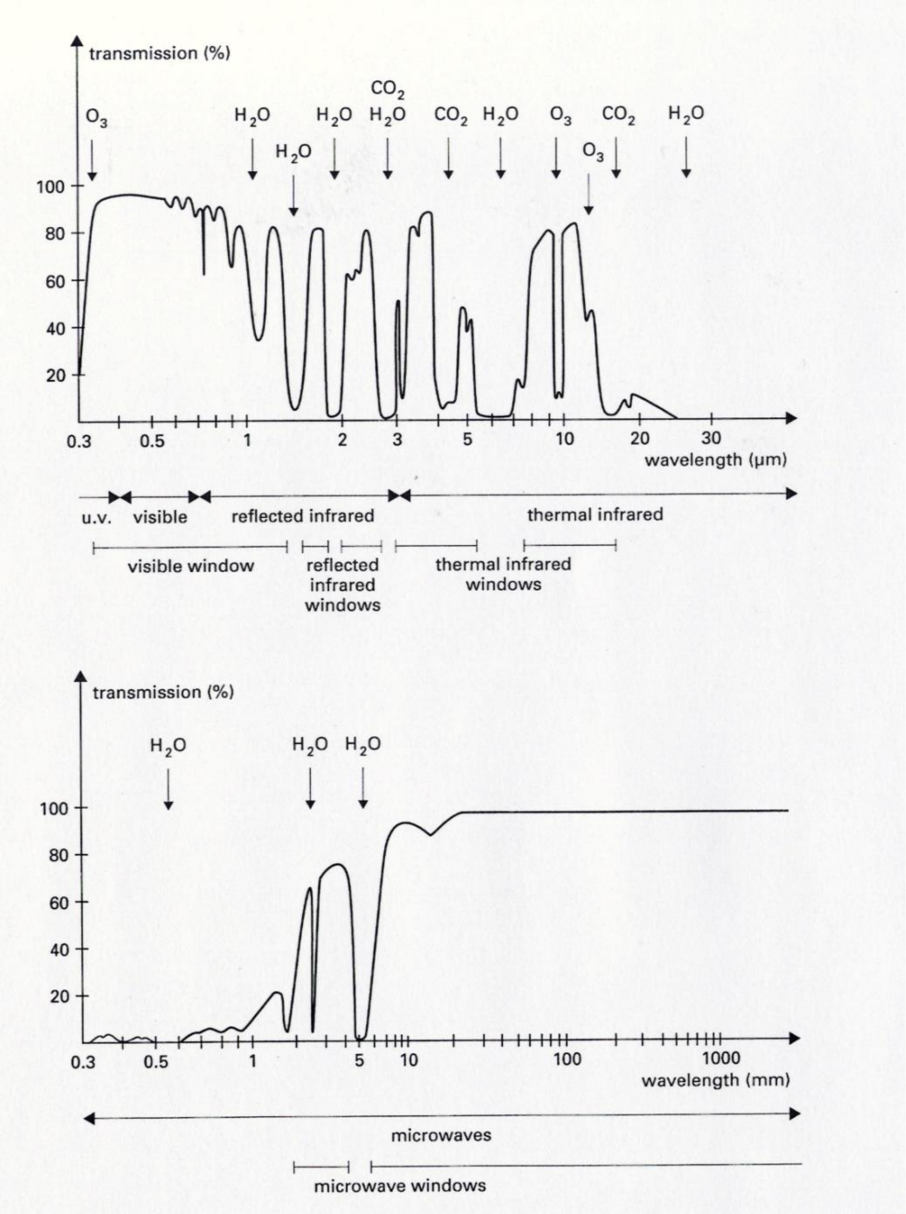

Radar = RAdio Detection And Ranging

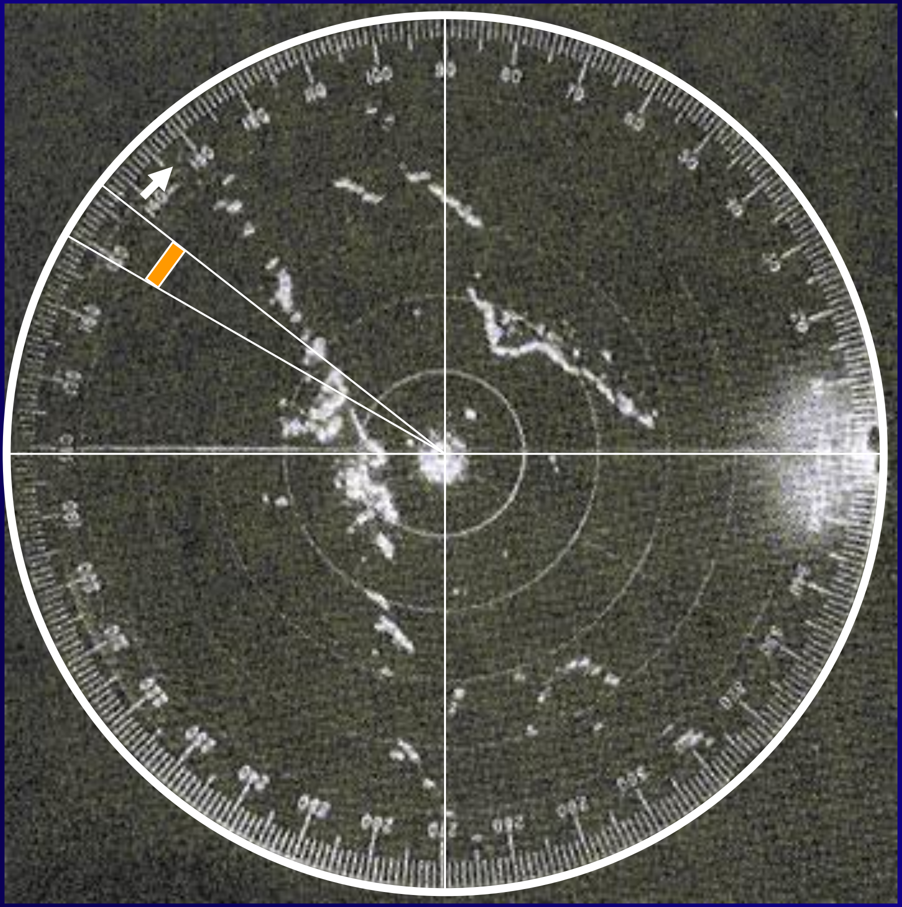

Side-Looking Airborne Radar

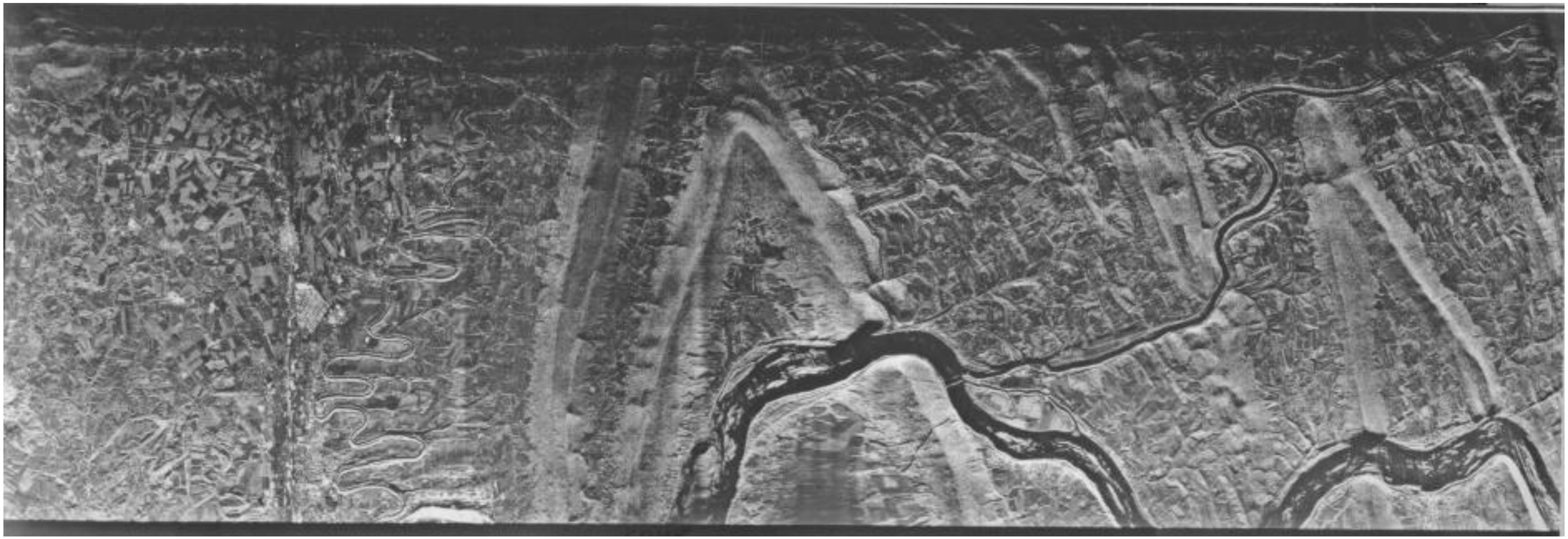

Side-Looking Airborne Radar

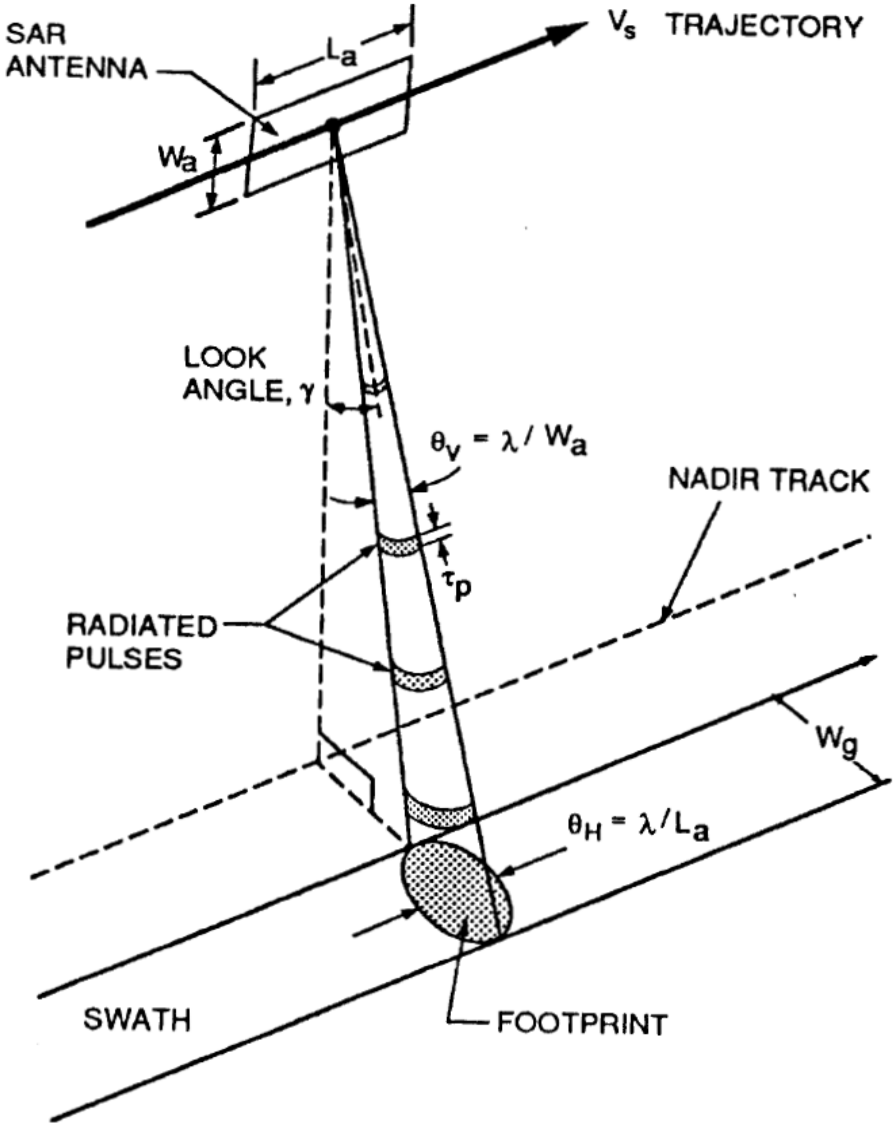

θ ~ λ / W

e.g. λ = 0.05 m

W = 10 m

θ ~ 0.005 radians

If at 800 km height, along-track footprint ~ 4 km

Trick – the Synthetic Aperture

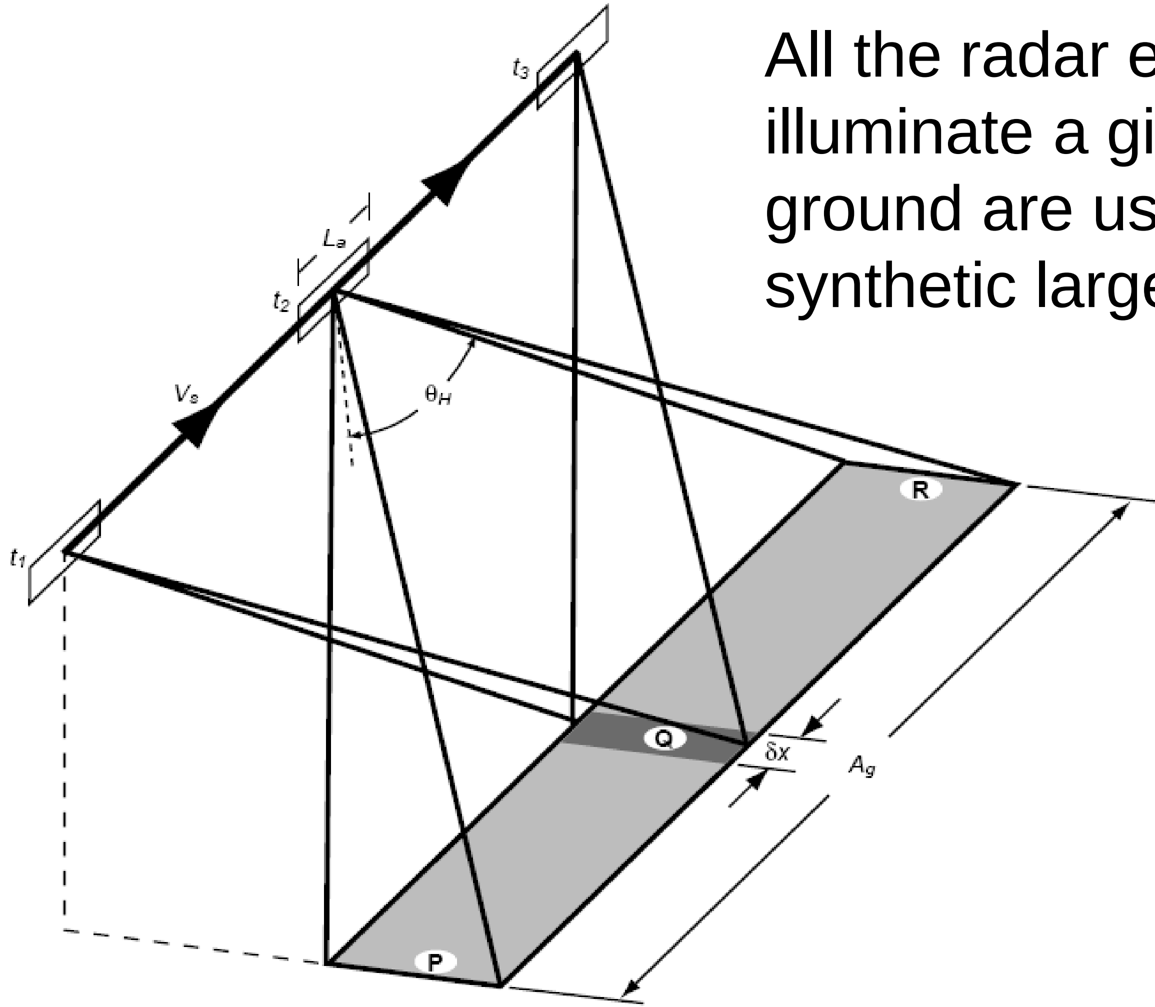

All the radar echoes that illuminate a given patch of ground are used to construct a synthetic larger antenna

Synthetic Aperture Radar (SAR)

ERS

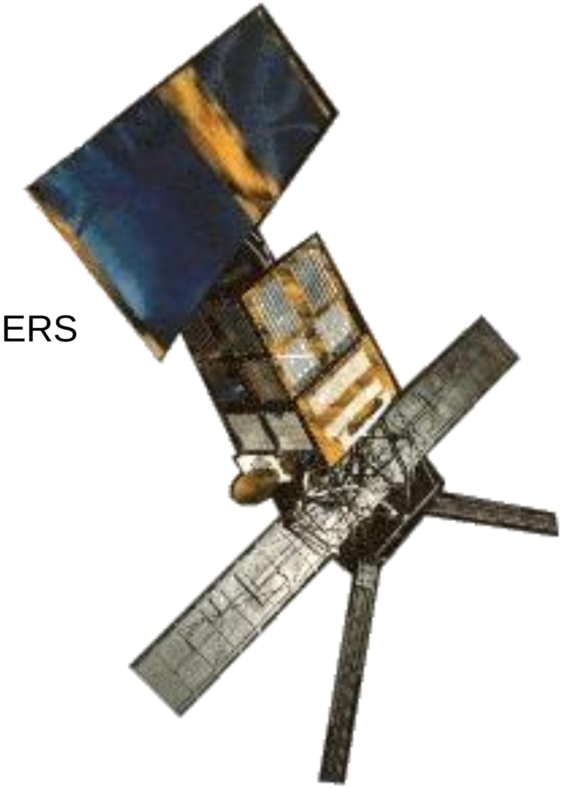

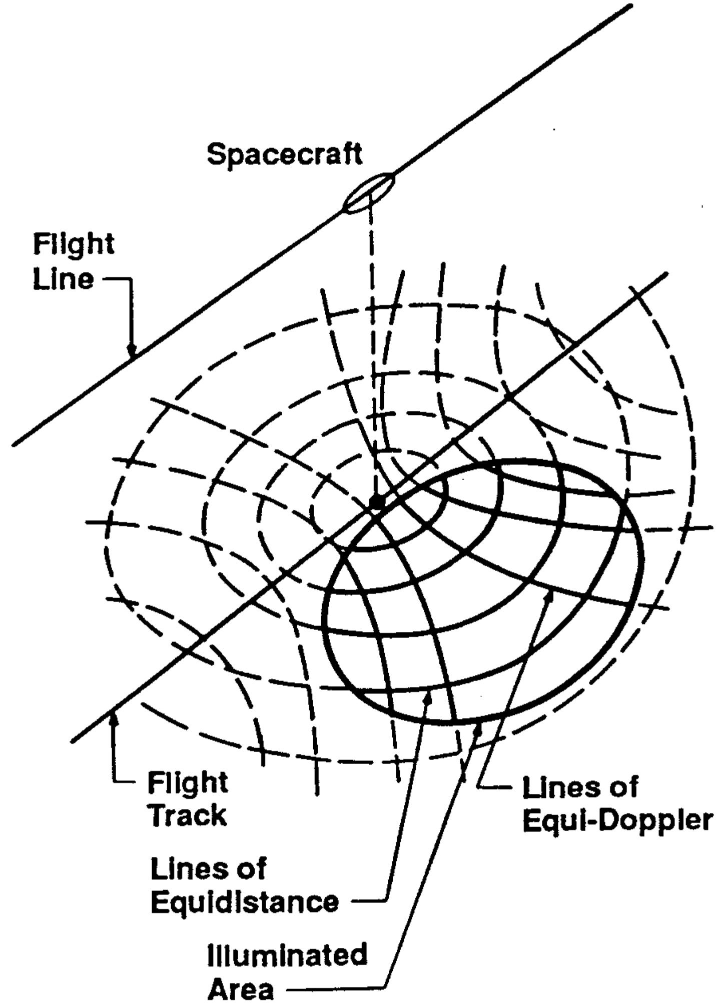

A SAR makes use of measurements of the range and Doppler shift of the radar returns to locate ground points. The signals from many returns are analysed together to image ground elements ~5x20m in size, much smaller than would be possible with a stationary antenna of the same size - hence the Synthetic Aperture.

InSAR – how it works

- Actively illuminate ground with radar waves.
- Operates day and night, can see through clouds
- ERS, Envisat (1991): very stable orbits and pointing ⇨ InSAR
- Followed by ERS-2 (1995) and Envisat (2003) for ~ 20 year time series

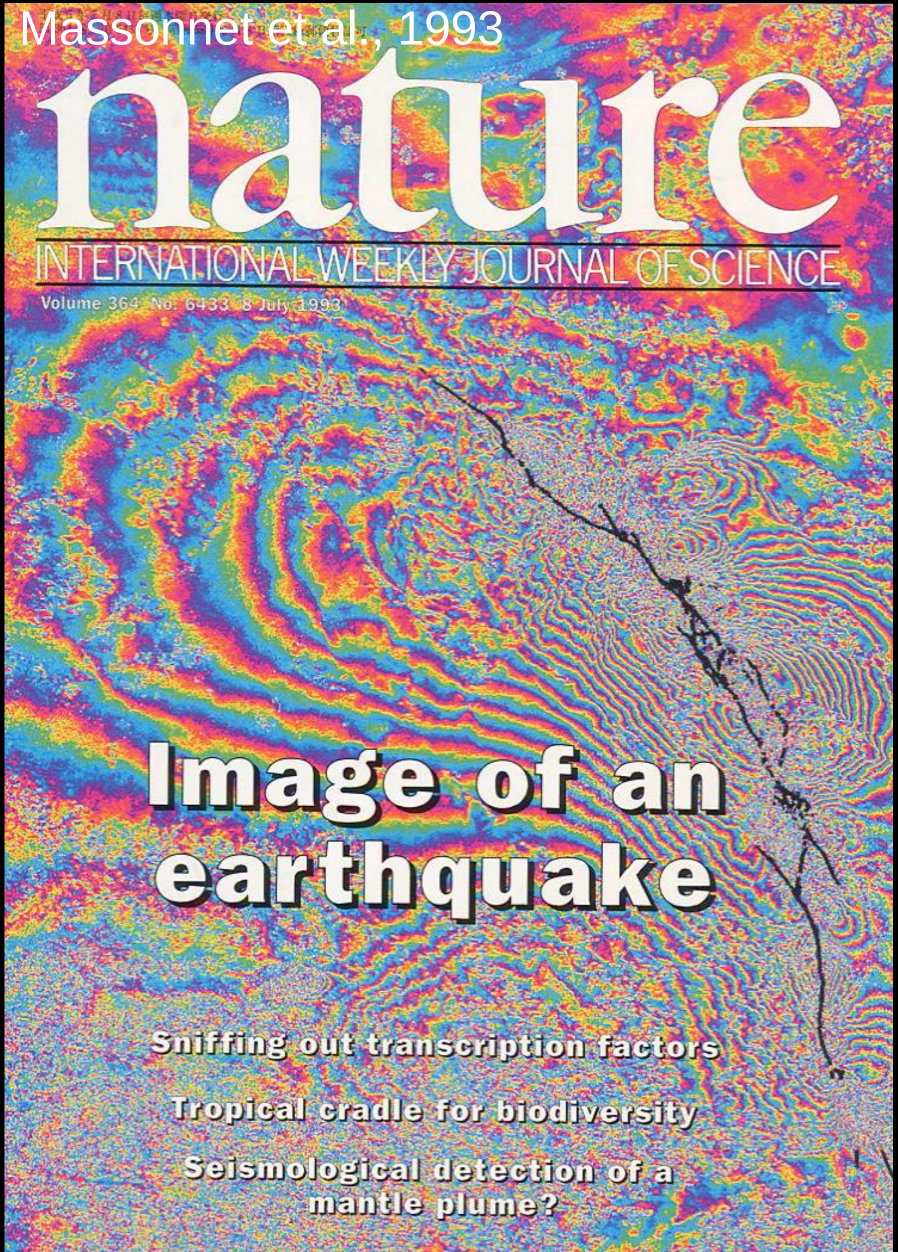

InSAR – how it works

Round trip ~ 30 million wavelengths

BUT we don't know the exact number

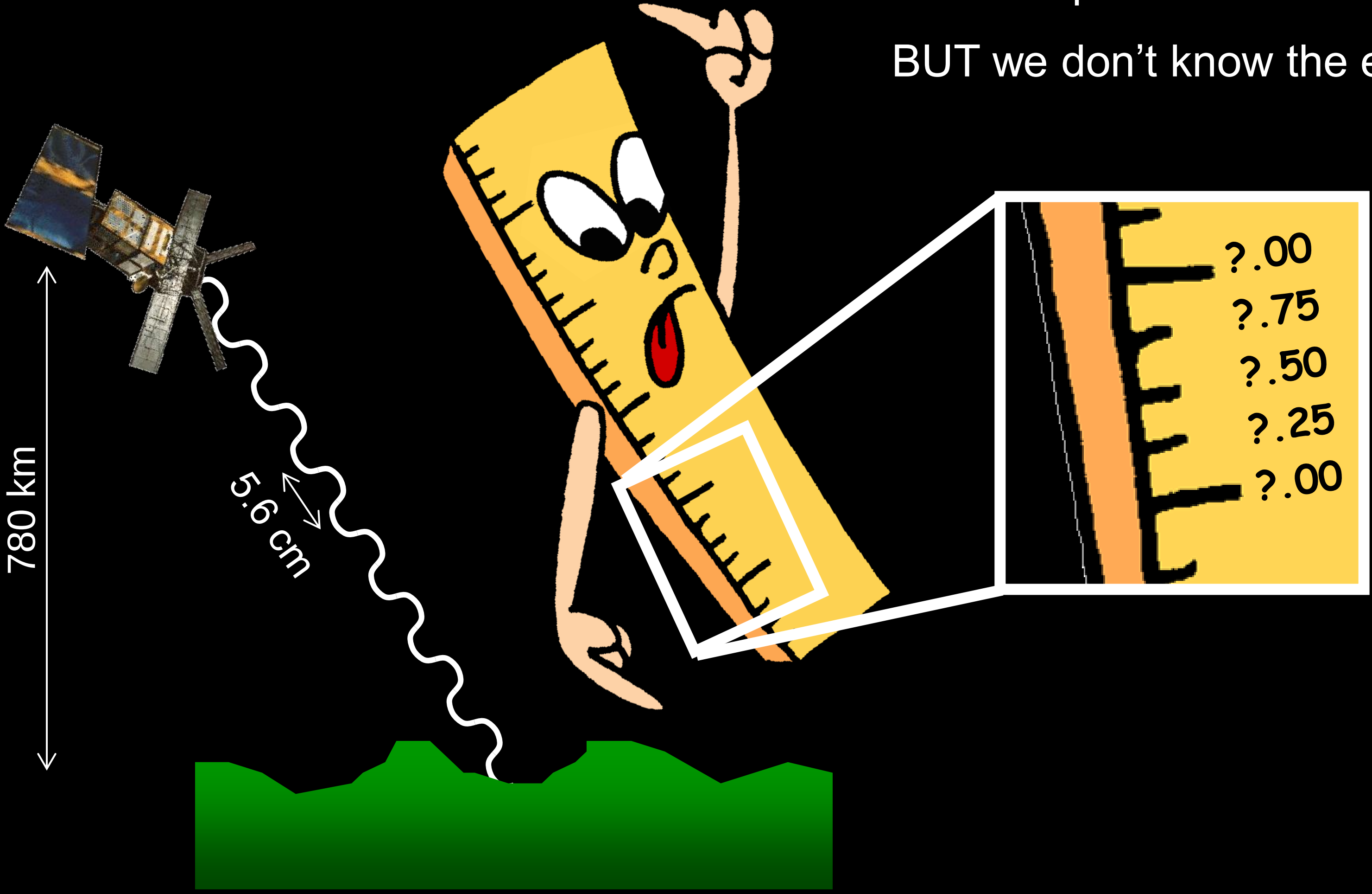

InSAR – how it works

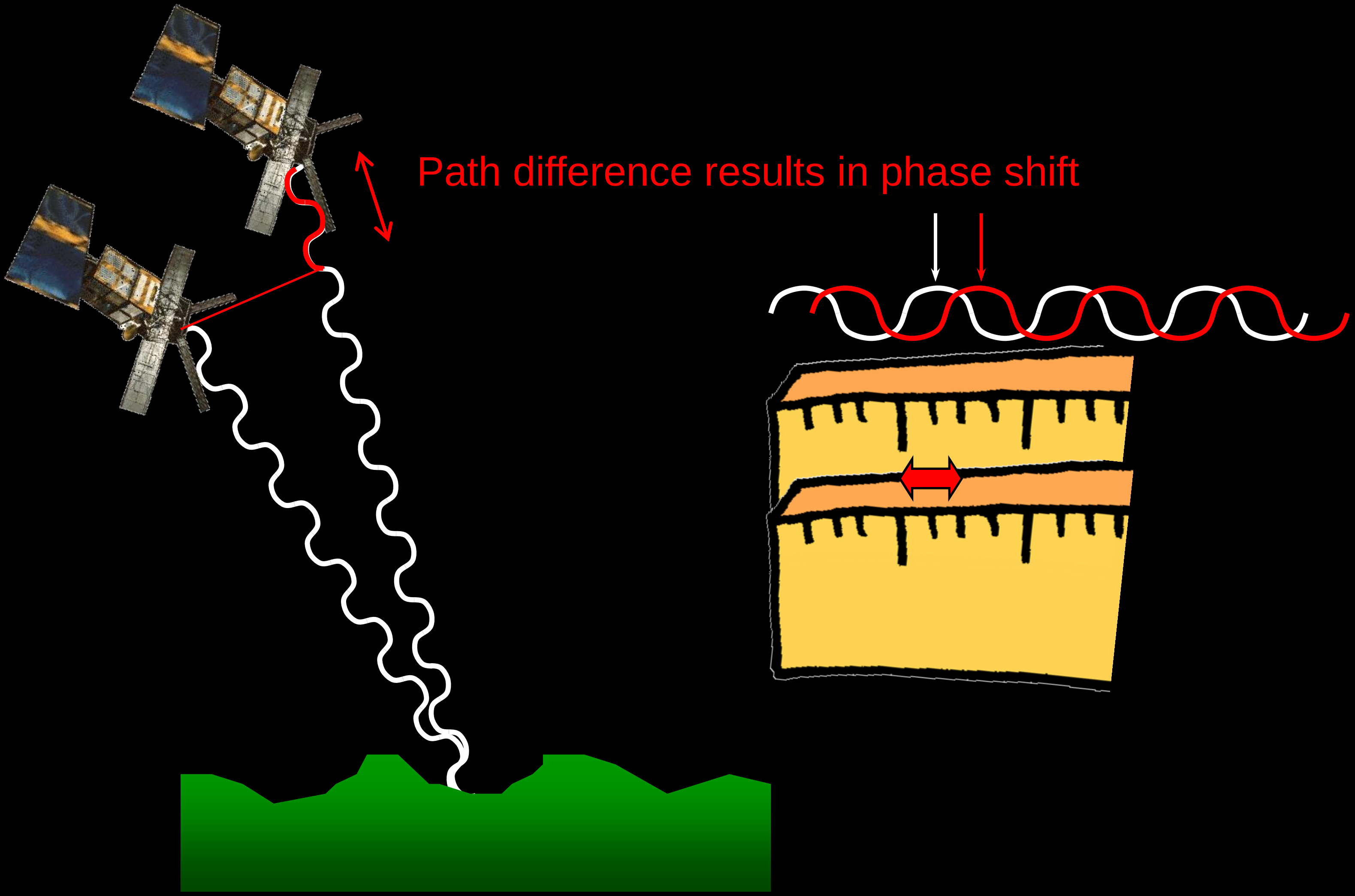

InSAR – how it works

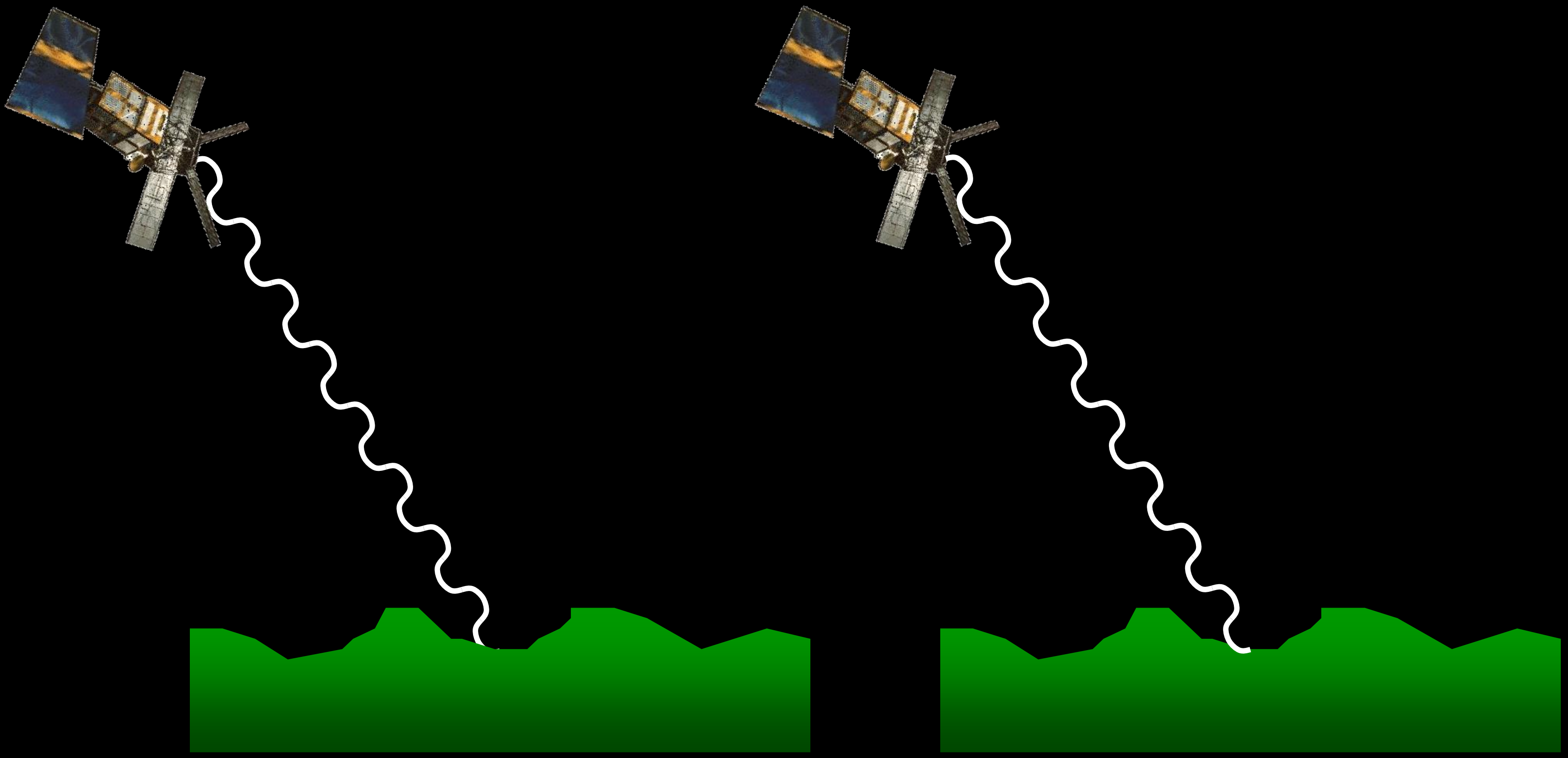

InSAR – how it works

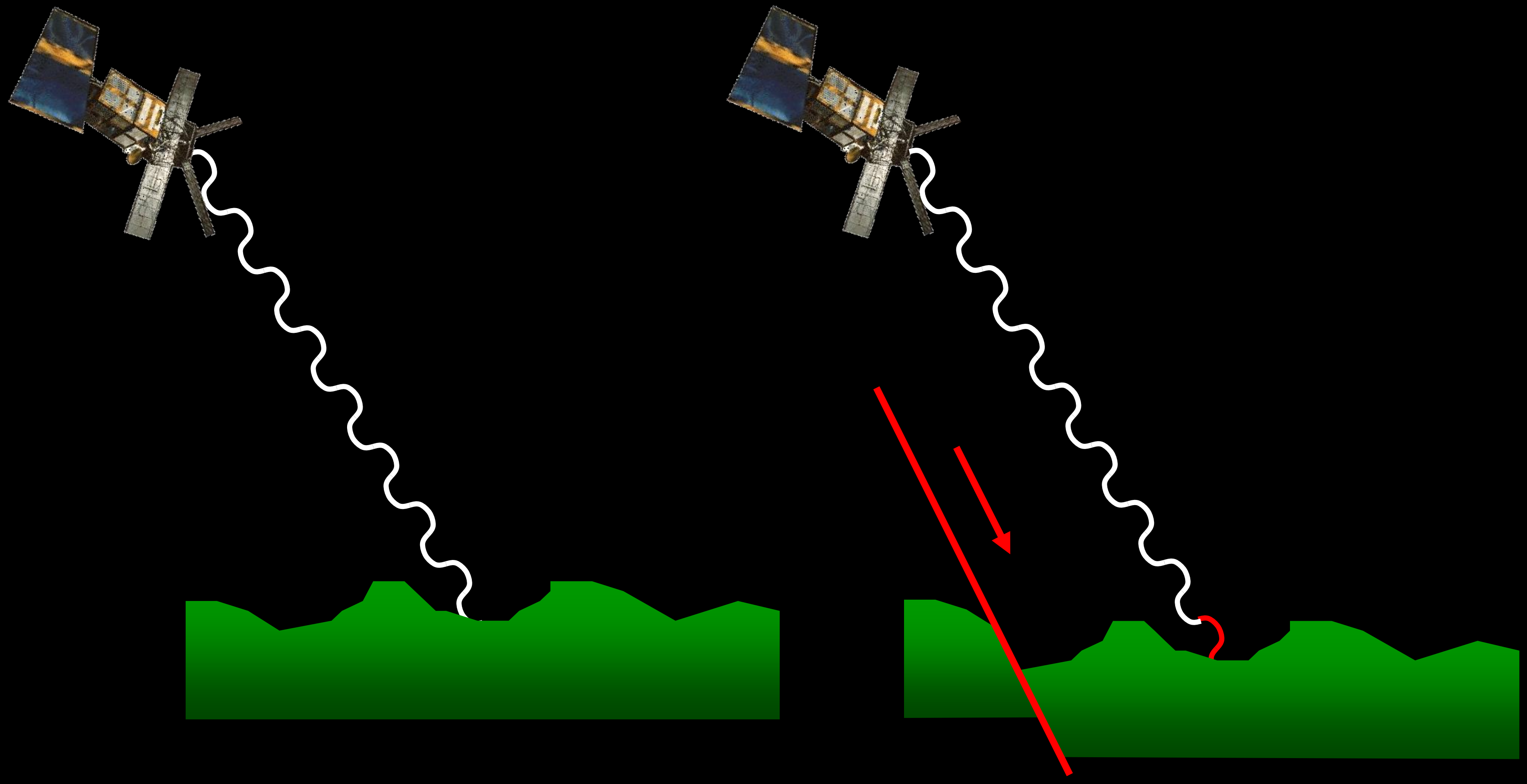

Image A - 12 August 1999

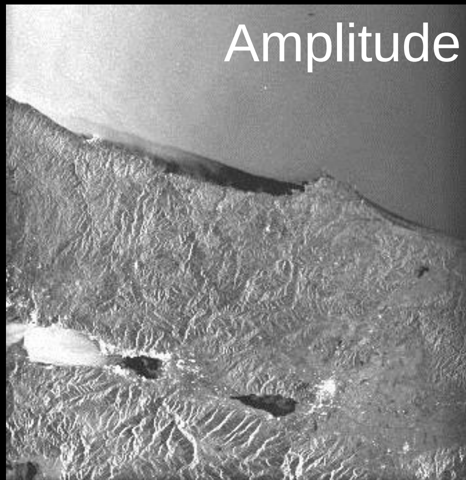

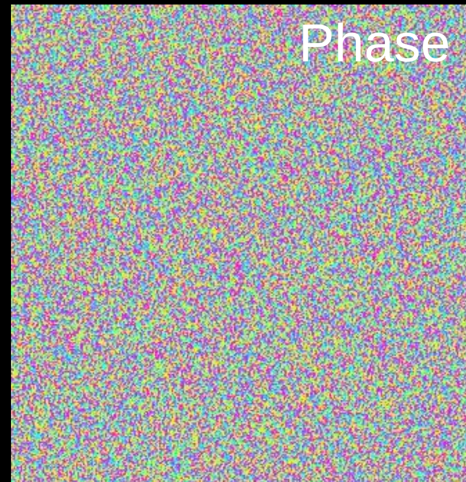

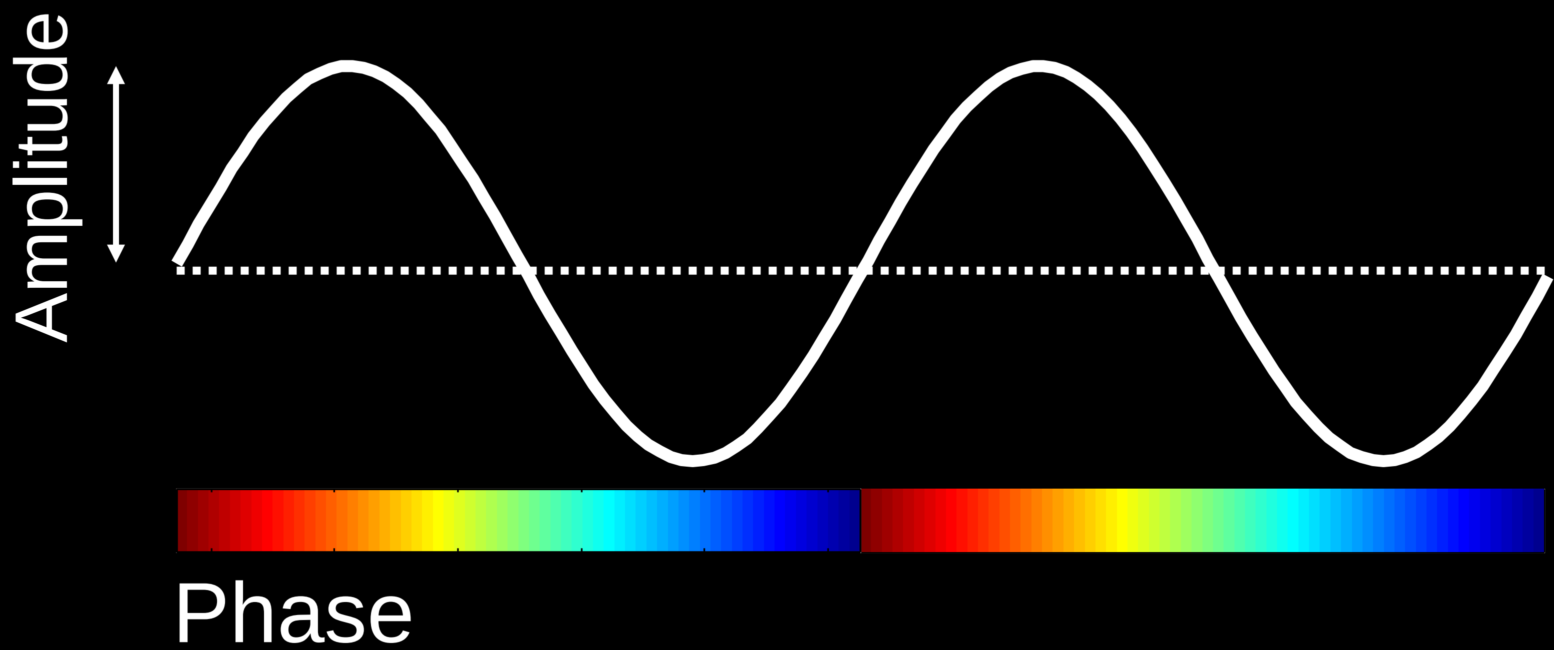

Image A - 12 August 1999

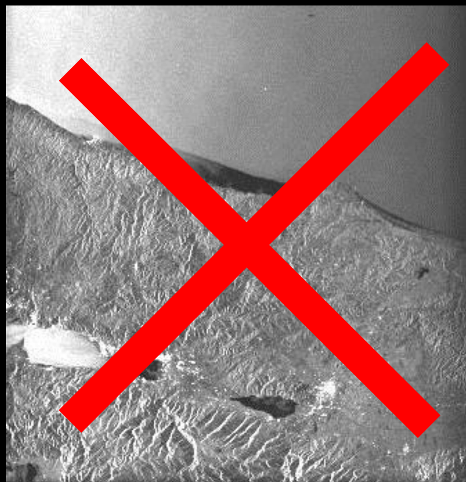

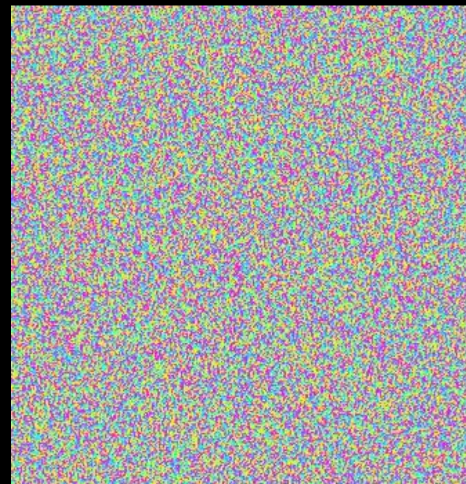

Interferogram =
Phase A - Phase B

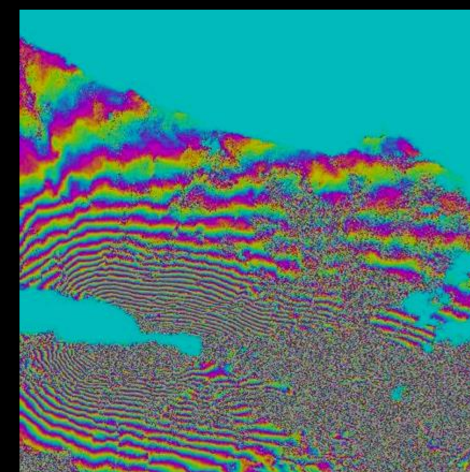

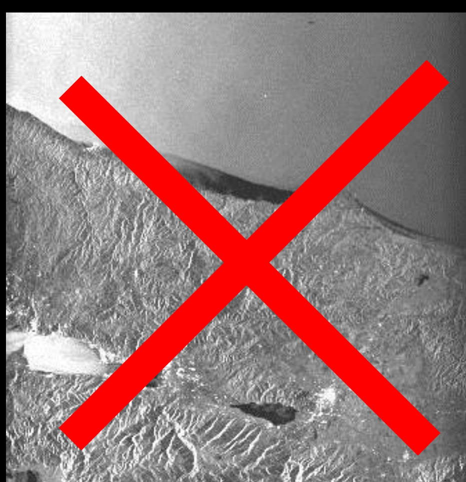

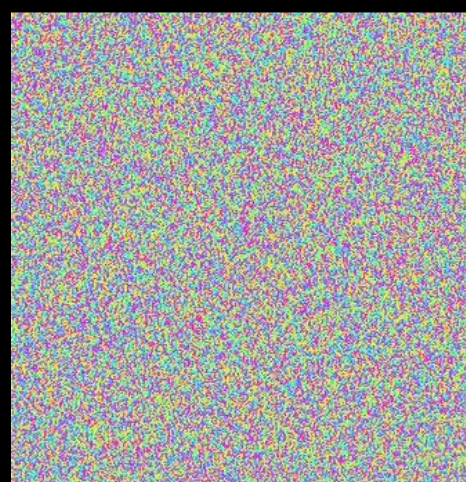

Image B - 16 September 1999

Remove phase from
topography
satellite positions
earth curvature

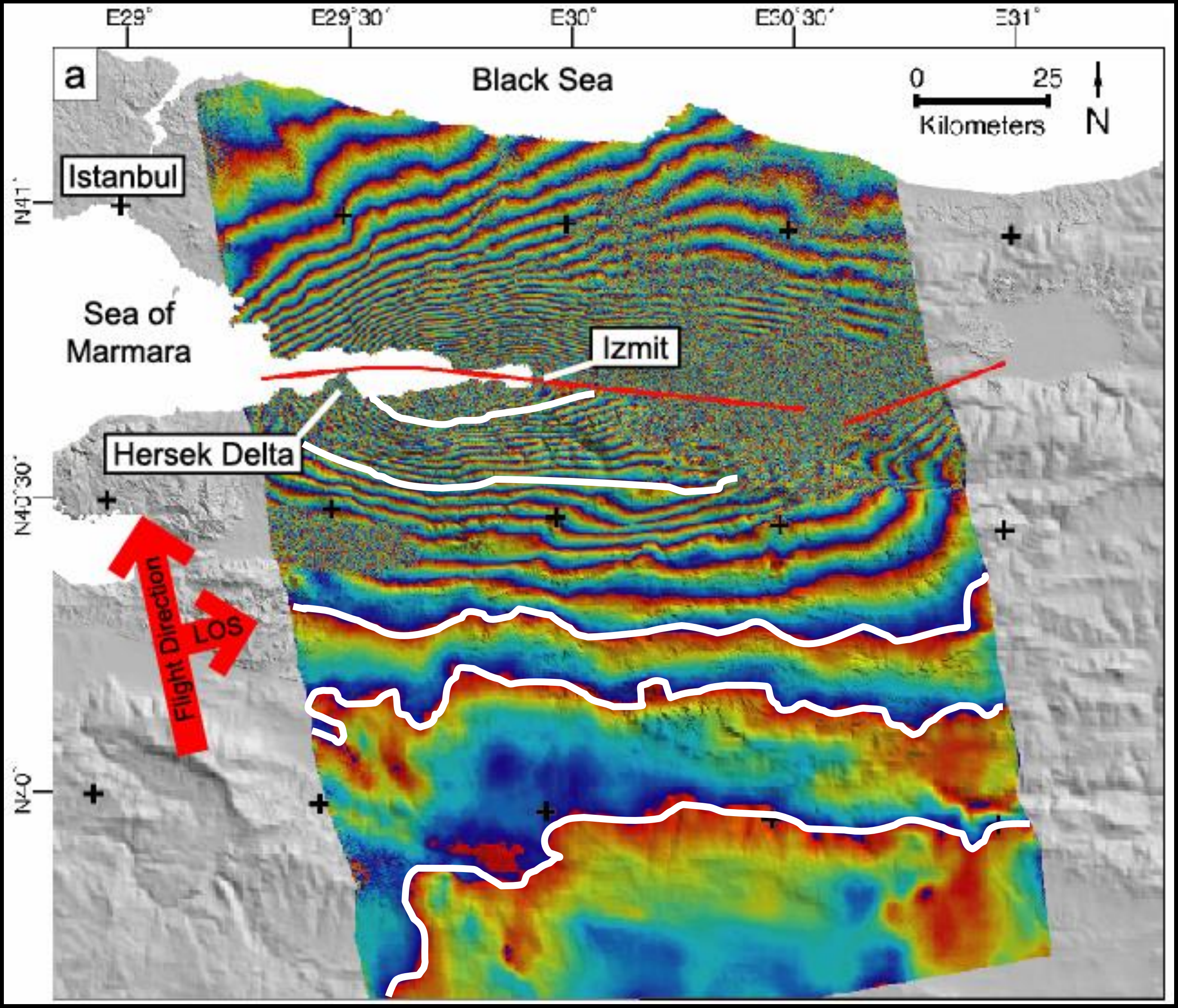

(-20) 567 mm range decrease

(-10) 283 mm range decrease

(-2) 57 mm range decrease

(-1) 28 mm range decrease

(0) 0 mm range change

17 August 1999, Izmit earthquake (Turkey)

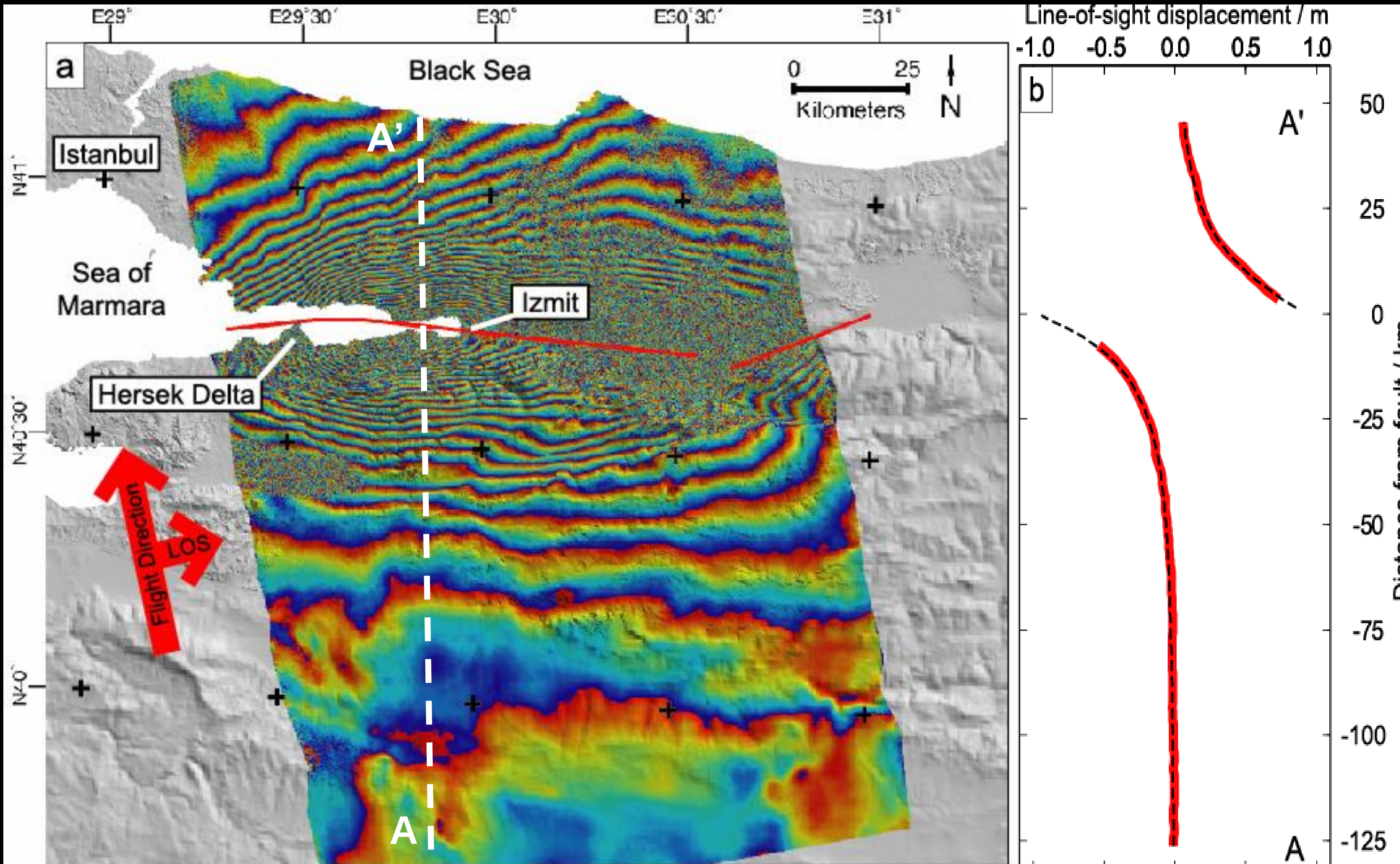

17 August 1999, Izmit earthquake (Turkey)

Components of interferometric phase

$$\Delta\phi_{\text{int}} = \Delta\phi_{\text{geom}} + \Delta\phi_{\text{topo}} + \Delta\phi_{\text{atm}} + \Delta\phi_{\text{noise}} + \Delta\phi_{\text{def}}$$

Components of interferometric phase

$$\Delta\phi_{int} = \Delta\phi_{geom} + \Delta\phi_{topo} + \Delta\phi_{atm} + \Delta\phi_{noise} + \Delta\phi_{def}$$

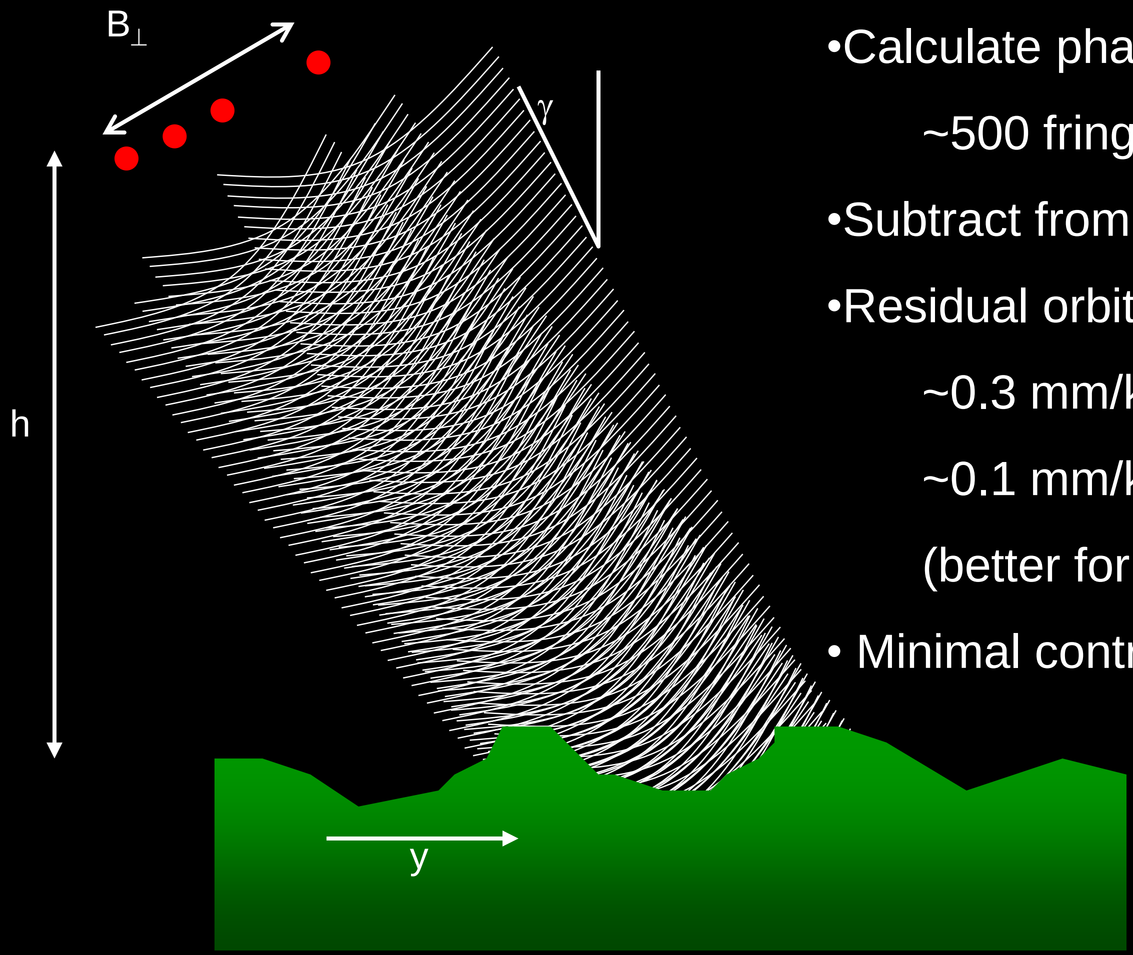

- Calculate phase ramp from satellite orbits
  - ~500 fringes across typical frame
- Subtract from interferogram
- Residual orbital errors:
  - ~0.3 mm/km (north, ERS)
  - ~0.1 mm/km (east, ERS)
  - (better for Envisat)
- Minimal control on v. long wavelength

Components of interferometric phase

$$\Delta\phi_{\text{int}} = \Delta\phi_{\text{geom}} + \Delta\phi_{\text{topo}} + \Delta\phi_{\text{atm}} + \Delta\phi_{\text{noise}} + \Delta\phi_{\text{def}}$$

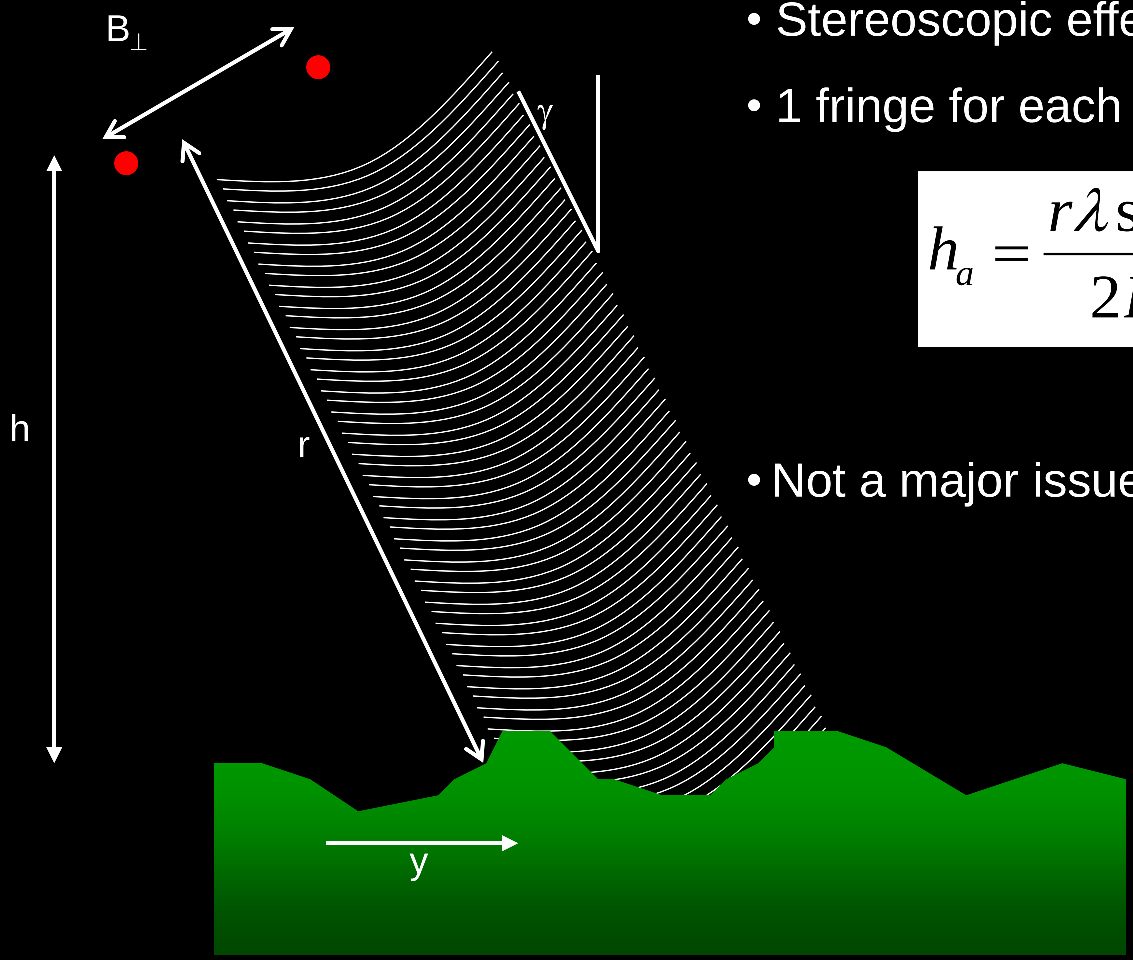

- Stereoscopic effect $\Rightarrow$ topographic fringes
- 1 fringe for each change in elevation h_a

$$h_a = \frac{r\lambda \sin\gamma}{2B_\perp} \approx \frac{10{,}000}{B_\perp}$$

- Not a major issue since SRTM

Components of interferometric phase

$$\Delta\phi_{\text{int}} = \Delta\phi_{\text{geom}} + \Delta\phi_{\text{topo}} + \Delta\phi_{\text{atm}} + \Delta\phi_{\text{noise}} + \Delta\phi_{\text{def}}$$

A foggy morning,

near ancient Mycenae,

Greece

Components of interferometric phase

$$\Delta\phi_{int} = \Delta\phi_{geom} + \Delta\phi_{topo} + \Delta\phi_{atm} + \Delta\phi_{noise} + \Delta\phi_{def}$$

Layered atmosphere

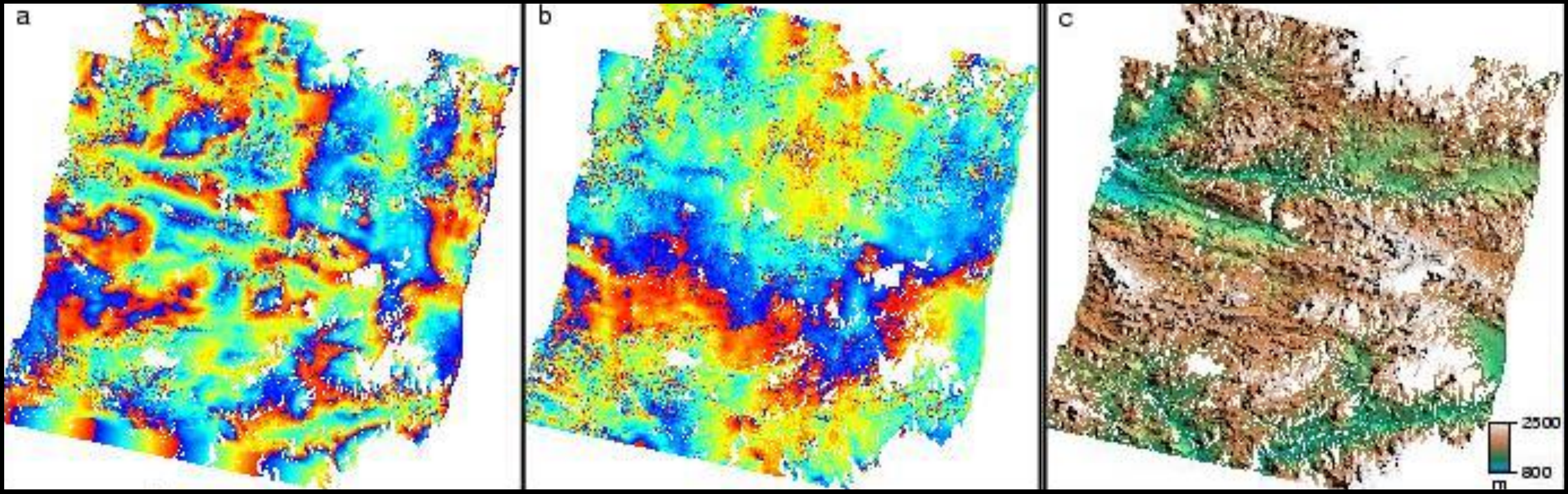

29/8/1995 to 29/7/1997 | 30/8/1995 to 29/7/1997 | Topography

Components of interferometric phase

$$\Delta\phi_{\text{int}} = \Delta\phi_{\text{geom}} + \Delta\phi_{\text{topo}} + \Delta\phi_{\text{atm}} + \Delta\phi_{\text{noise}} + \Delta\phi_{\text{def}}$$

Layered atmosphere

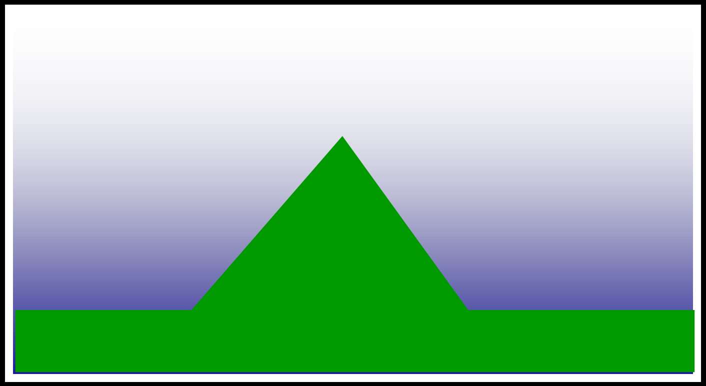

Pass 1

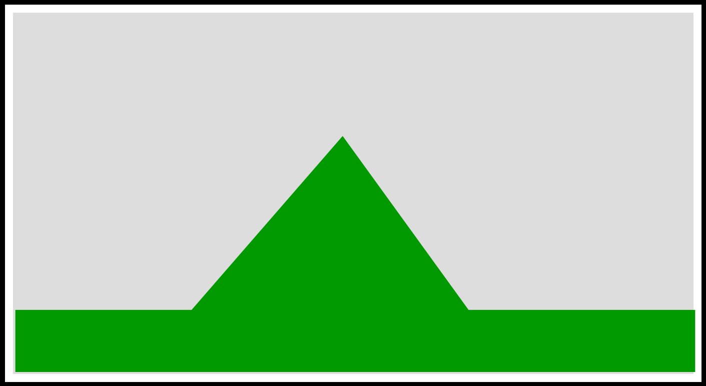

Pass 2

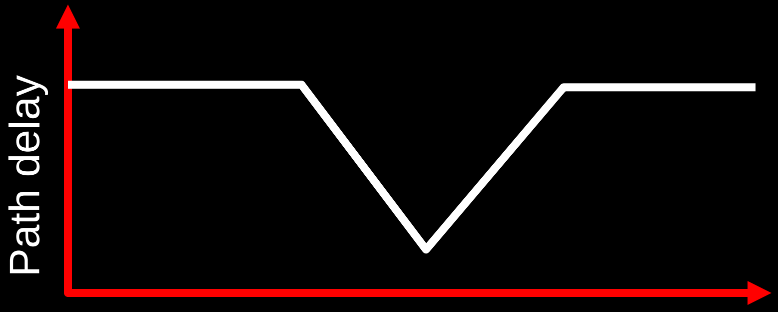

Components of interferometric phase

$$\Delta\phi_{\text{int}} = \Delta\phi_{\text{geom}} + \Delta\phi_{\text{topo}} + \Delta\phi_{\text{atm}} + \Delta\phi_{\text{noise}} + \Delta\phi_{\text{def}}$$

Turbulent atmosphere

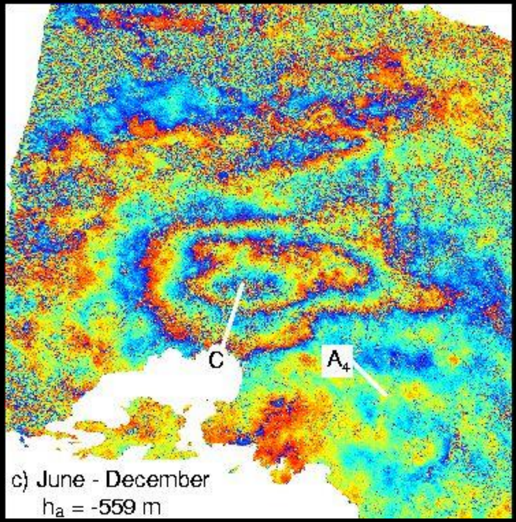

June to December

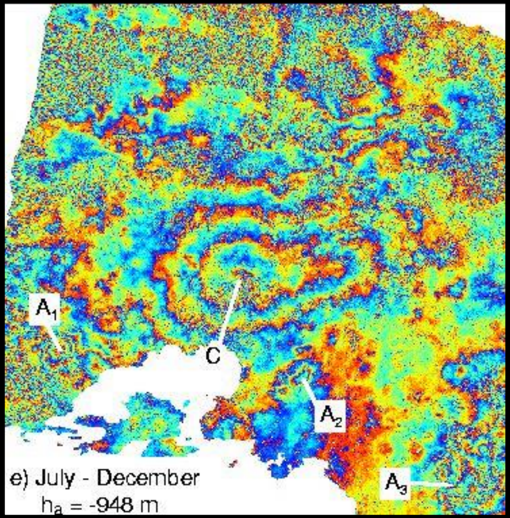

July to December

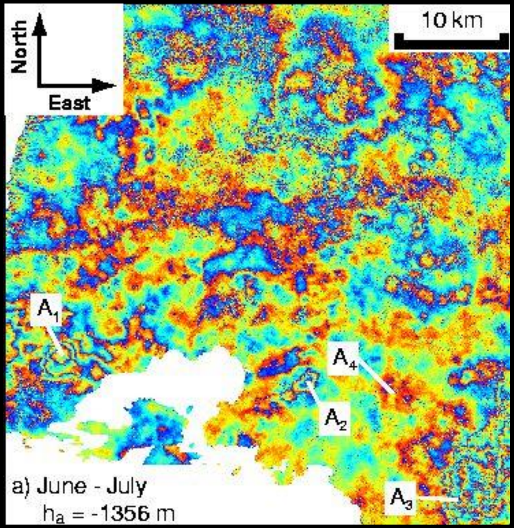

June to July

Athens Earthquake – September 1999

Components of interferometric phase

$$\Delta\phi_{int} = \Delta\phi_{geom} + \Delta\phi_{topo} + \Delta\phi_{atm} + \Delta\phi_{noise} + \Delta\phi_{def}$$

- Size of $\Delta\phi_{atm}$ (at sea level) scales with distance, but can be +/- 10 cm or more.
- Methods for dealing with $\Delta\phi_{atm}$
  - Ignore (most common)
  - Quantify
  - Model based on other observations (e.g. GPS, meteorology…)
  - Increase SNR by stacking or time series analysis

Components of interferometric phase

$$\Delta\phi_{int} = \Delta\phi_{geom} + \Delta\phi_{topo} + \Delta\phi_{atm} + \Delta\phi_{noise} + \Delta\phi_{def}$$

- Biggest source of noise is due to changing ground surface
- *Coherence* is convenient measure

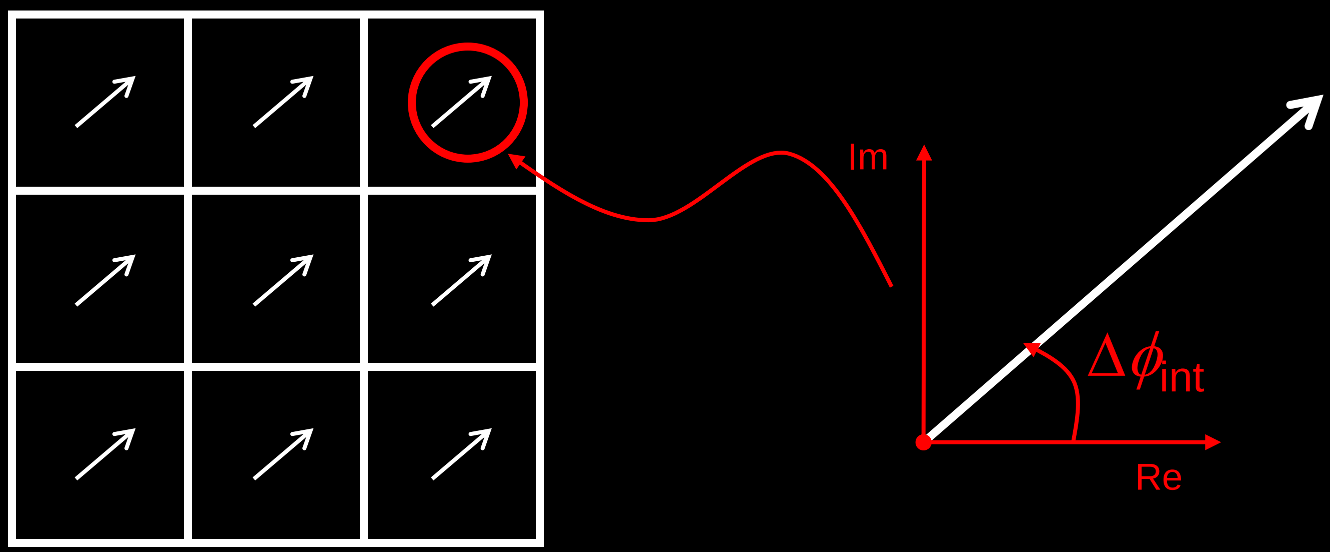

Components of interferometric phase

$$\Delta\phi_{int} = \Delta\phi_{geom} + \Delta\phi_{topo} + \Delta\phi_{atm} + \Delta\phi_{noise} + \Delta\phi_{def}$$

- Biggest source of noise is due to changing ground surface
- *Coherence* is convenient measure

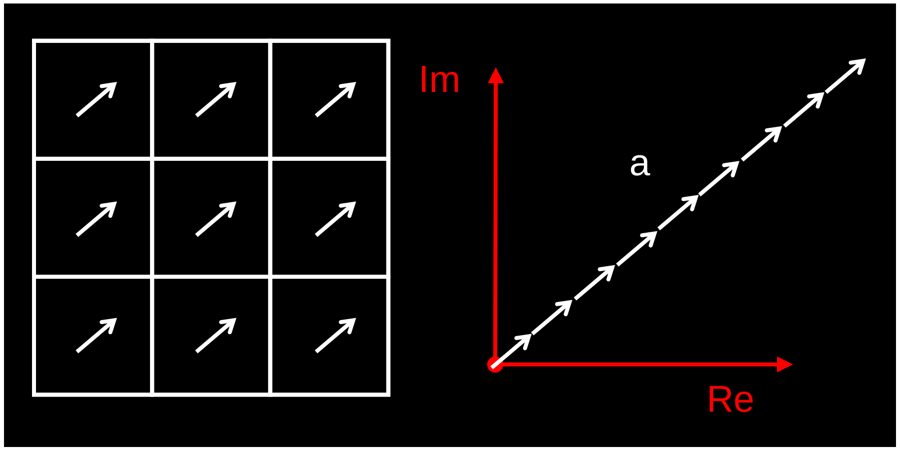

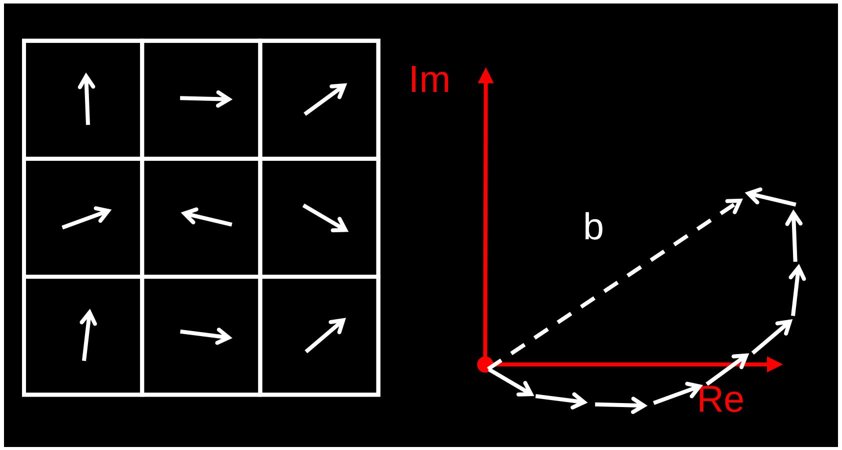

Coherence = b / a

Components of interferometric phase

$$\Delta\phi_{int} = \Delta\phi_{geom} + \Delta\phi_{topo} + \Delta\phi_{atm} + \Delta\phi_{noise} + \Delta\phi_{def}$$

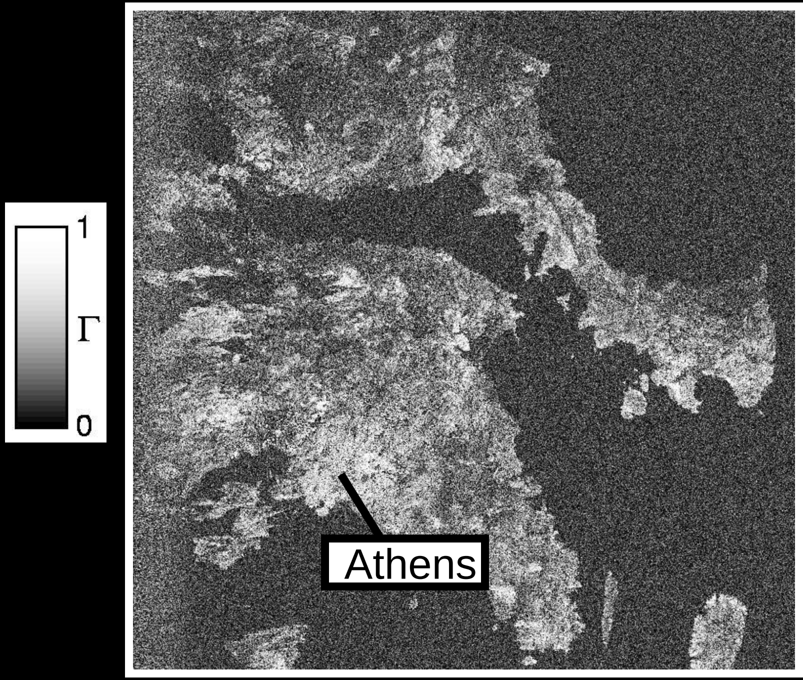

Coherent surface types

- Bare Rock
- Buildings esp. towns/cities

- Grassland
- Agricultural fields
- Ice

Incoherent surface types

- Leafy Trees
- Water

Components of interferometric phase

$$\Delta\phi_{\text{int}} = \Delta\phi_{\text{geom}} + \Delta\phi_{\text{topo}} + \Delta\phi_{\text{atm}} + \Delta\phi_{\text{noise}} + \Delta\phi_{\text{def}}$$

1. incoherence

- Changes in the ground cover cause a random phase shift for each pixel
- Large baselines

2. Unwrapping errrors

- Phase in interferograms is wrapped (each fringe is 2 π radians).
- Discontinuities or data gaps can cause phase unwrapping errors

Components of interferometric phase

$$\Delta\phi_{int} = \Delta\phi_{geom} + \Delta\phi_{topo} + \Delta\phi_{atm} + \Delta\phi_{noise} + \Delta\phi_{def}$$

InSAR ONLY MEASURES THE COMPONENT OF SURFACE DEFORMATION IN THE SATELLITE'S LINE OF SIGHT

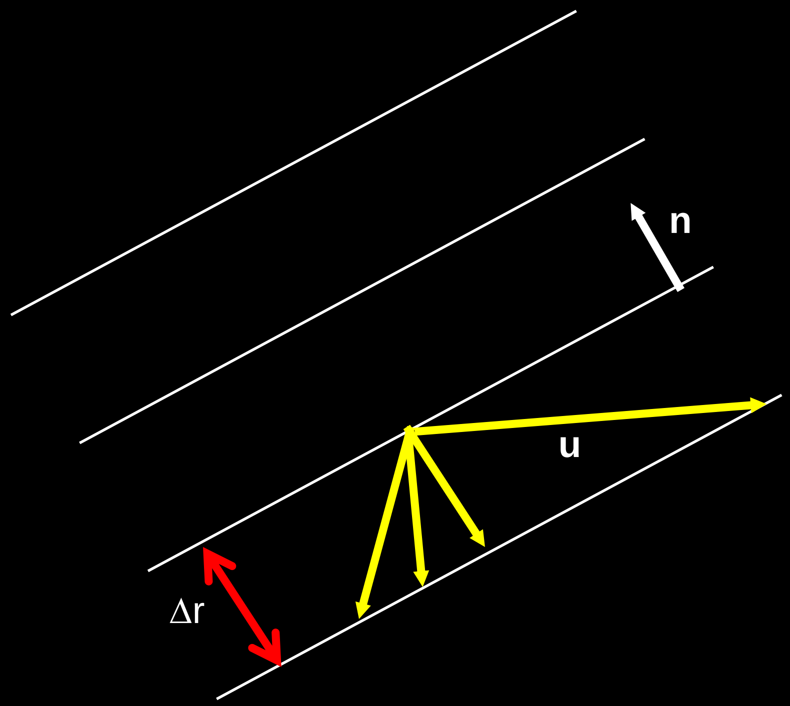

$$\Delta r = -\,\mathbf{n.u}$$

where n is a unit vector pointing from the ground to the satellite

$$\Delta\phi_{def} = (4\pi / \lambda)\, \Delta r$$

i.e. 1 fringe = 28.3 mm l.o.s. deformation for ERS

Error Budget (1)
Single interferogram

$$\sigma_{def}^2 = \sigma_{gm}^2 + \sigma_{topo}^2 + \sigma_{atm}^2 + \sigma_{coh}^2 + \sigma_{sys}^2 + \sigma_{unw}^2$$

- Orbital errors ⇨ long-wavelength ramps.
- Envisat: ~0.3 mm/km (across-track) and 0.1 mm/km (along-track) [Wang, Wright and Biggs, GRL 2009].
- Can correct by processing long strips and tying to GPS **(see. Fringe presentations by Wang, Pagli and Hamlyn)**
- Should be negligible for future missions with onboard GPS receivers.

Error Budget (1)
Single interferogram

$$\sigma_{def}^2 = \sigma_{gm}^2 + \sigma_{topo}^2 + \sigma_{atm}^2 + \sigma_{coh}^2 + \sigma_{sys}^2 + \sigma_{unw}^2$$

$$\sigma_{topo} = \frac{\bar{r}_{slant} B_{\perp}}{\sin \theta_{inc}} \sigma_{DEM}$$

- SRTM error ~ 4 m absolute, of which 2.5 m is not spatially correlated [Rodriguez et al., PERS 2006]

B_{perp}	σ_{topo} (40° incidence)
150 m	1.1 mm
300 m	2.3 mm
1000 m	7.8 mm

Error Budget (1)
Single interferogram

$$\sigma_{def}^2 = \sigma_{gm}^2 + \sigma_{topo}^2 + \sigma_{atm}^2 + \sigma_{coh}^2 + \sigma_{sys}^2 + \sigma_{unw}^2$$

- Troposhere

Emardson et al., 2003:
$\sigma = cL^{\alpha}$ [c~2.5, α~0.5]
σ= 25 mm at 100 km

(assume no corrections)

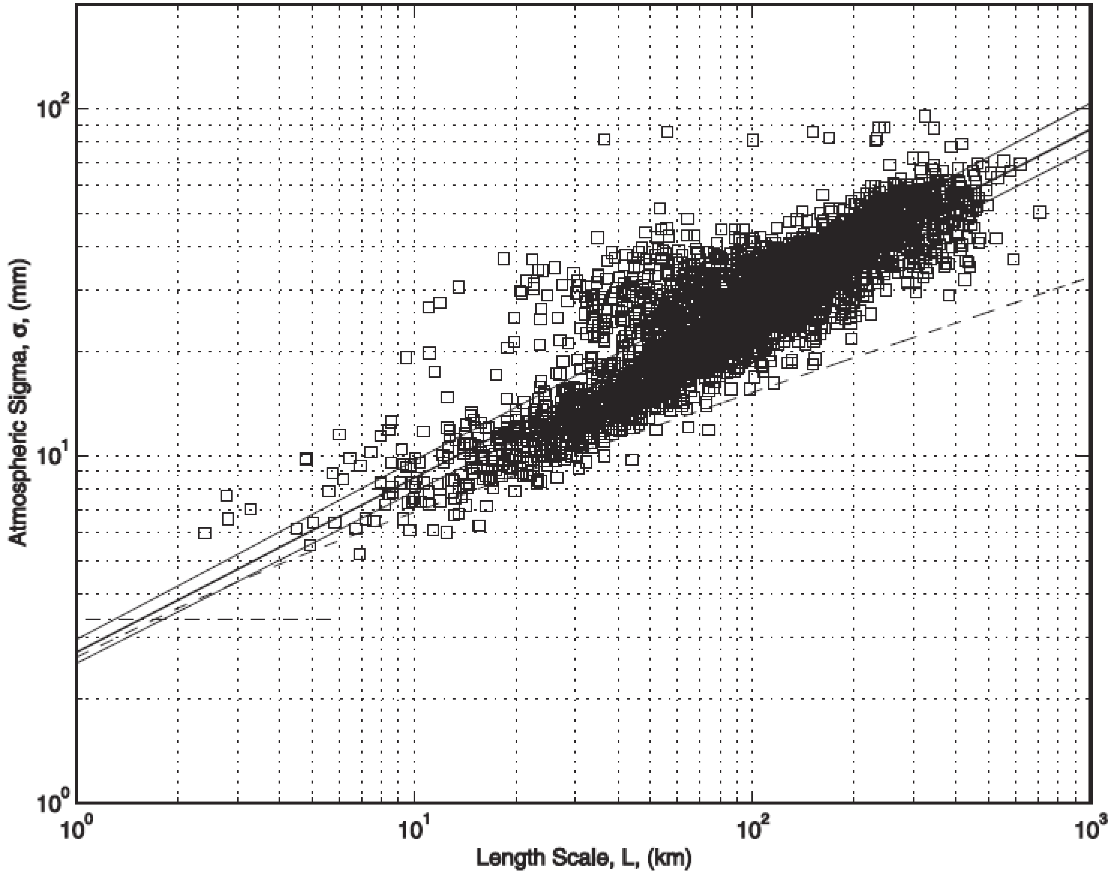

Error Budget (1)
Single interferogram

$$\sigma_{def}^2 = \sigma_{gm}^2 + \sigma_{topo}^2 + \sigma_{atm}^2 + \sigma_{coh}^2 + \sigma_{sys}^2 + \sigma_{unw}^2$$

- Ionosphere ($1/f^2$ dependence). Important at L-band, but not at C-band.
- Can correct with split band processing (e.g. 1200 and 1260 MHz) in future missions
- Ionospheric error on 100 km wavelength ~ 1mm after spatial averaging

Error Budget (1)
Single interferogram

$$\sigma_{def}^2 = \sigma_{gm}^2 + \sigma_{topo}^2 + \sigma_{atm}^2 + \sigma_{coh}^2 + \sigma_{sys}^2 + \sigma_{unw}^2$$

- Coherence, γ
  - important at short wavelengths, but can be averaged through multilooking to < 1 mm for most ground cover types

Error Budget (1)
Single interferogram

$$\sigma^2_{def} = \sigma^2_{gm} + \sigma^2_{topo} + \sigma^2_{atm} + \sigma^2_{coh} + \sigma^2_{sys} + \sigma^2_{unw}$$

- Coherence, γ
  - important at short wavelengths, but can be averaged through multilooking to < 1 mm for most ground cover types
- System (thermal) - modifies coherence
  - reduces effective coherence, but still insignificant after spatial averaging.

$$\sigma_{coh} = \left(\frac{\lambda}{4\pi}\right)\frac{1}{\sqrt{N_L}}\frac{\sqrt{1-\gamma^2}}{\gamma}$$

$$\gamma_c = \frac{\gamma}{1+SNR^{-1}}$$

Error Budget (1)
Single interferogram

$$\sigma_{def}^2 = \sigma_{gm}^2 + \sigma_{topo}^2 + \sigma_{atm}^2 + \sigma_{coh}^2 + \sigma_{sys}^2 + \sigma_{unw}^2$$

- Unwrapping errors difficult to quantify.
- Assume = 0 in this analysis (probably OK for L-band missions or missions with short revisits).

Error Budget (1)
Single interferogram

$$\sigma^2_{def} = \sigma^2_{gm} + \sigma^2_{topo} + \sigma^2_{atm} + \sigma^2_{coh} + \sigma^2_{sys} + \sigma^2_{unw}$$

Atmospheric (tropospheric) error dominates at 100 km length scales, at which single interferograms have error of ~25 mm.

Improving SNR: 1. Stacking

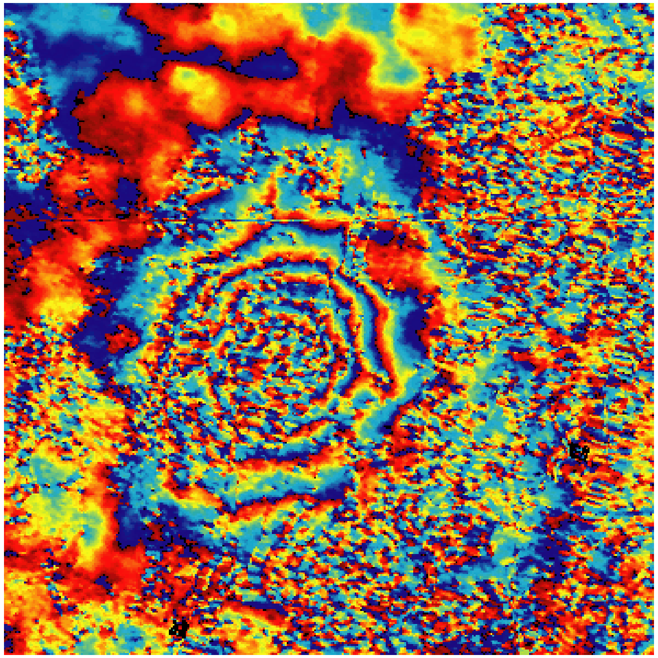

Individual Interferogram

Typical atmospheric noise for individual interferogram ~ 1cm

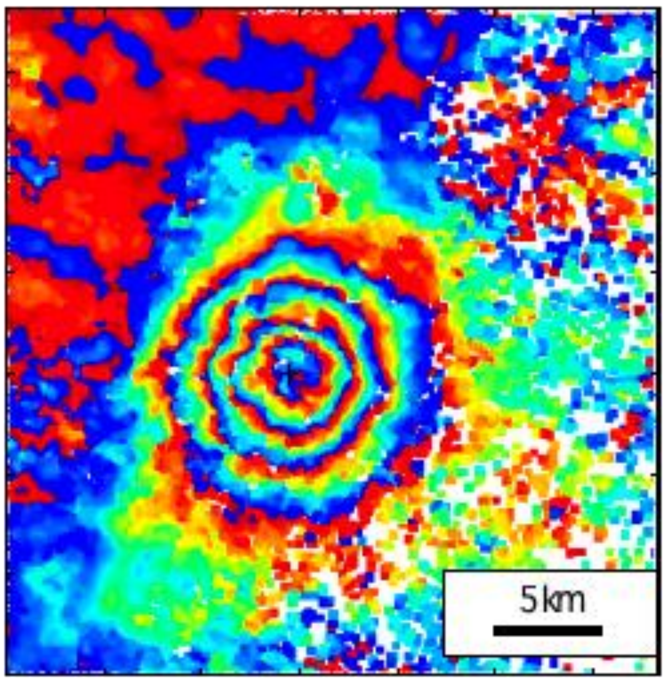

Stack of 5 images

Stack: Add together 5 interferograms

Signal increases by a factor of 5

Noise increases by a factor of √5

Signal:Noise ratio increases by 5/√5 = √5 ~ 2.23

For continuous phenomena (e.g. interseismic strain) or discrete events (e.g earthquakes)

Biggs et al, 2009 (Geology)

Improving SNR: 2. Time Series Methods

All time series methods are essentially the same – rely on large stacks of imagery to separate signal from noise

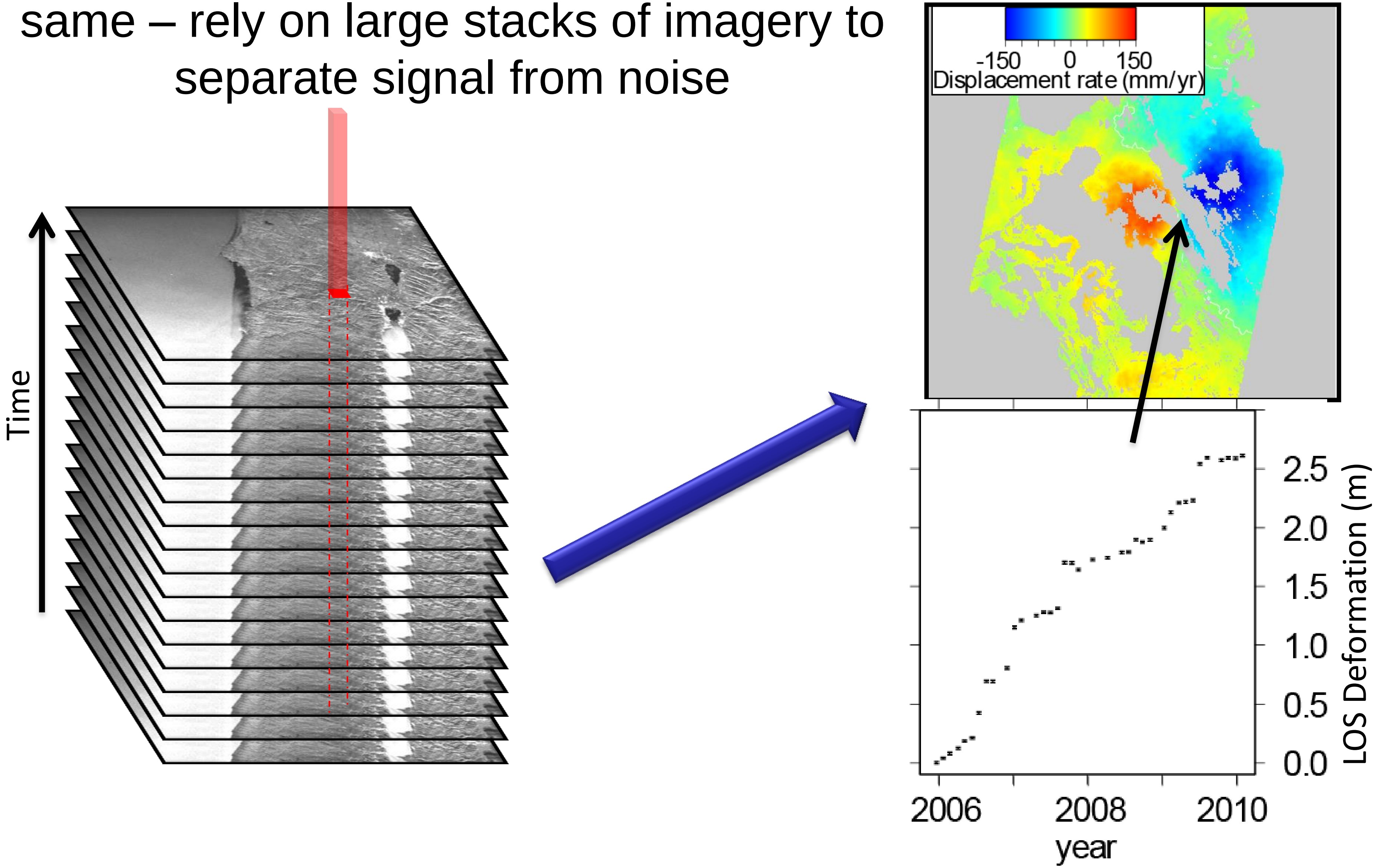

The Future

Sentinel-1 (ESA, GMES)

- “Operational” C-band InSAR
- 12 day repeat, 2 satellites ⇨ 3 day revisit
- Funded for 20 years, Launch early 2014

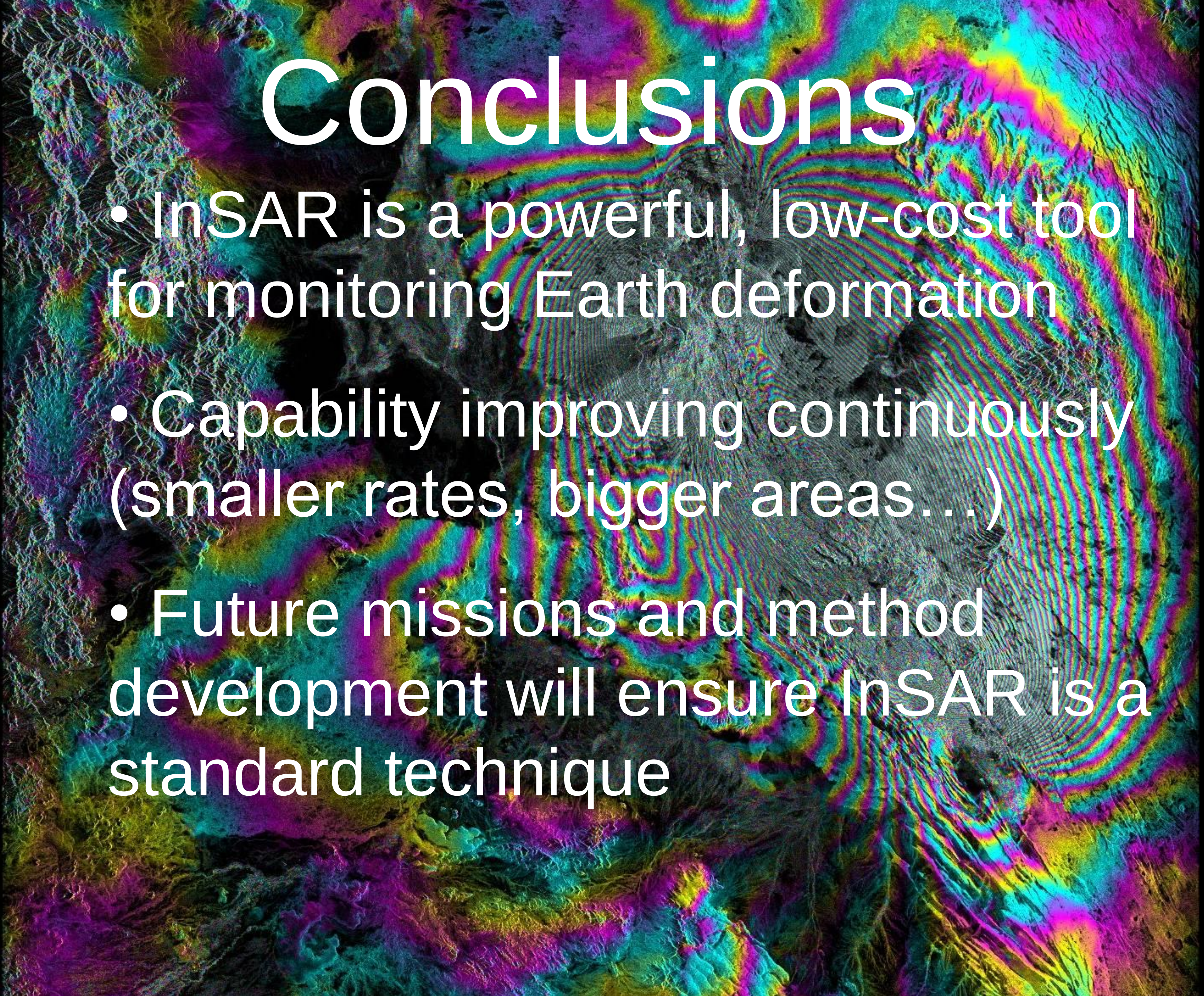

Conclusions

- InSAR is a powerful, low-cost tool for monitoring Earth deformation
- Capability improving continuously (smaller rates, bigger areas…)
- Future missions and method development will ensure InSAR is a standard technique

Part 2: “Advanced” InSAR Methods

Outline for Advanced Methods

1. Combining interferograms
   - Stacking
   - Time series
   - SBAS/Permanent Scatterers
   - Error budget for Time Series Methods
2. Determining 3D displacements/velocities
   - Direct inversion
   - Combination with GPS
3. Atmospheric Corrections
   - Linear/Smooth Velocity Assumption
   - MERIS/MODIS
   - GPS
   - Weather Models

Stacking

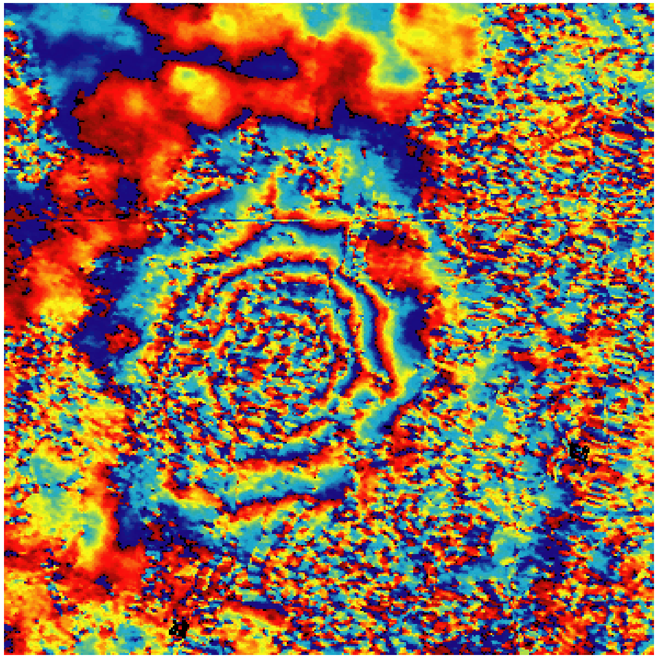

Individual Interferogram

Typical atmospheric noise for individual interferogram ~ 1cm

Stack: Add together 5 interferograms

Signal increases by a factor of 5

Noise increases by a factor of √5

Signal:Noise ratio increases by $5/\sqrt{5} = \sqrt{5} \sim 2.23$

For continuous phenomena (e.g. interseismic strain) or discrete events (e.g earthquakes)

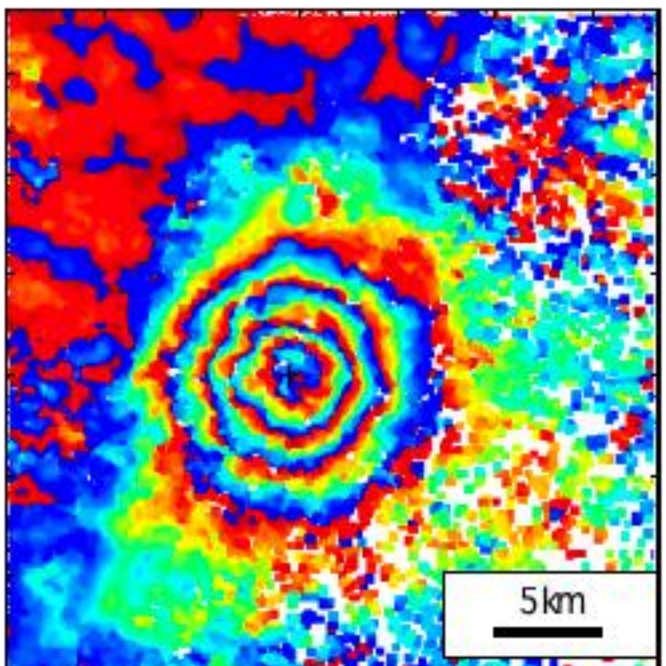

Stack of 5 images

Biggs et al, 2009 (Geology)

All time series methods are essentially the same – rely on large stacks of imagery to separate signal from noise

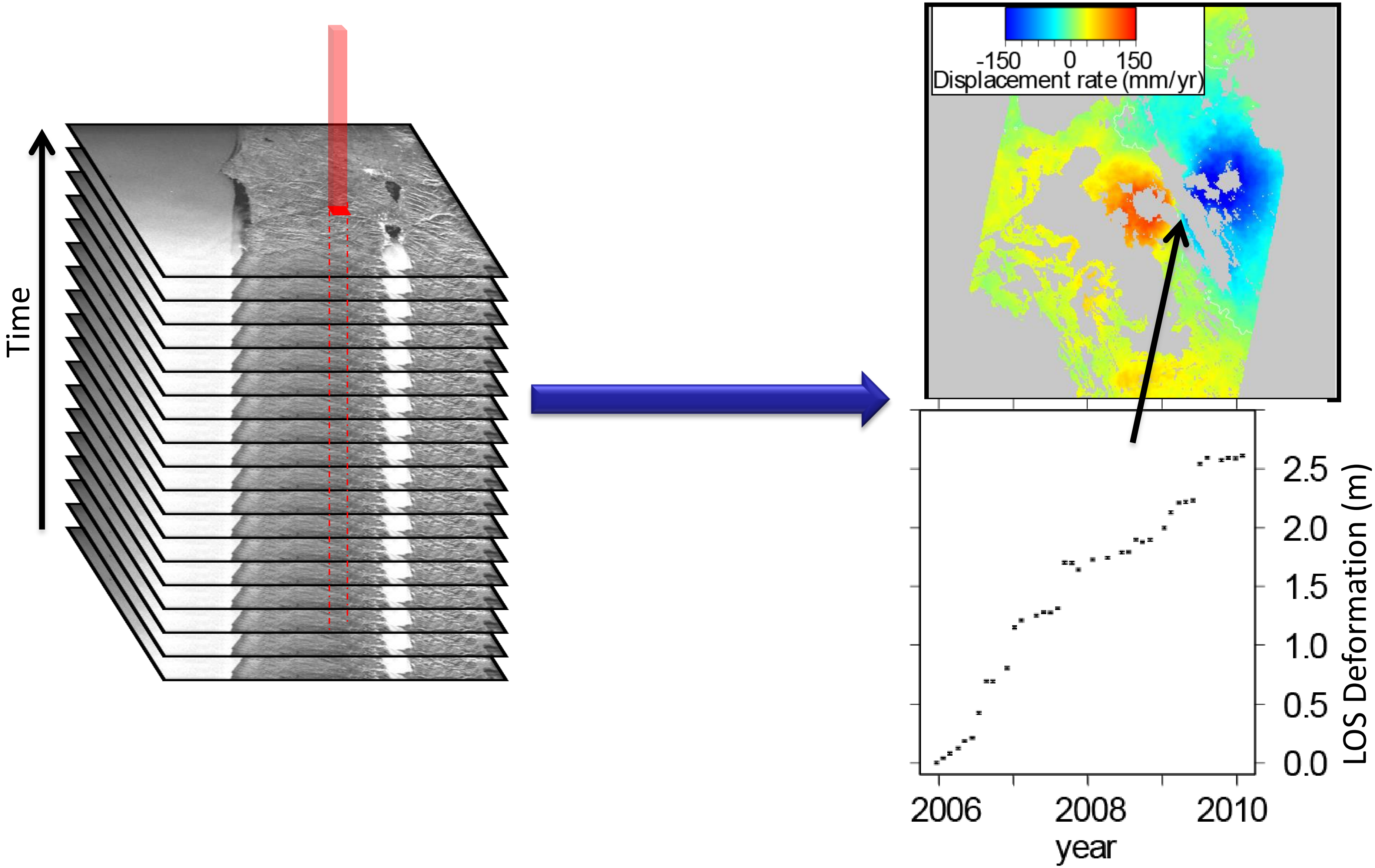

Time Series Example

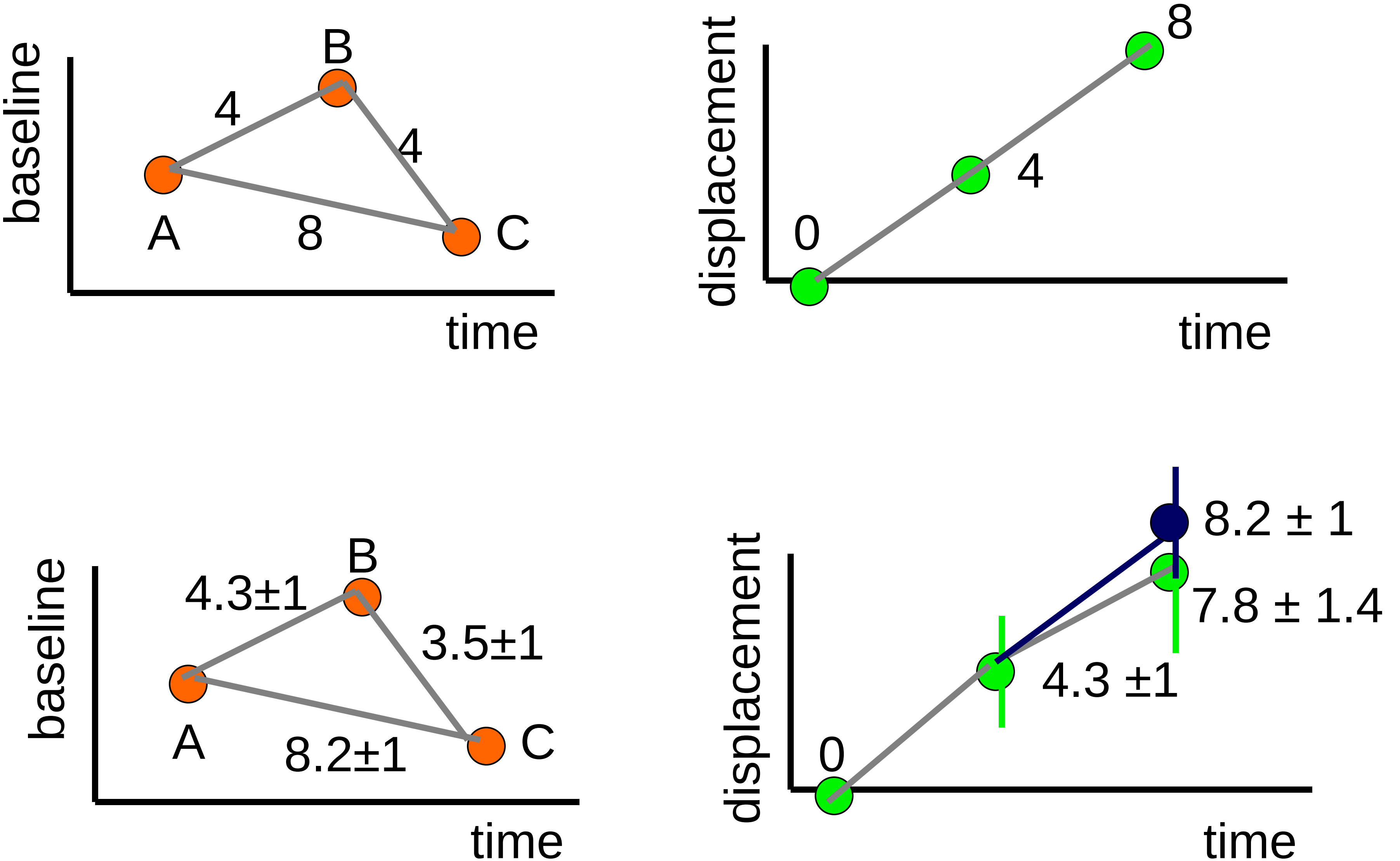

Time Series Inversion

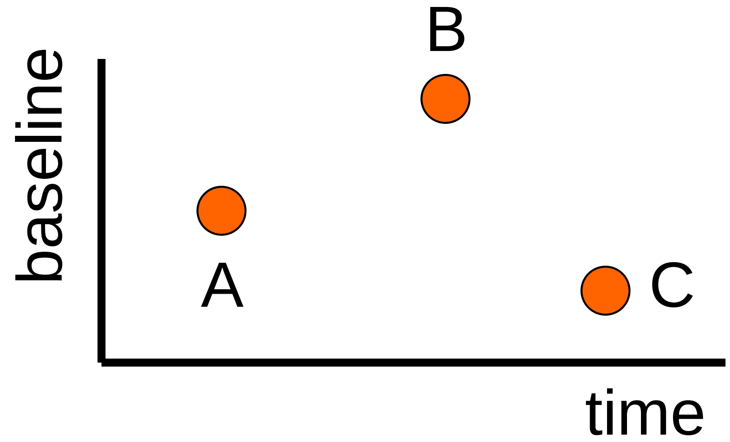

Acquisitions A,B,C

$i_{AB} = d_B - d_A \qquad = v_{AB} t_{AB}$

$i_{BC} = d_C - d_B \qquad = v_{BC} t_{BC}$

$i_{AC} = d_C - d_A \qquad = (d_C - d_B) + (d_B - d_A) \qquad = v_{AB} t_{AB} + v_{BC} t_{BC}$

$$\begin{bmatrix} t_{AB} & 0 \\ 0 & t_{BC} \\ t_{AB} & t_{BC} \end{bmatrix} \begin{bmatrix} v_{AB} \\ v_{BC} \end{bmatrix} = \begin{bmatrix} i_{AB} \\ i_{BC} \\ i_{AC} \end{bmatrix}$$

$G_{INS}\, m = d_{INS}$

To get correct answer with this method, weighting with covariances is essential

$\Sigma^{-1} G_{INS}\, m = \Sigma^{-1} d_{INS}$

SBAS: Short BAseline Subset

Example: Campi Flegrei caldera (Italy).

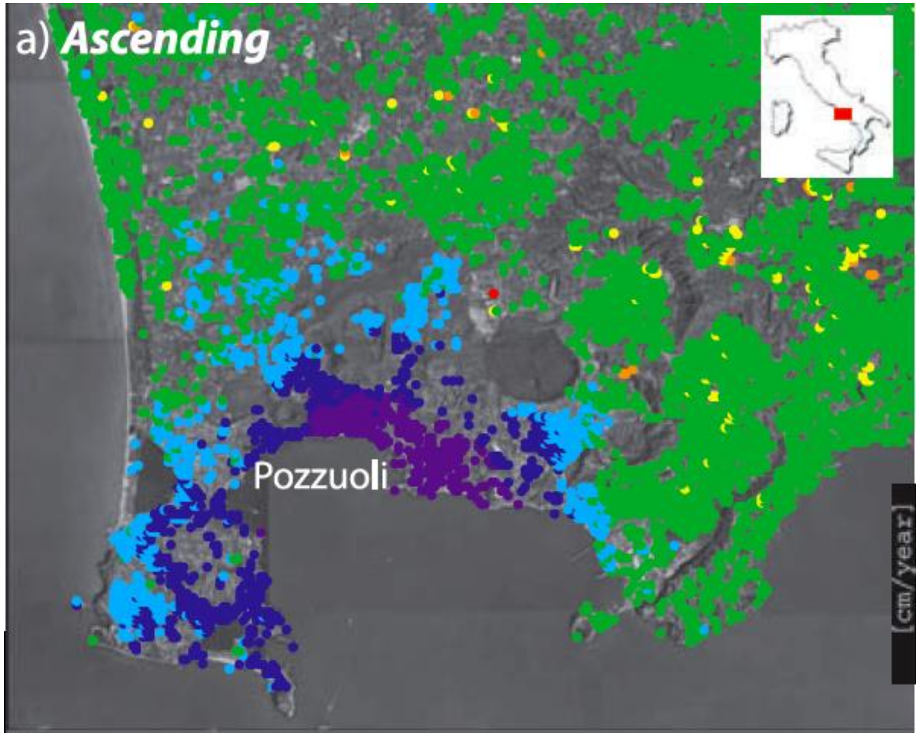

30 ascending images
=> 180 interferograms

Max uplift of 2 cm/yr in Pozzuoli Harbour

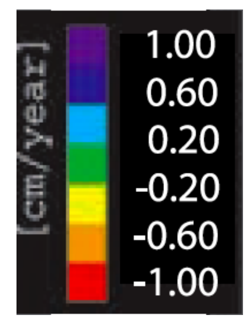

Modelled by an inflation rate of a magma chamber at a depth of 3.2 km with a volume change of 1.1 x 10^6 m^3/yr

(Trasatti et al, 2008; Casu et al, 2006)

SBAS

Pozzuoli Harbour time series:

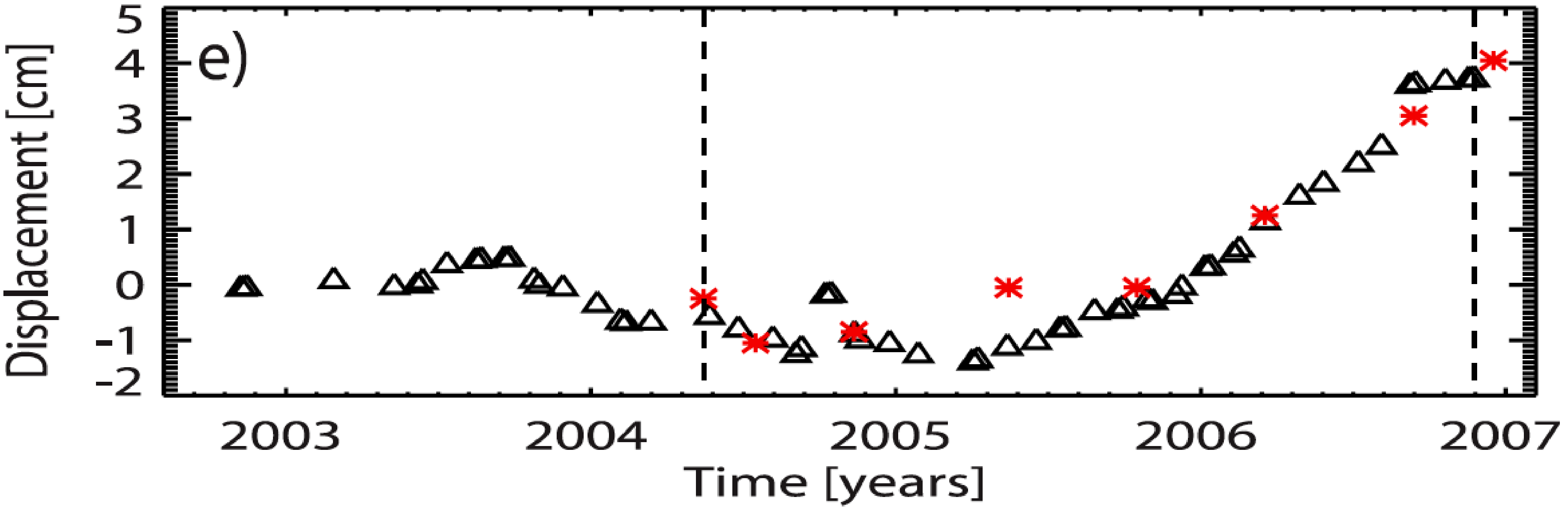

Stated accuracy: 1 mm/yr in rate. 5 mm in displacement.

Good match with levelling data (red).

PI-RATE: Poly-Interferogram Rate And Time-series Estimator

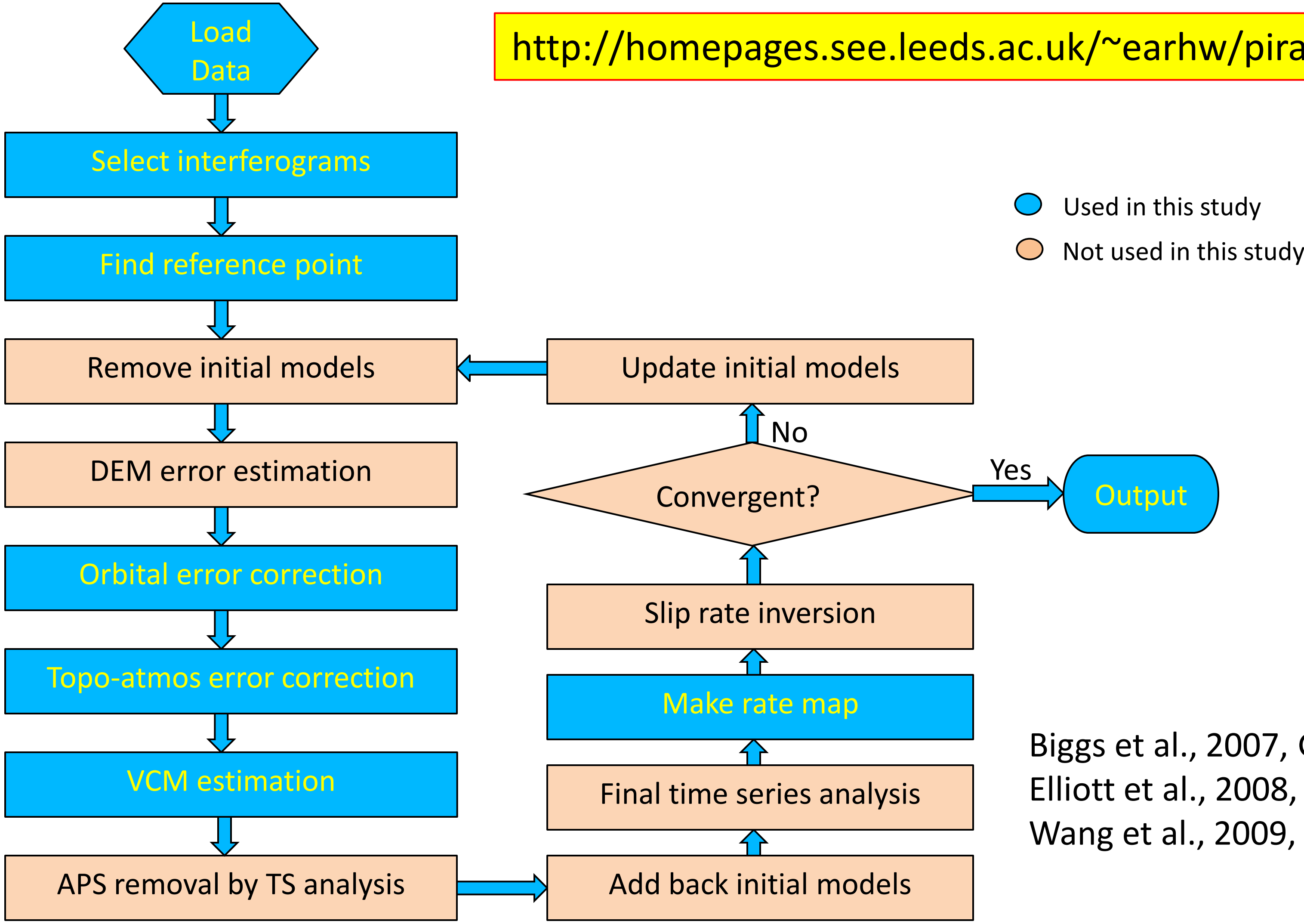

http://homepages.see.leeds.ac.uk/~earhw/pirate

Biggs et al., 2007, GJI;
Elliott et al., 2008, GRL;
Wang et al., 2009, GRL.

PS InSAR:

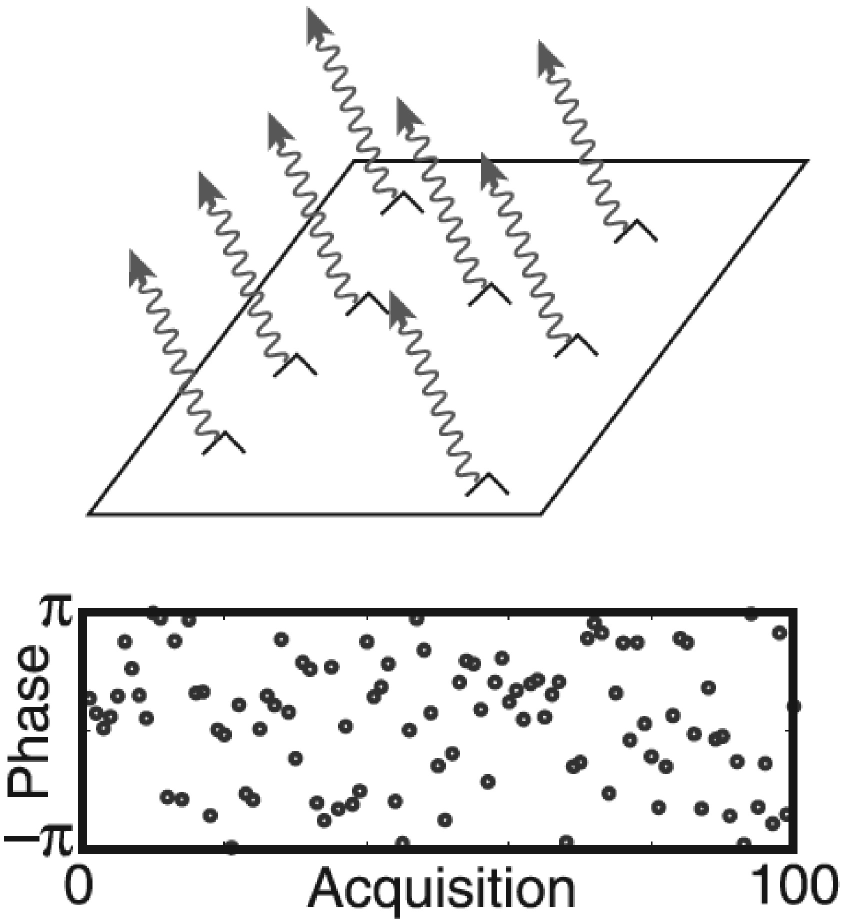

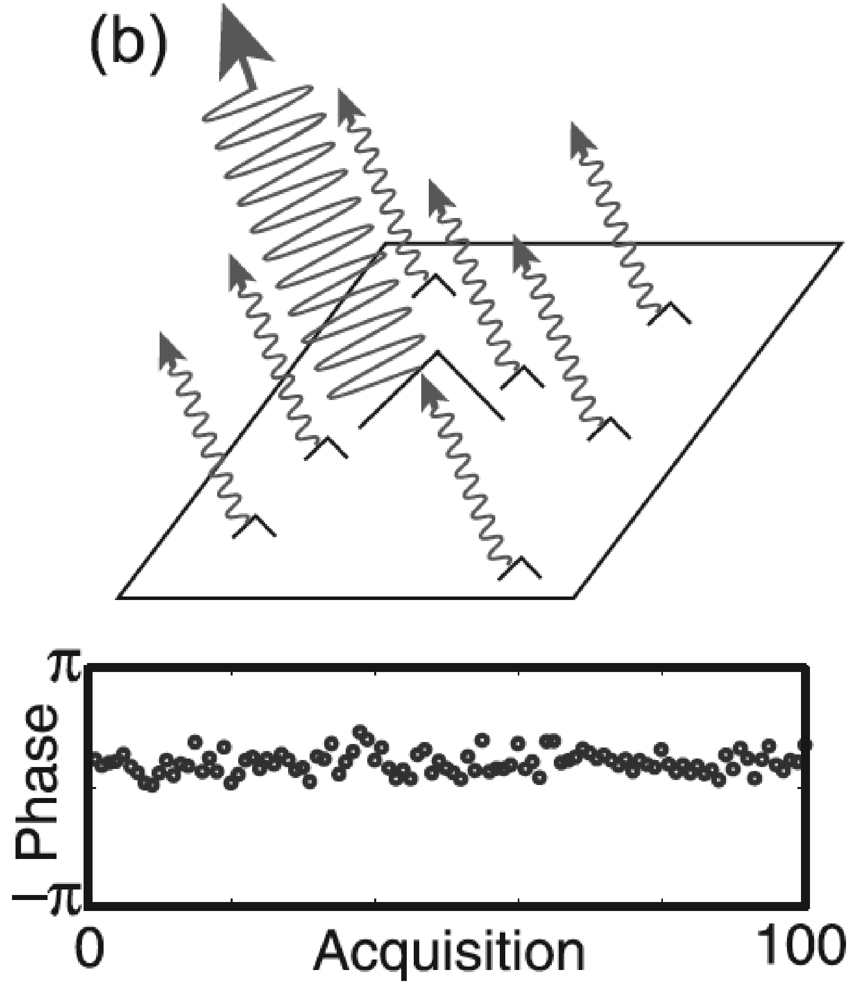

ns

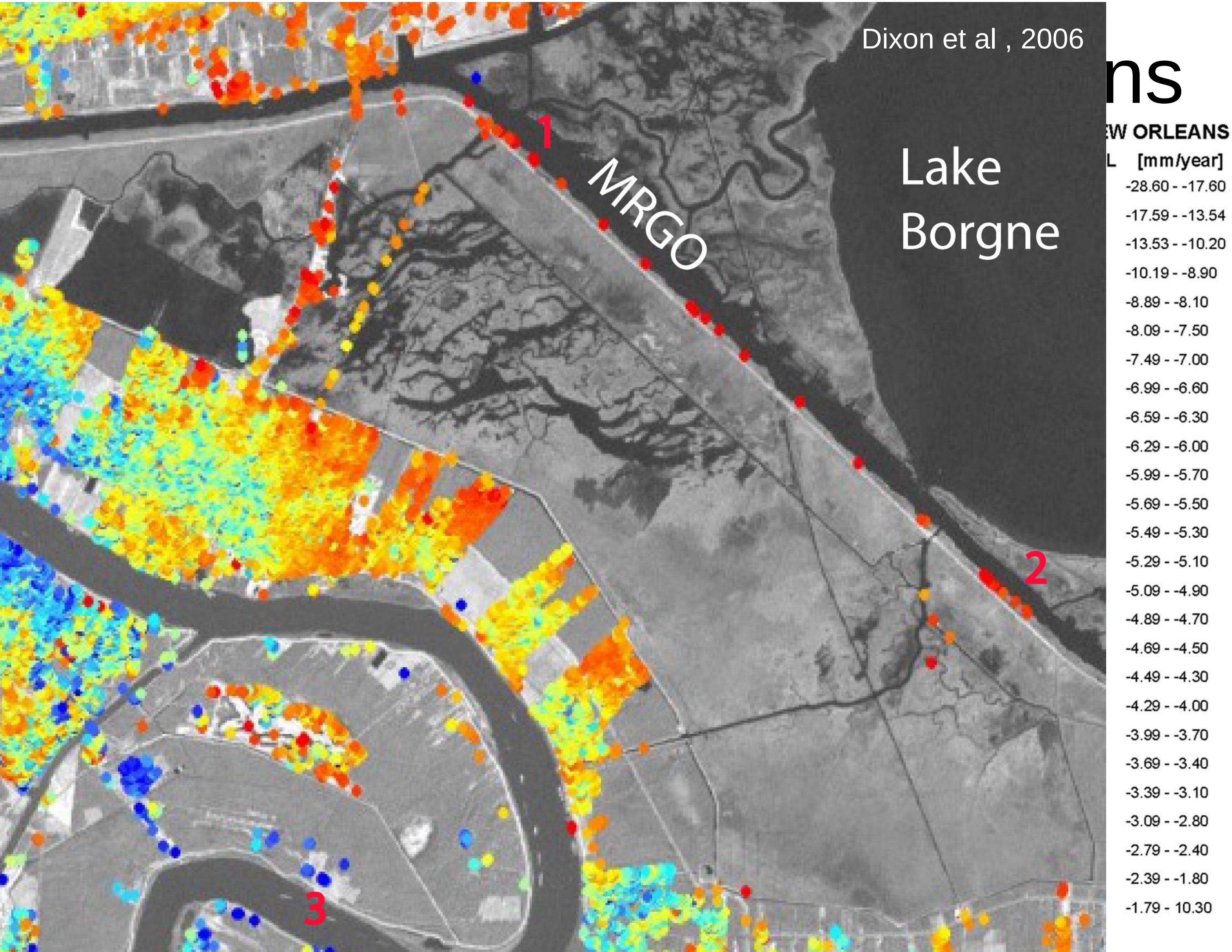

Dixon et al , 2006
1
MRGO
Lake
Borgne
2
3
W ORLEANS
L [mm/year]
-28.60 - -17.60
-17.59 - -13.54
-13.53 - -10.20
-10.19 - -8.90
-8.89 - -8.10
-8.09 - -7.50
-7.49 - -7.00
-6.99 - -6.60
-6.59 - -6.30
-6.29 - -6.00
-5.99 - -5.70
-5.69 - -5.50
-5.49 - -5.30
-5.29 - -5.10
-5.09 - -4.90
-4.89 - -4.70
-4.69 - -4.50
-4.49 - -4.30
-4.29 - -4.00
-3.99 - -3.70
-3.69 - -3.40
-3.39 - -3.10
-3.09 - -2.80
-2.79 - -2.40
-2.39 - -1.80
-1.79 - 10.30

STAMPS: Volcan Alcedo, Galapagos

Hooper et al, 2007

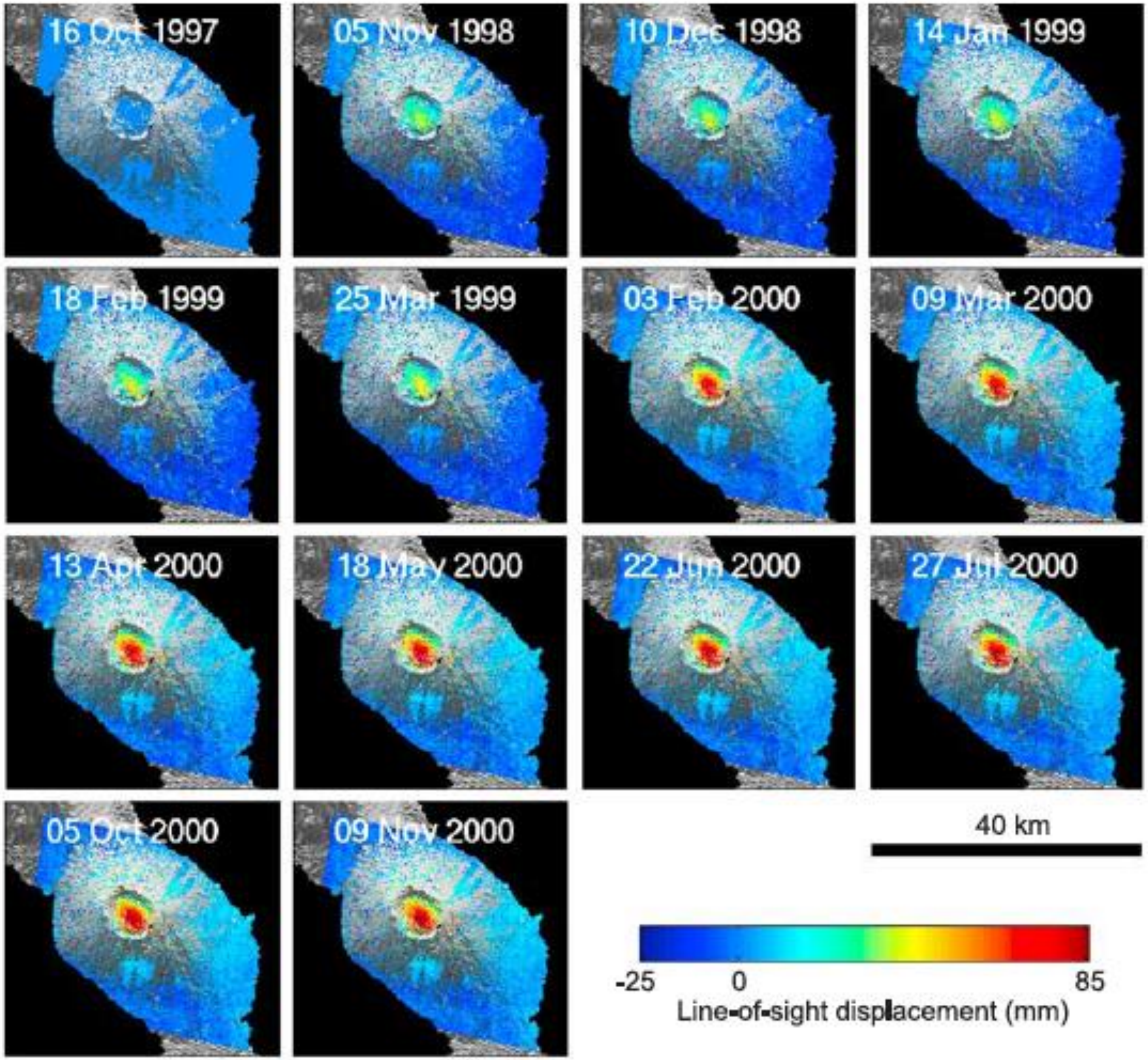

Error Budget (2)

Optimum determination of Linear Deformation Rates

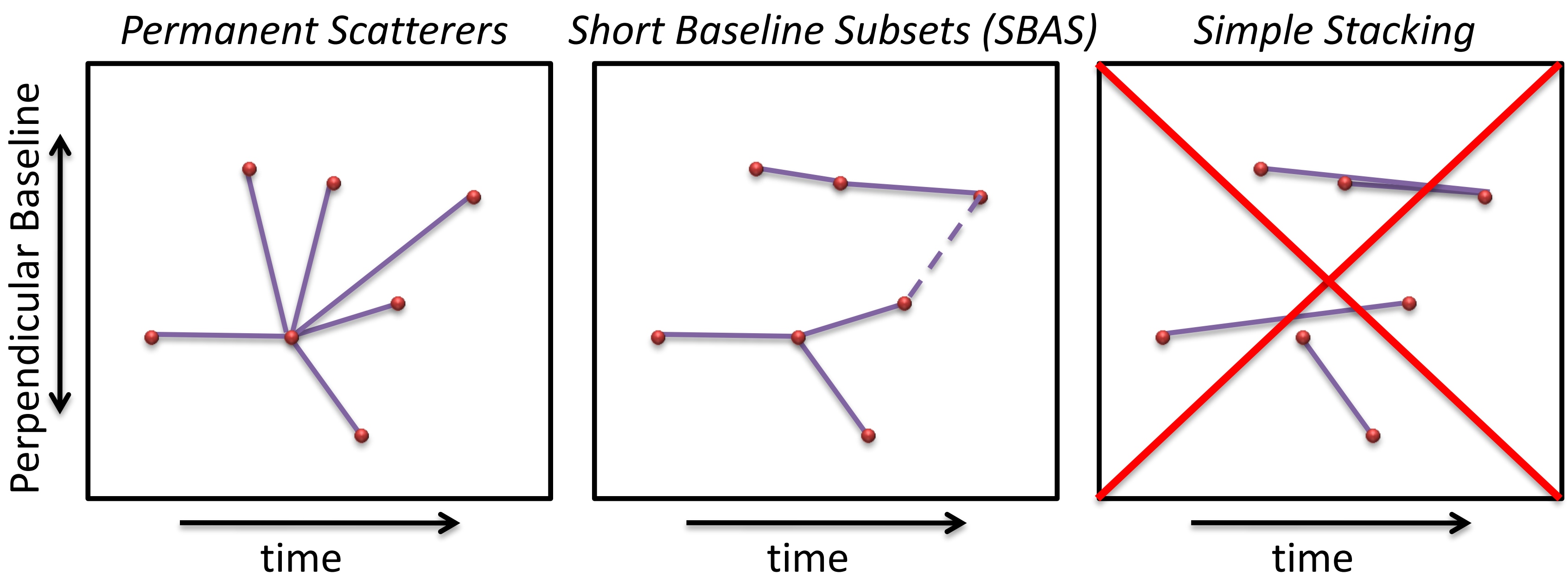

For the determination of linear deformation rates, optimum errors are determined through a connected network, since noise terms are associated with individual acquisitions not interferograms.

Error Budget (2)

Optimum determination of Linear Deformation Rates

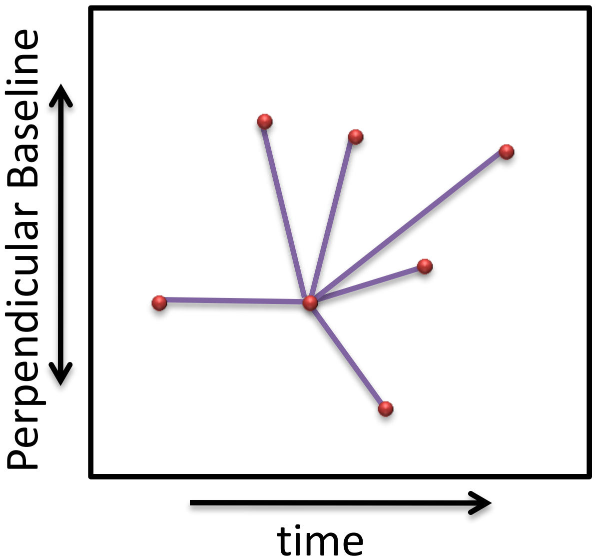

- Error on linear rate is independent of how network is connected (but of course short-baseline, short-time interferograms are best).

Error Budget (2)

Optimum determination of Linear Deformation Rates

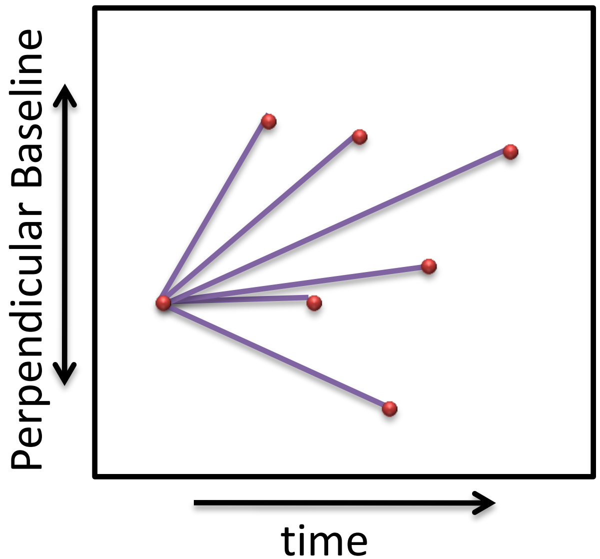

• Error on linear rate is independent of how network is connected (but of course short-baseline, short-time interferograms are best).

• To simplify mathematics, assume all connections to date d1...

Error Budget (2)

Optimum determination of Linear Deformation Rates

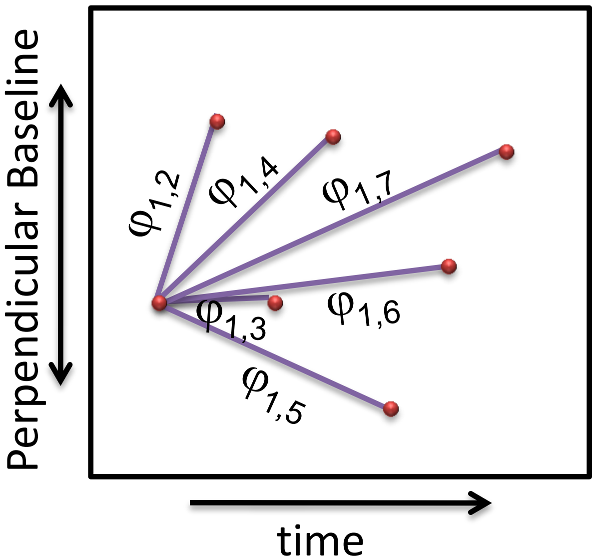

- Error on linear rate is independent of how network is connected (but of course short-baseline, short-time interferograms are best).
- To simplify mathematics, assume all connections to date d1...

...and regular acquisition spacing, t_m

Error Budget (2)

Optimum determination of Linear Deformation Rates

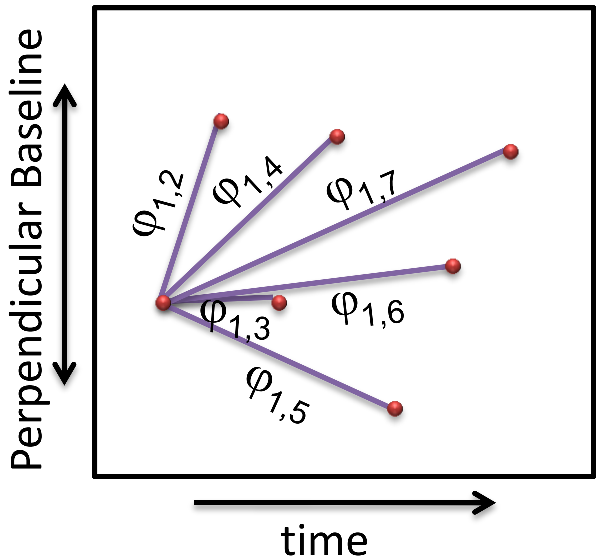

- Error on linear rate is independent of how network is connected (but of course short-baseline, short-time interferograms are best).
- To simplify mathematics, assume all connections to date d1...

...and regular acquisition spacing, t_r

- We can determine the best-fit linear rate of phase change due to deformation, $\frac{d\varphi}{dt}$, using weighted least squares:

$$\mathbf{\Sigma_P^{-1}T}\frac{d\varphi}{dt} = \mathbf{\Sigma_P^{-1}P}$$

where **T** = $[t_r, 2t_r, \ldots Nt_r]^T$, **P** = $[\varphi_{1,2}, \varphi_{1,3}, \ldots \varphi_{1,N}]^T$, and $\mathbf{\Sigma_P^{-1}}$ is the inverse of the variance-covariance matrix for the range change observations, **P**.

Error Budget (2)

Optimum determination of Linear Deformation Rates

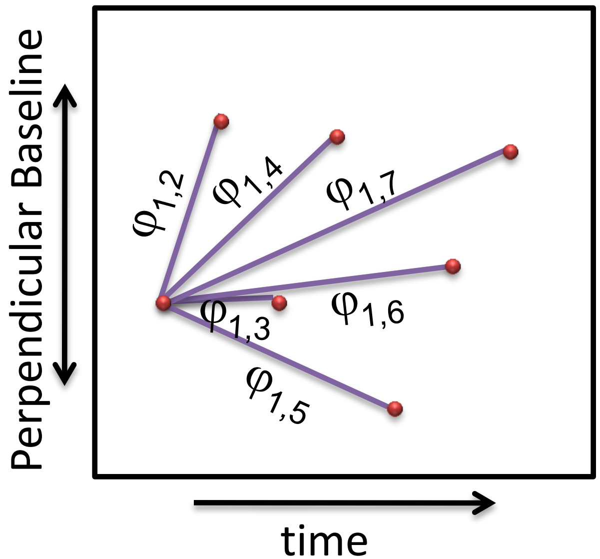

- Using the correct VCM, $\mathbf{\Sigma_P}$, is essential.
- In this particular network, all interferograms share a common acquisition (epoch 1).

⇨ Cov $(\varphi_{1,i} , \varphi_{1,j}) = \sigma_1^2$ (the variance on epoch 1)

and Var $(\varphi_{1,i}) = \sigma_1^2 + \sigma_i^2$

$= 2\sigma^2$ (assuming noise is identical on all epochs)

Error Budget (2)

Optimum determination of Linear Deformation Rates

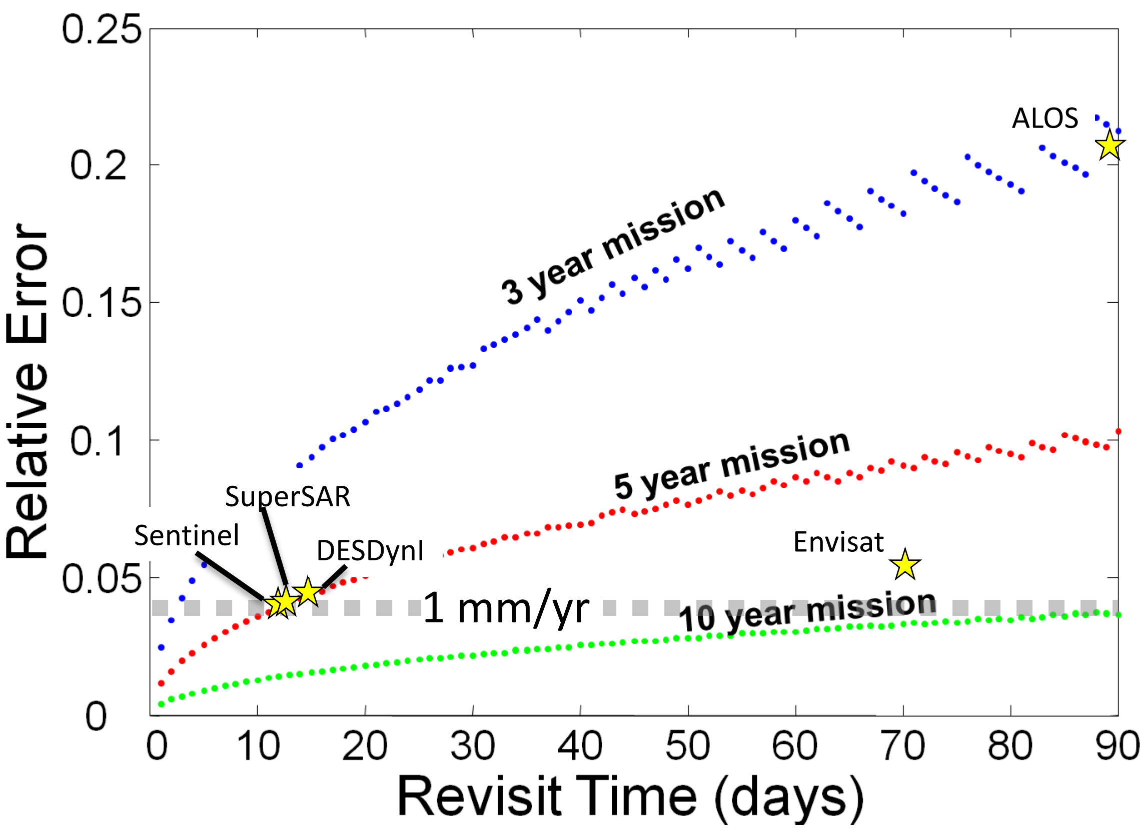

Error ∝ (*revisit time*)$^{0.5}$

∝ (*mission length*)$^{-1.5}$

i.e.

- For a **fixed length mission**, cut revisit time by 4 to halve the linear rate error.
- For a **fixed revisit time**, increase mission length by ~60% to halve the linear rate error.

Error Budget (2)

Optimum determination of Linear Deformation Rates

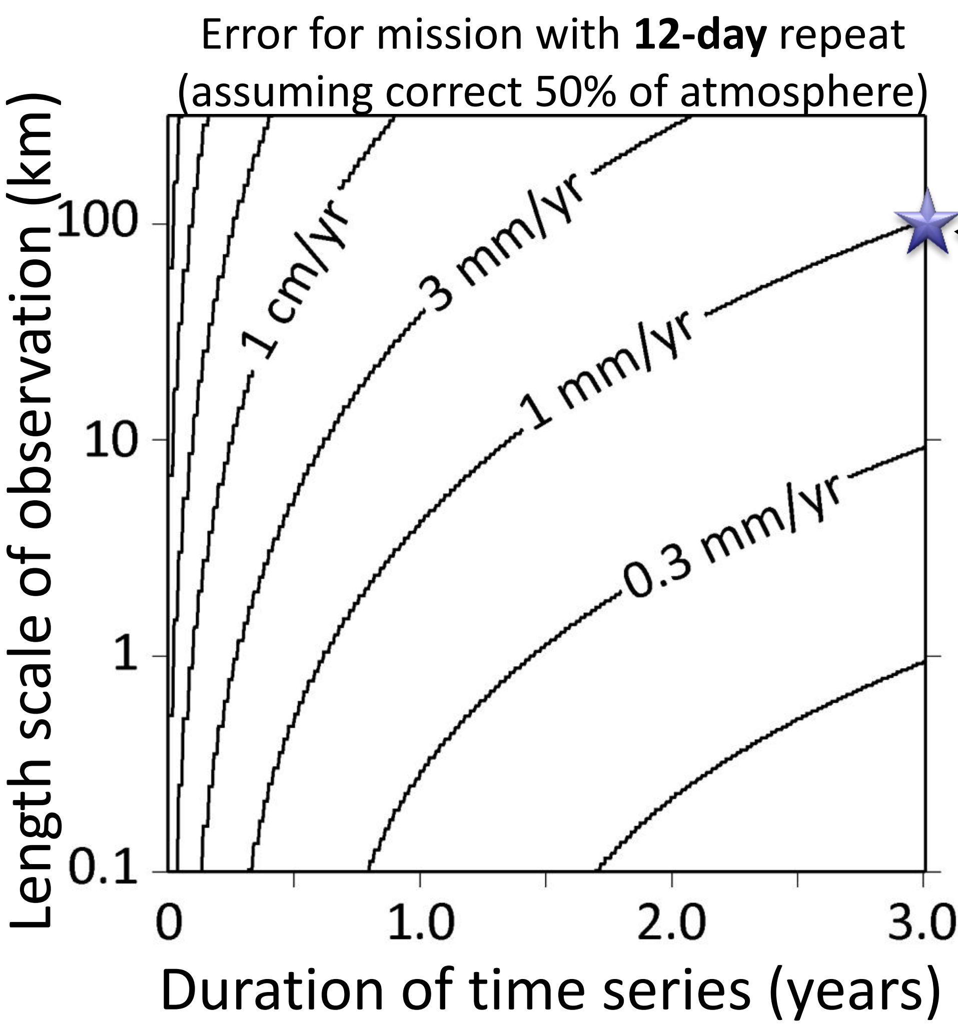

Reaching the target precision is tough!

Everything so far has been for Line-of-sight deformation

Combining Viewing Geometries

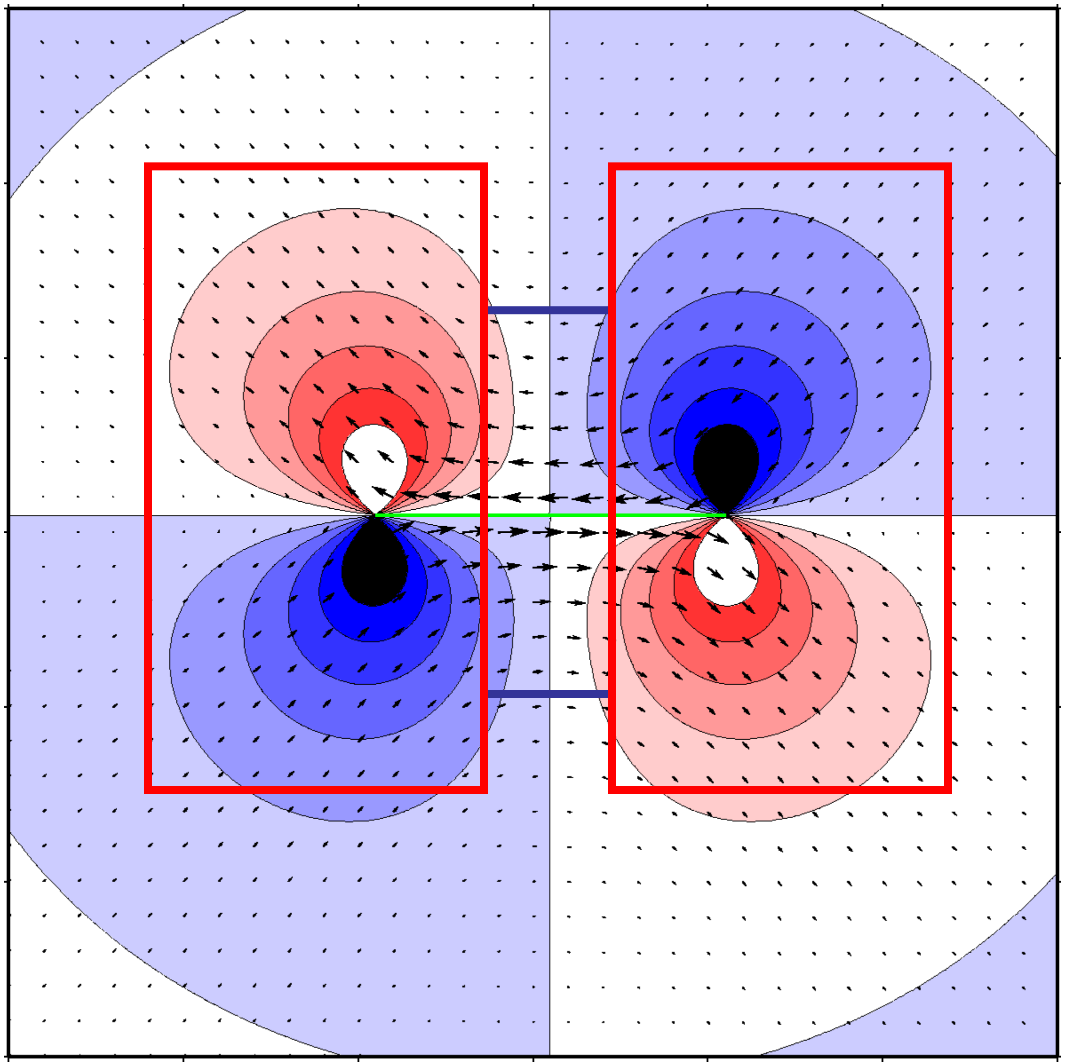

Surface Displacements of Strike Slip Faults

Combining Viewing Geometries

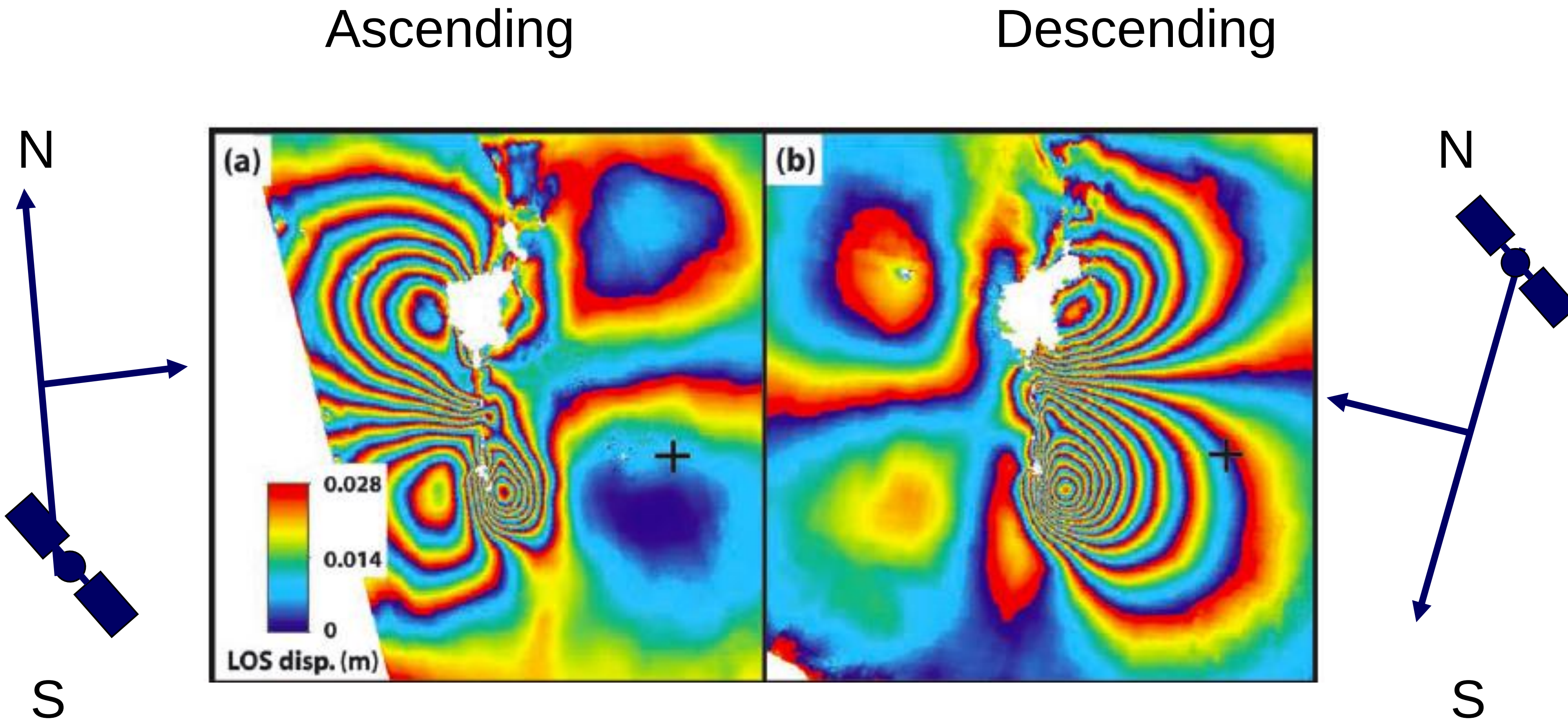

Bam, Earthquake, Iran, 2003. (Funning et al, 2006)

Combining Viewing Geometries

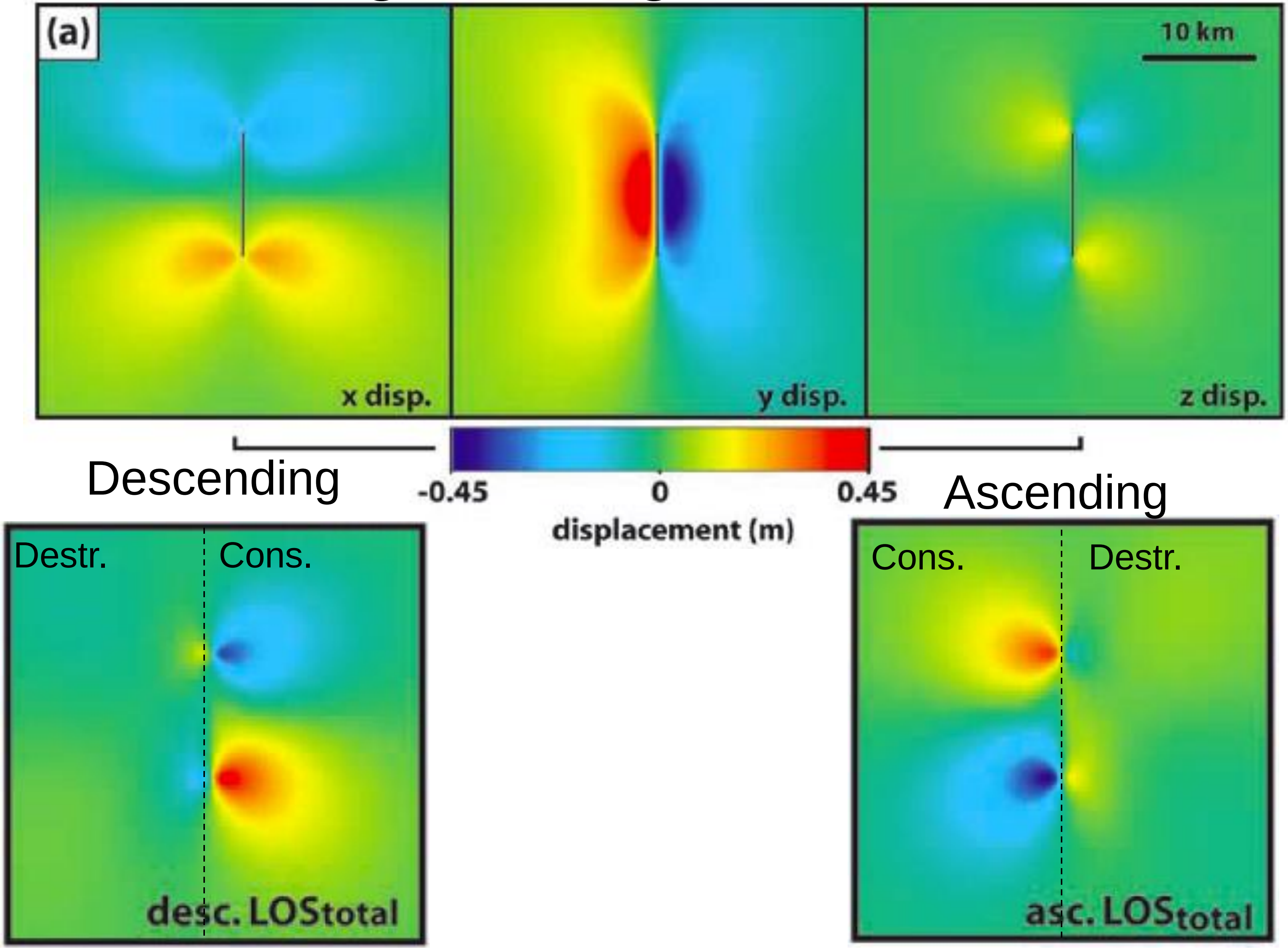

Azimuth offsets

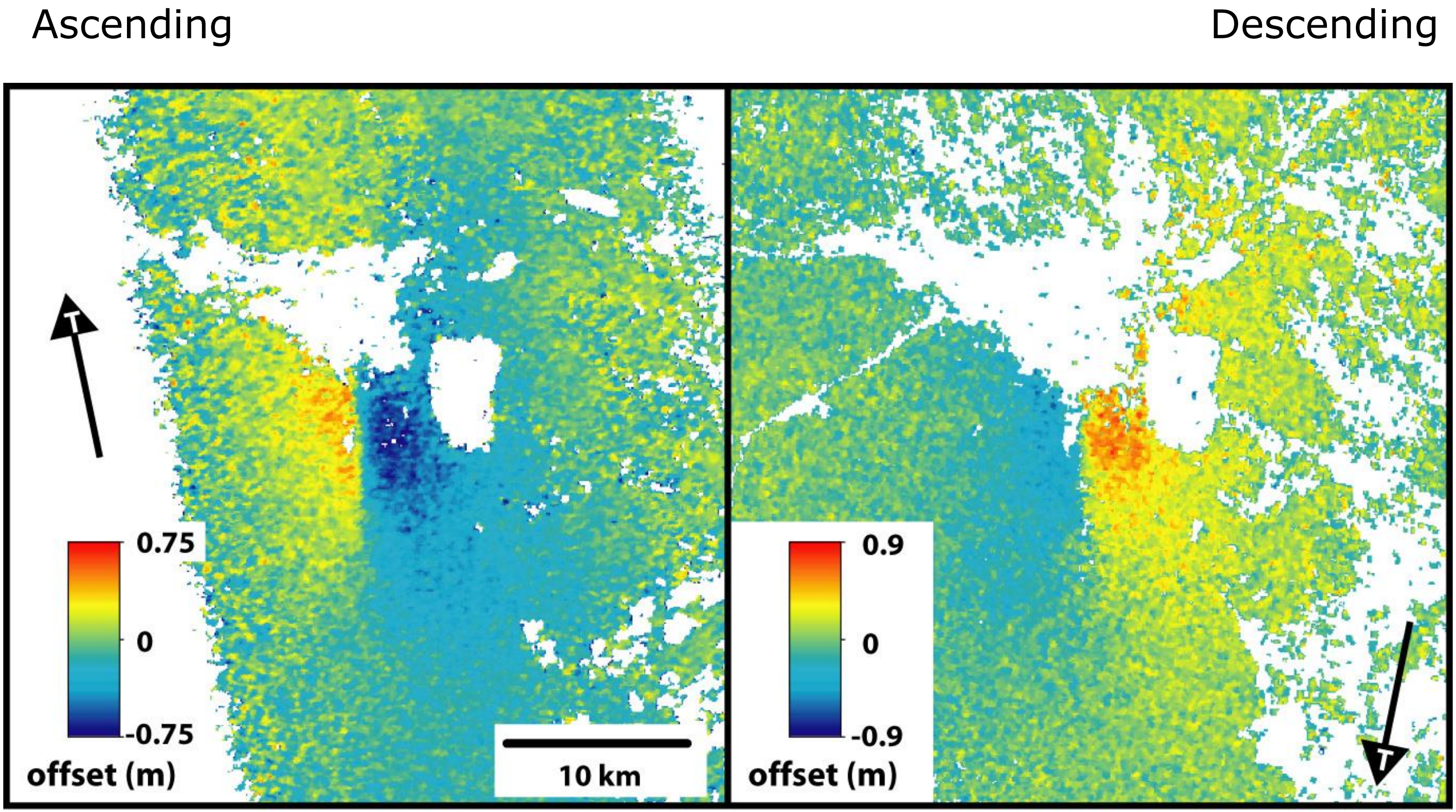

MAI: Split Beam Processing

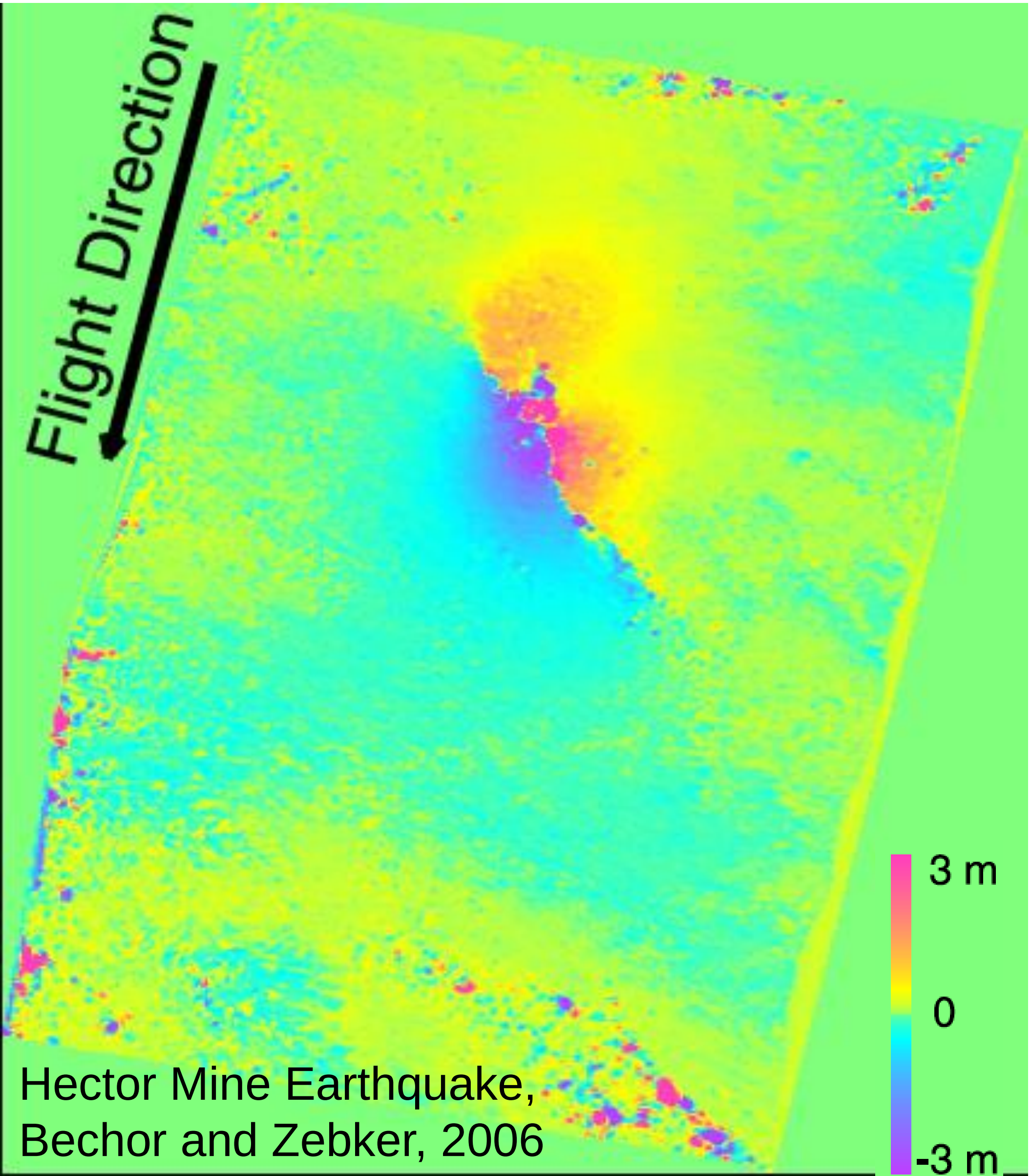

Hector Mine Earthquake,
Bechor and Zebker, 2006

Split beam into forward- and backward- looking sections to measure displacement in flight direction.

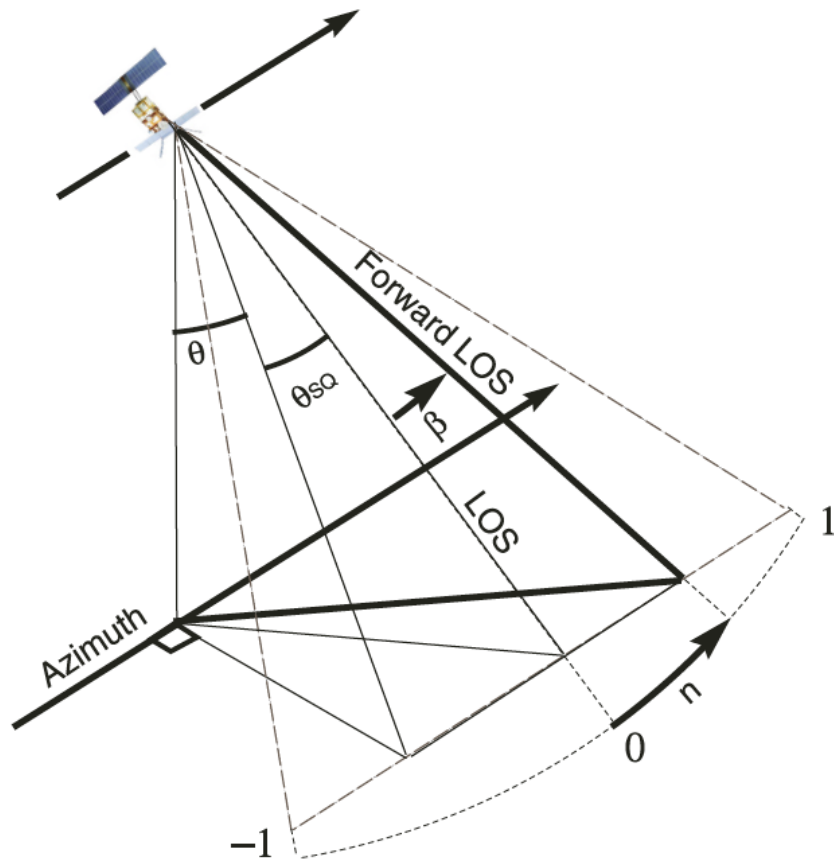

Accuracy depends on coherence and SNR.
Up to 3 cm.

Determining 3D displacements

If the 3D displacement at a pixel is given by $\mathbf{u} = [u_x, u_y, u_z]$, then…

Ascending interferogram, $d_1 = \mathbf{los_A} \bullet \mathbf{u}$

Descending interferogram, $d_2 = \mathbf{los_D} \bullet \mathbf{u}$

Ascending az. offsets, $d_3 = \mathbf{los_{AO}} \bullet \mathbf{u}$

Descending az. offsets, $d_4 = \mathbf{los_{DO}} \bullet \mathbf{u}$

Which can be rewritten as a matrix equation, $\mathbf{d} = \mathbf{Lu}$**,** and solved for $\mathbf{u}$.

See e.g. Wright, T.J, B. Parsons, Z. Lu., Geophys Res. Lett. 30(18), p.1974, 2003

Bam earthquake 3D displacements

East North Up

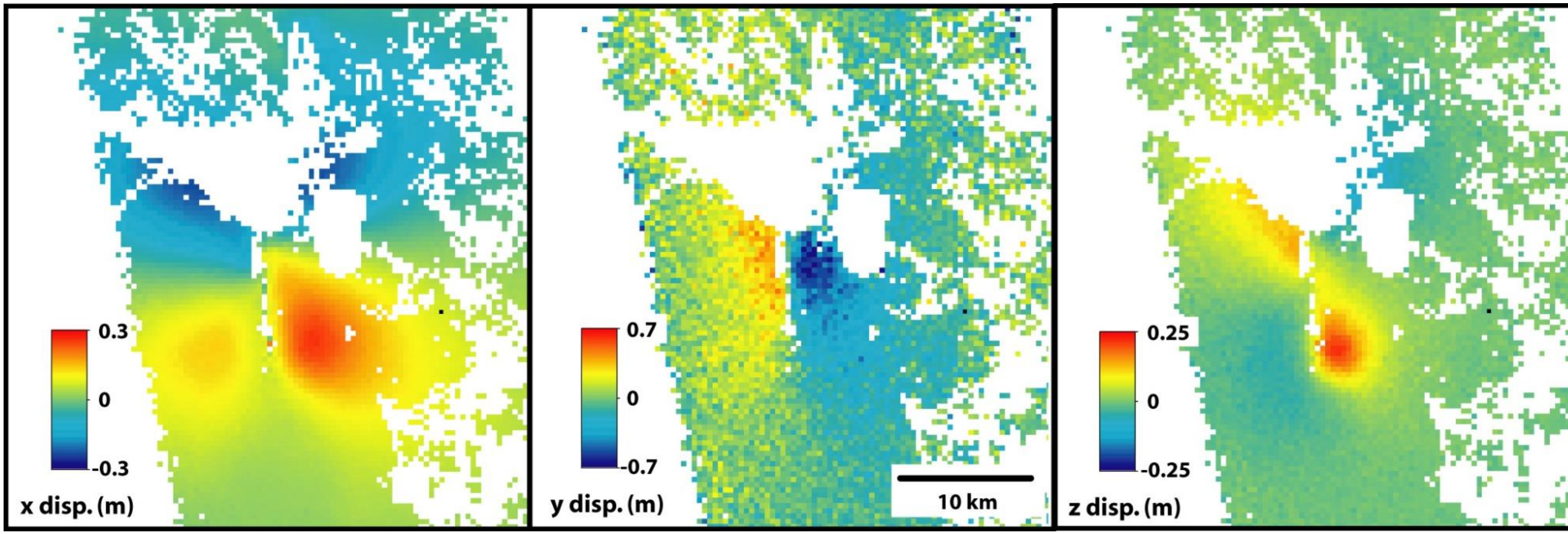

$\sigma = 0.01$ m $\sigma = 0.09$ m $\sigma = 0.01$ m

Combining Viewing Geometries

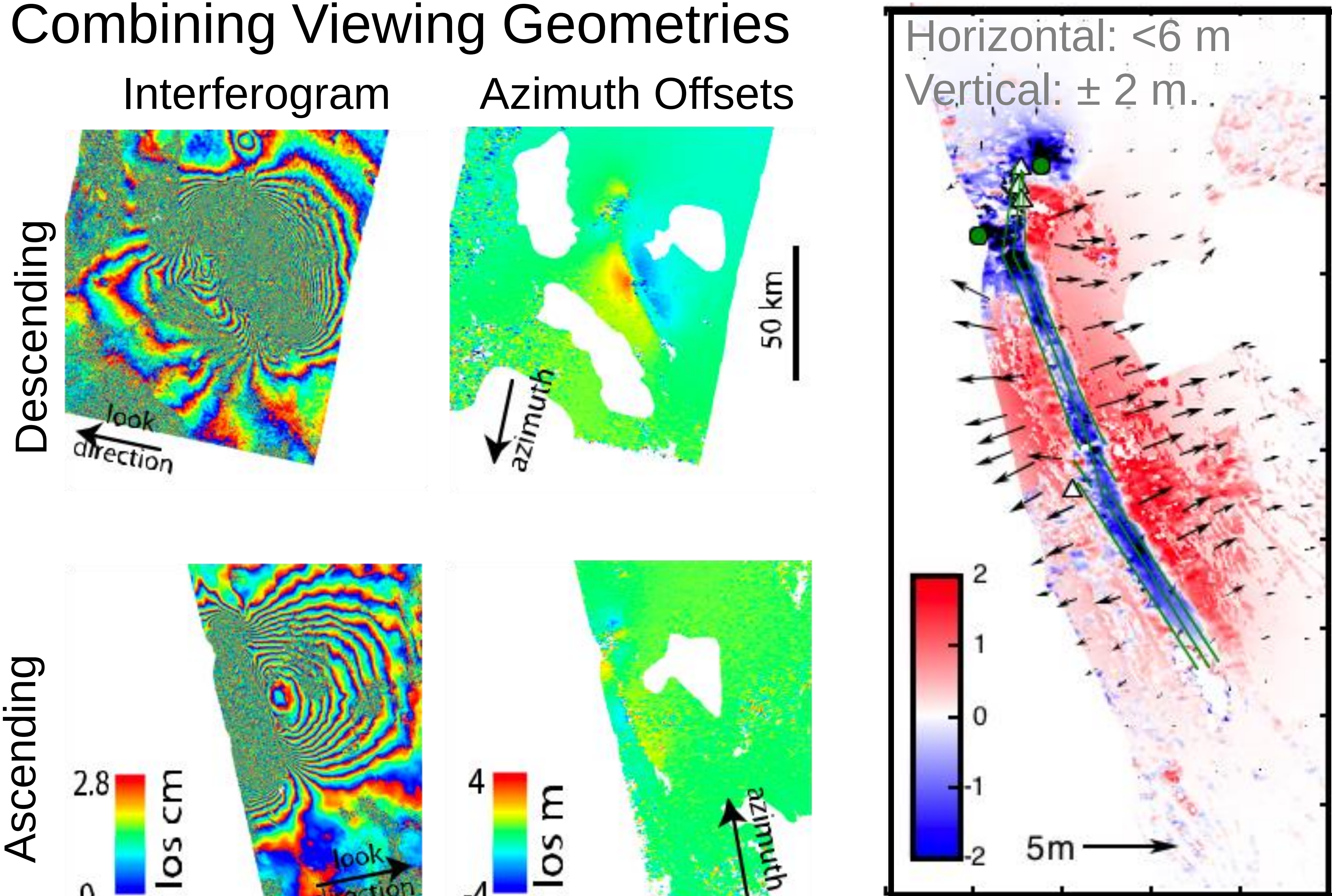

Afar Rift, Wright et al, Nature 2006

Tibet Case Study

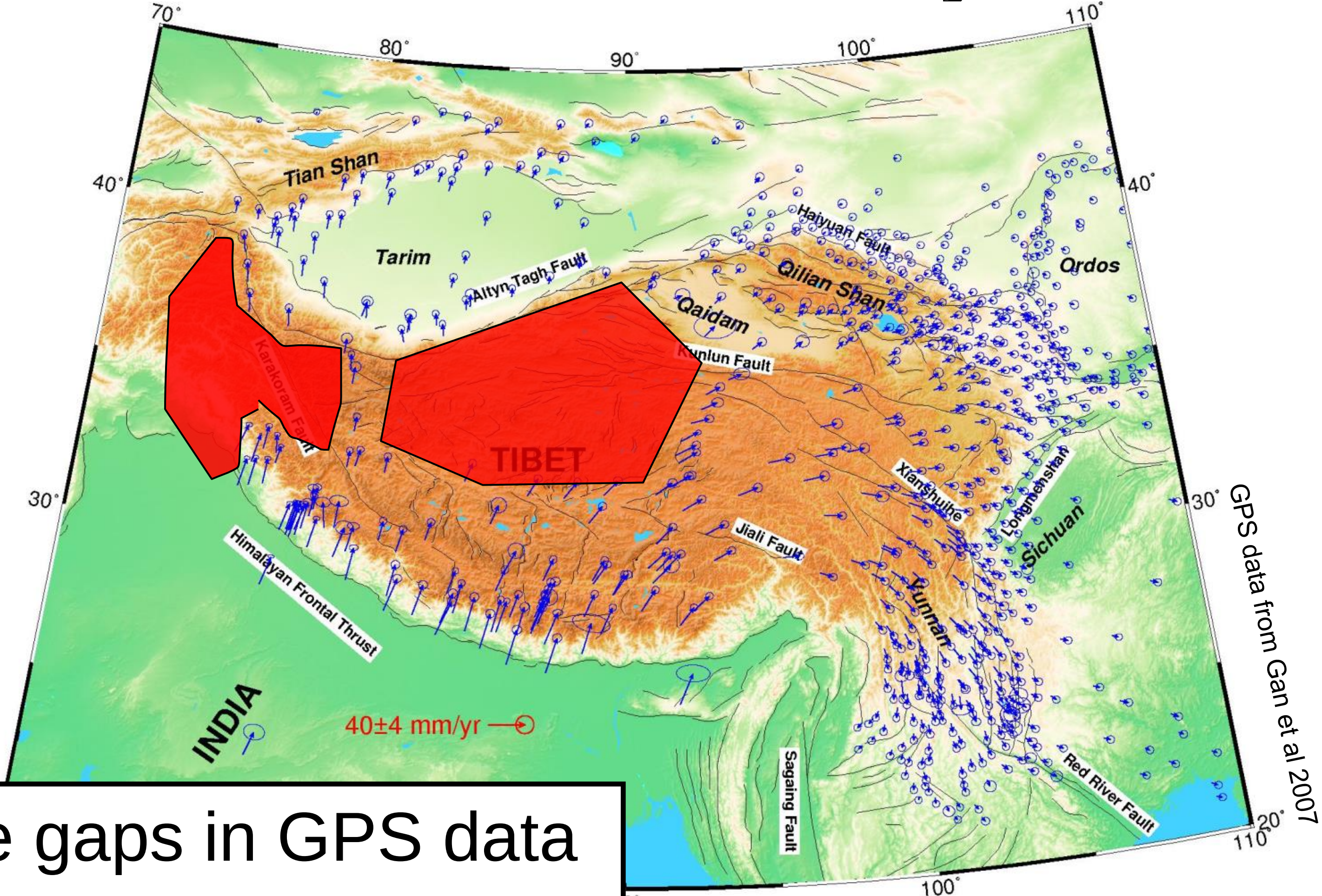

- Large gaps in GPS data
- Station spacing > 50 km

Tibet Case Study

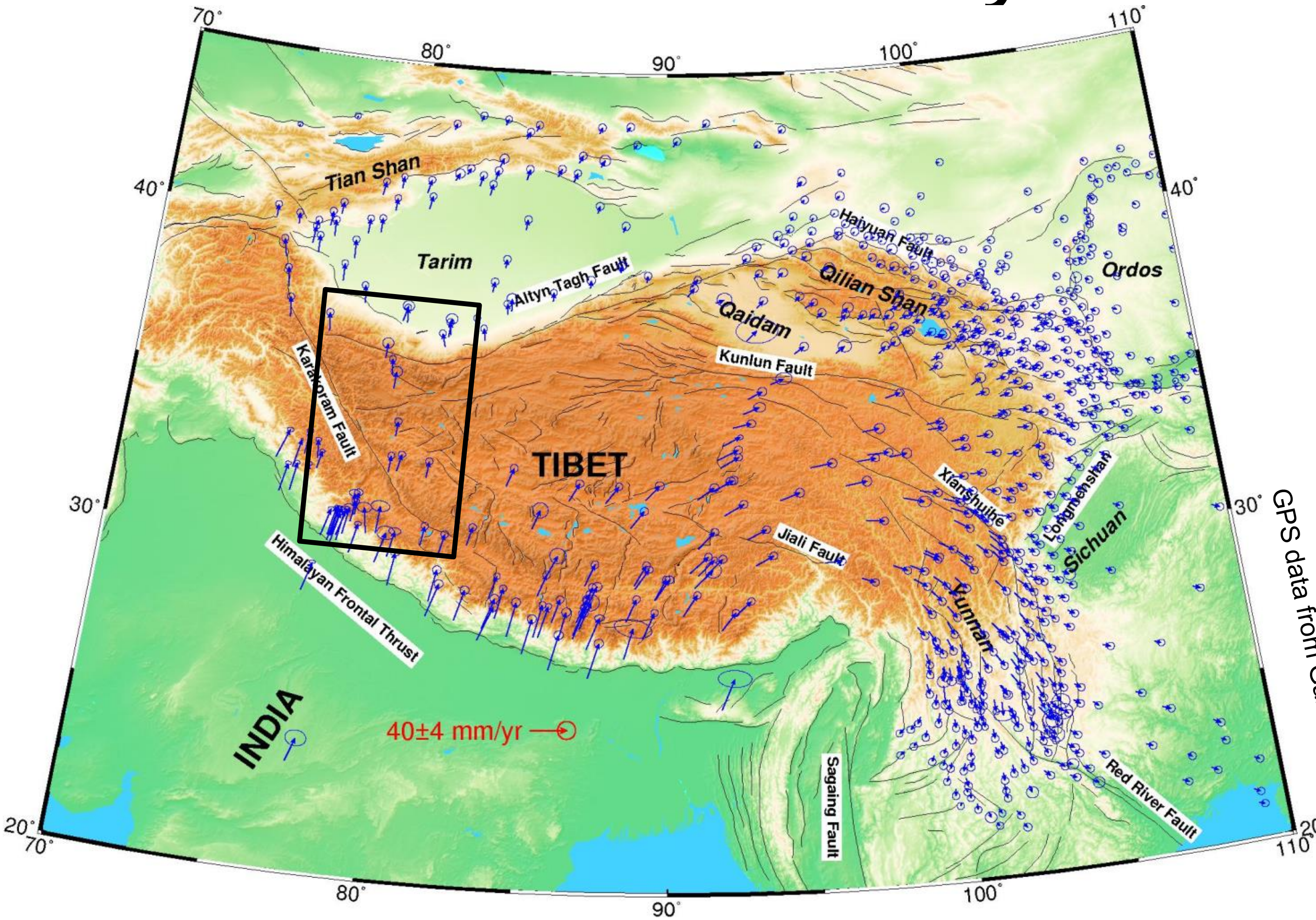

GPS data from Gan et al 2007

Tibet Case Study

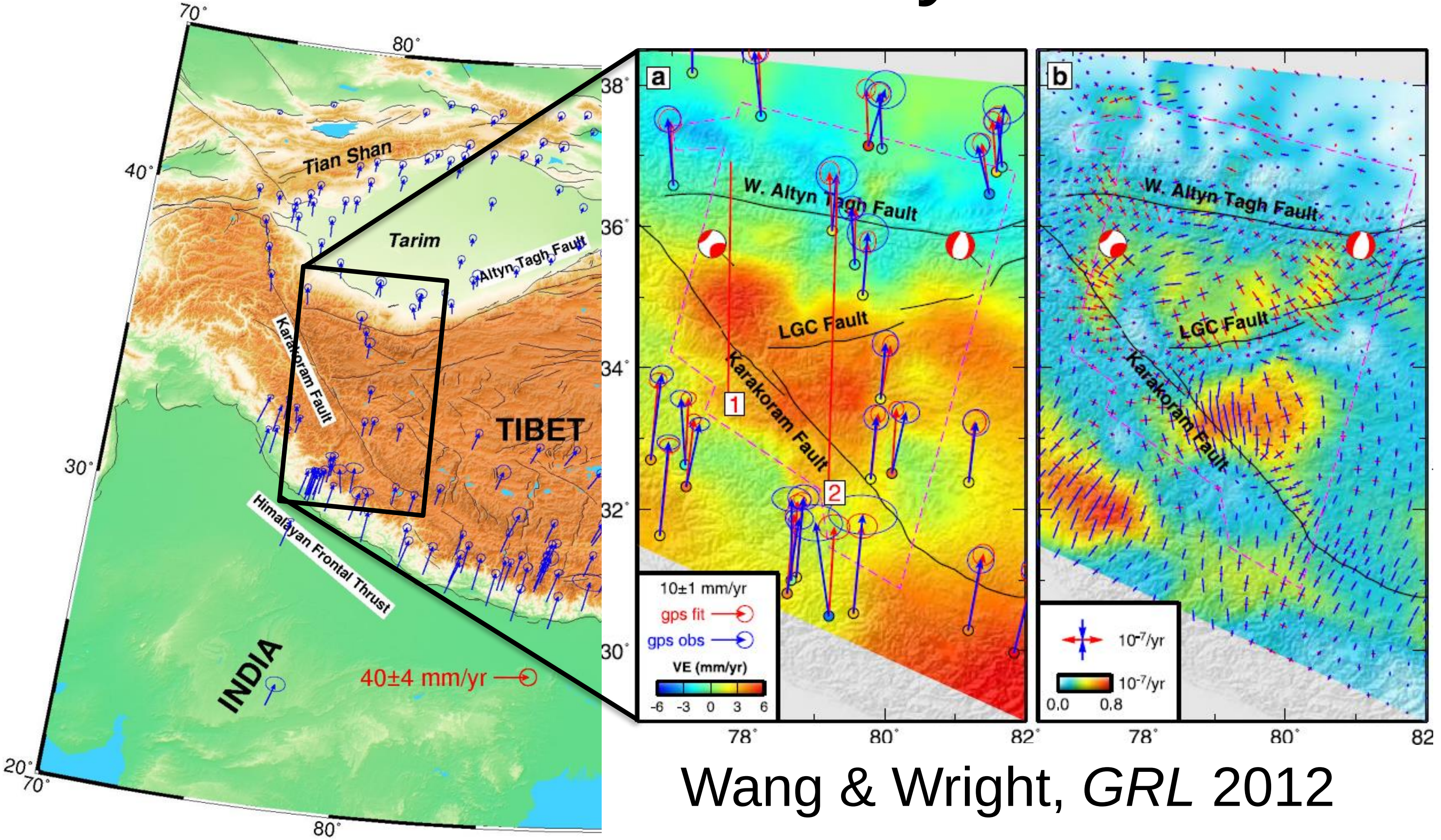

Wang & Wright, *GRL* 2012

InSAR Rate Maps from PI-RATE

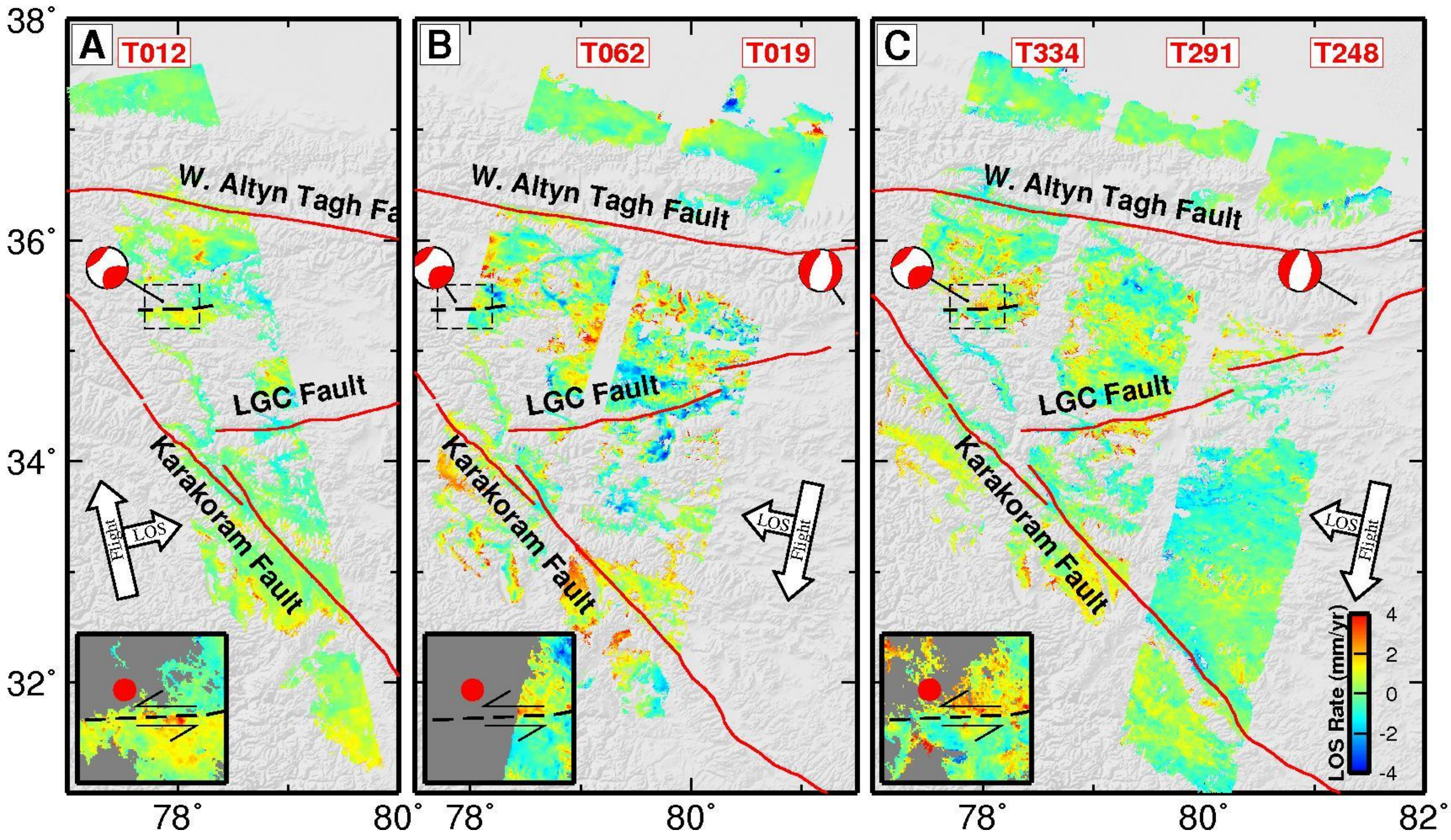

RATE MAP = DEFORM + ORB + ATM + NOISE

InSAR Error Maps from PI-RATE

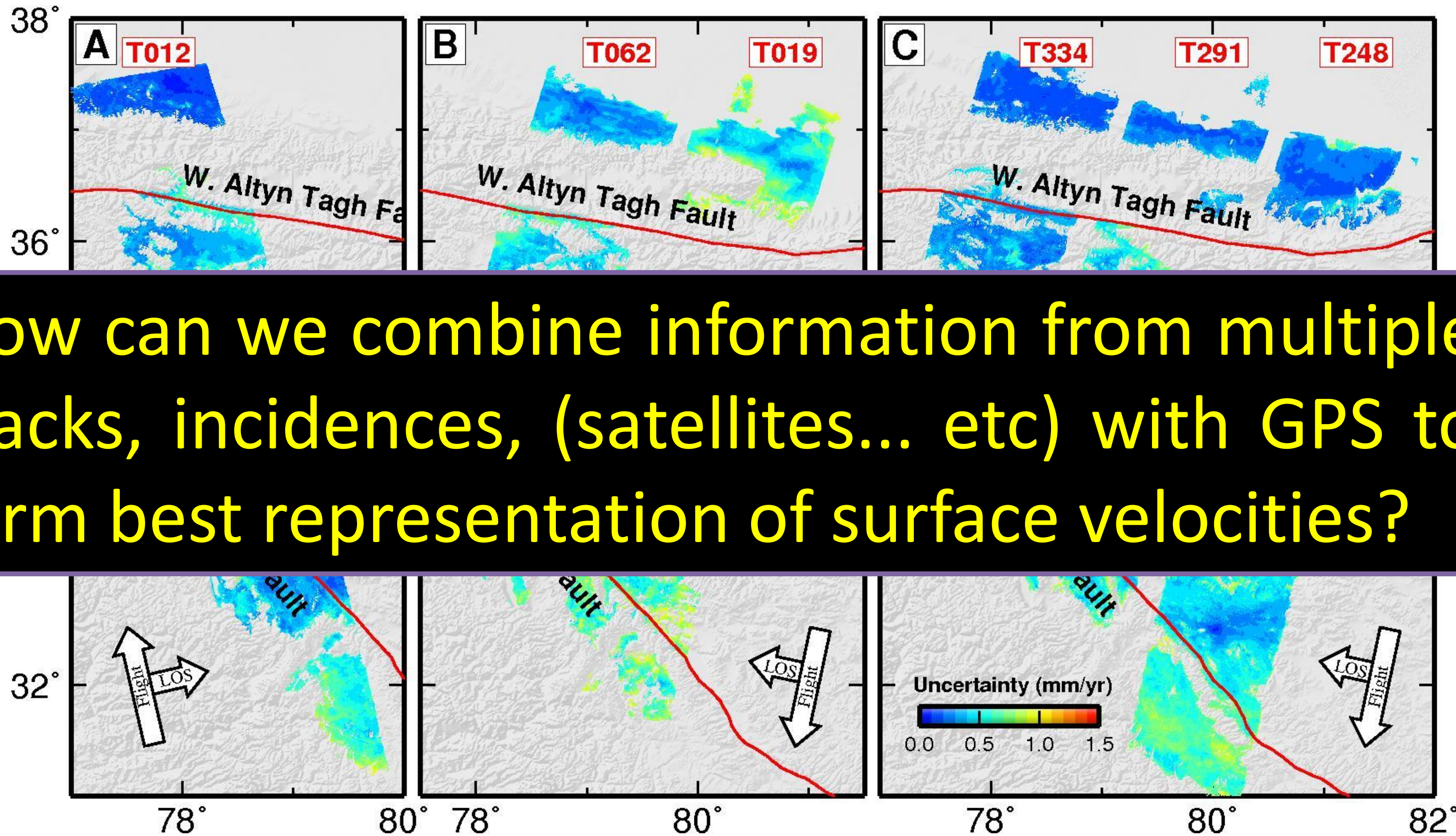

How can we combine information from multiple tracks, incidences, (satellites... etc) with GPS to form best representation of surface velocities?

Velocity Field Method

e.g. England and Molnar, JGR 2005

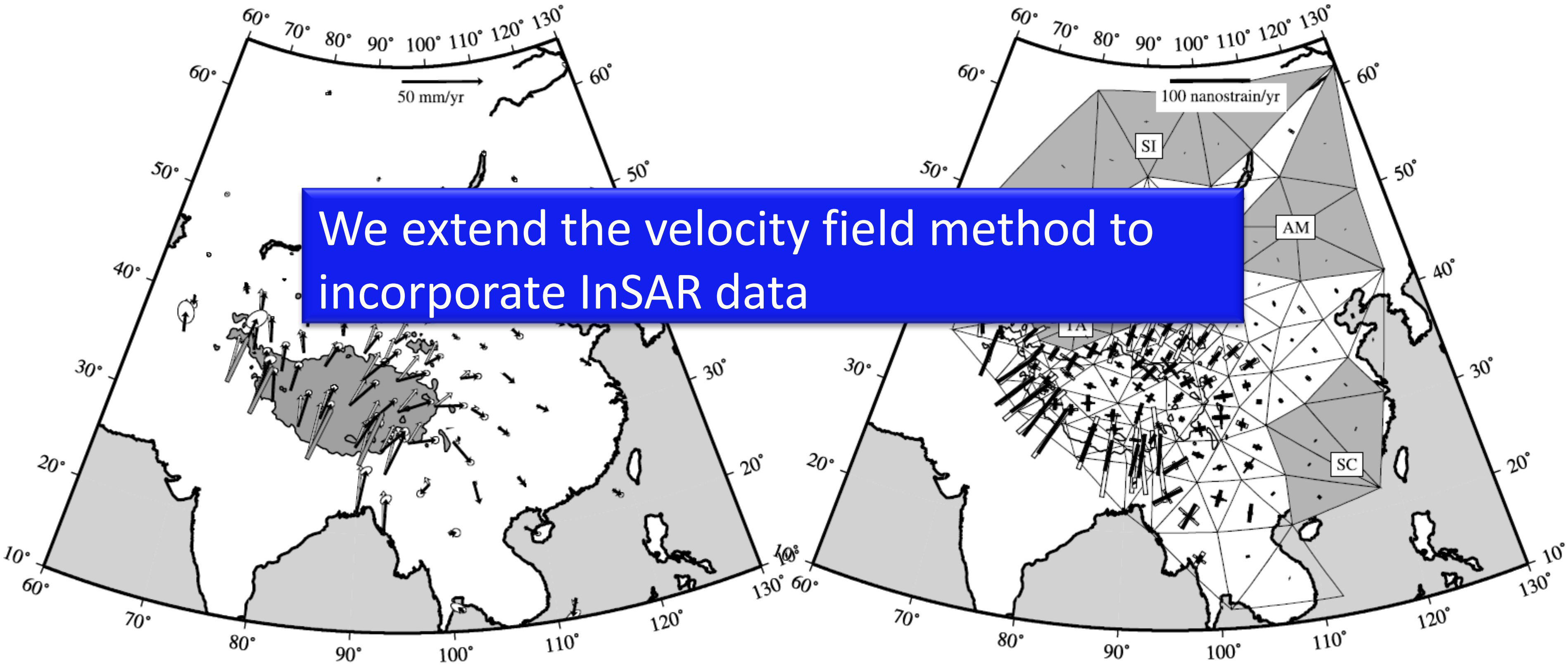

We extend the velocity field method to incorporate InSAR data

Velocities (left) and strain (right) from GPS, quaternary fault data and earthquake focal mechanisms

Velocity Field Method: Mesh and Interpolation

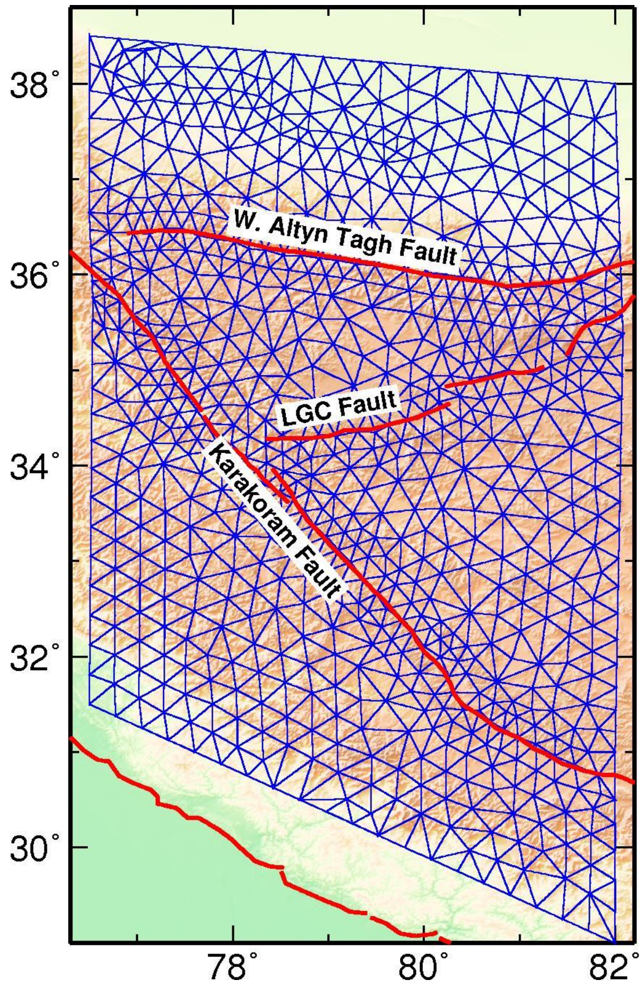

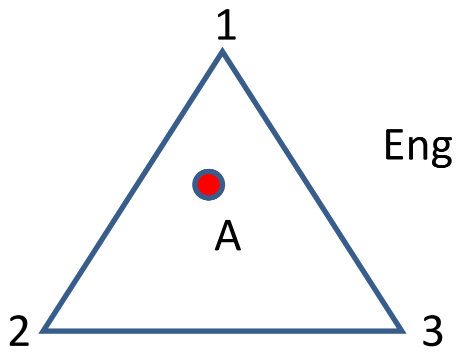

England & Molnar, 2005, JGR

[24] We divide the surface of the region of interest into spherical triangles and assume that within each triangle, the velocity varies linearly with latitude and longitude across the triangle. We may express the velocity in the interior of the triangle in terms of the velocities of its vertices:

$$\mathbf{U} = \sum_{m=1}^{3} N_m \mathbf{u}_m, \tag{5}$$

where $\mathbf{u}_m$ is the velocity of vertex m and N_m are interpolation functions:

$$N_i = a_i + b_i\phi + c_i\theta, \tag{6}$$

where ϕ is longitude and θ is latitude.

Wang and Wright, GRL 2012

Velocity Field Method: LS Solutions

$$\begin{bmatrix} \mathbf{G}_{sar} & \mathbf{G}_{orb} & \mathbf{G}_{atm} \\ \mathbf{G}_{gps} & \mathbf{0} & \mathbf{0} \\ \kappa^2 \nabla^2 & \mathbf{0} & \mathbf{0} \end{bmatrix} \begin{bmatrix} \mathbf{M}_{vel} \\ \mathbf{M}_{orb} \\ \mathbf{M}_{atm} \end{bmatrix} = \begin{bmatrix} \mathbf{d}_{sar} \\ \mathbf{d}_{gps} \\ \mathbf{0} \end{bmatrix}$$

Weighted LS solution:

$$\hat{\mathbf{M}} = (\mathbf{G}^{\mathrm{T}}\mathbf{W}\mathbf{G})^{-1}\mathbf{G}^{\mathrm{T}}\mathbf{W}\mathbf{d}$$

Weighting by full data covariances

Wang and Wright, GRL 2012

Velocity Field: From Vertices to Continuous

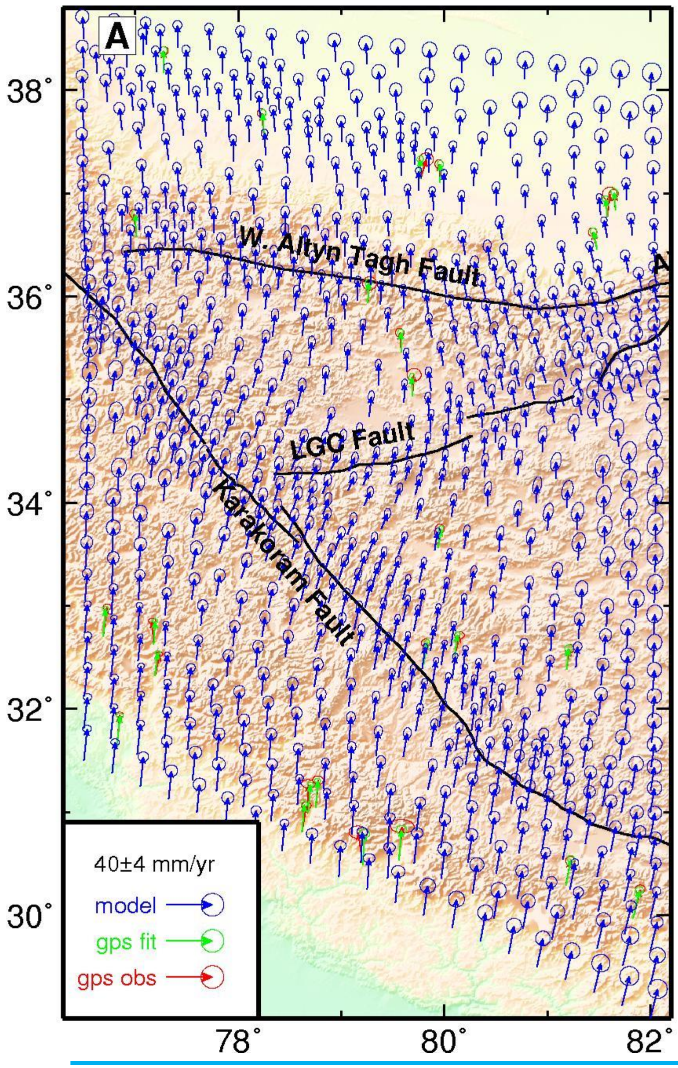

Wang and Wright, GRL 2012

Laplacian Smoothing: Over-smoothed

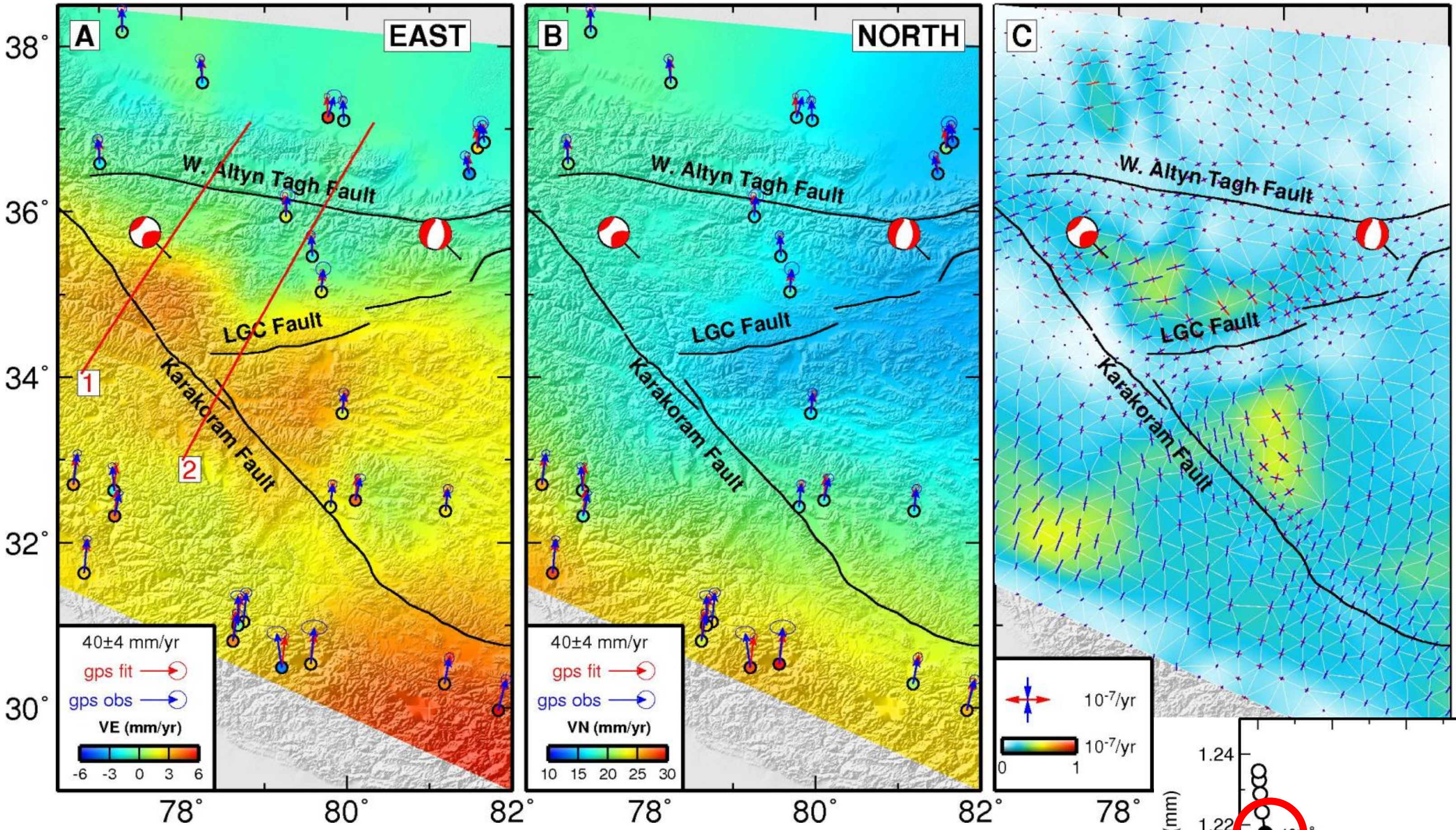

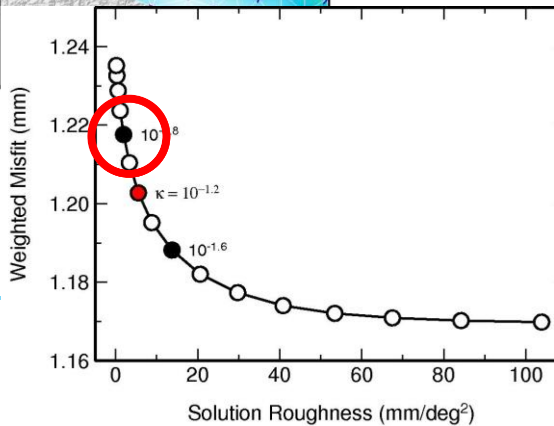

Wang and Wright, GRL 2012

Laplacian Smoothing: Little-smoothed

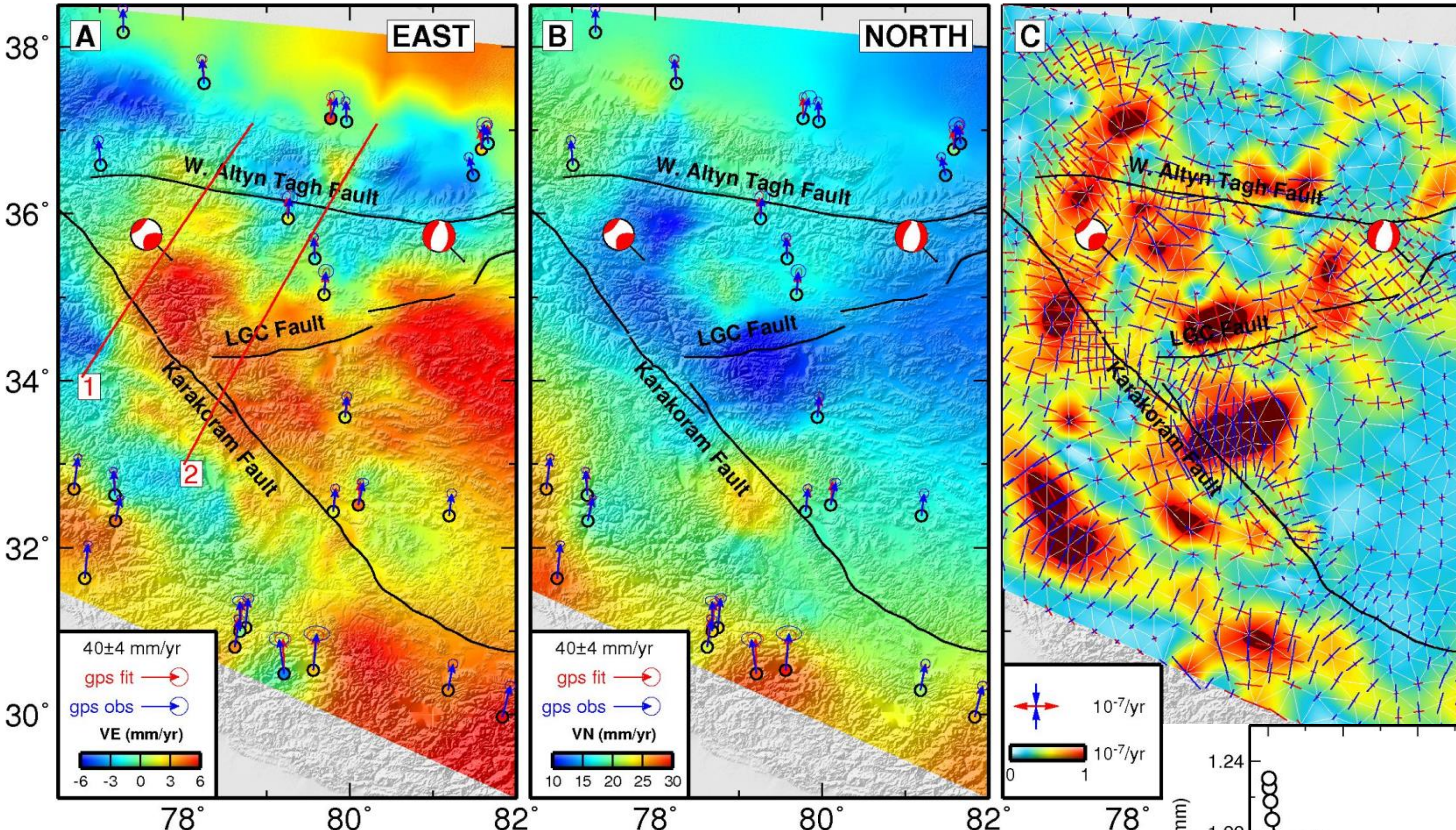

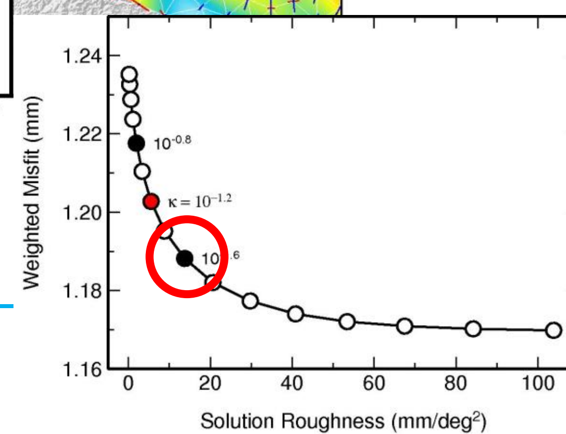

Wang and Wright, GRL 2012

Laplacian Smoothing: Best Solution

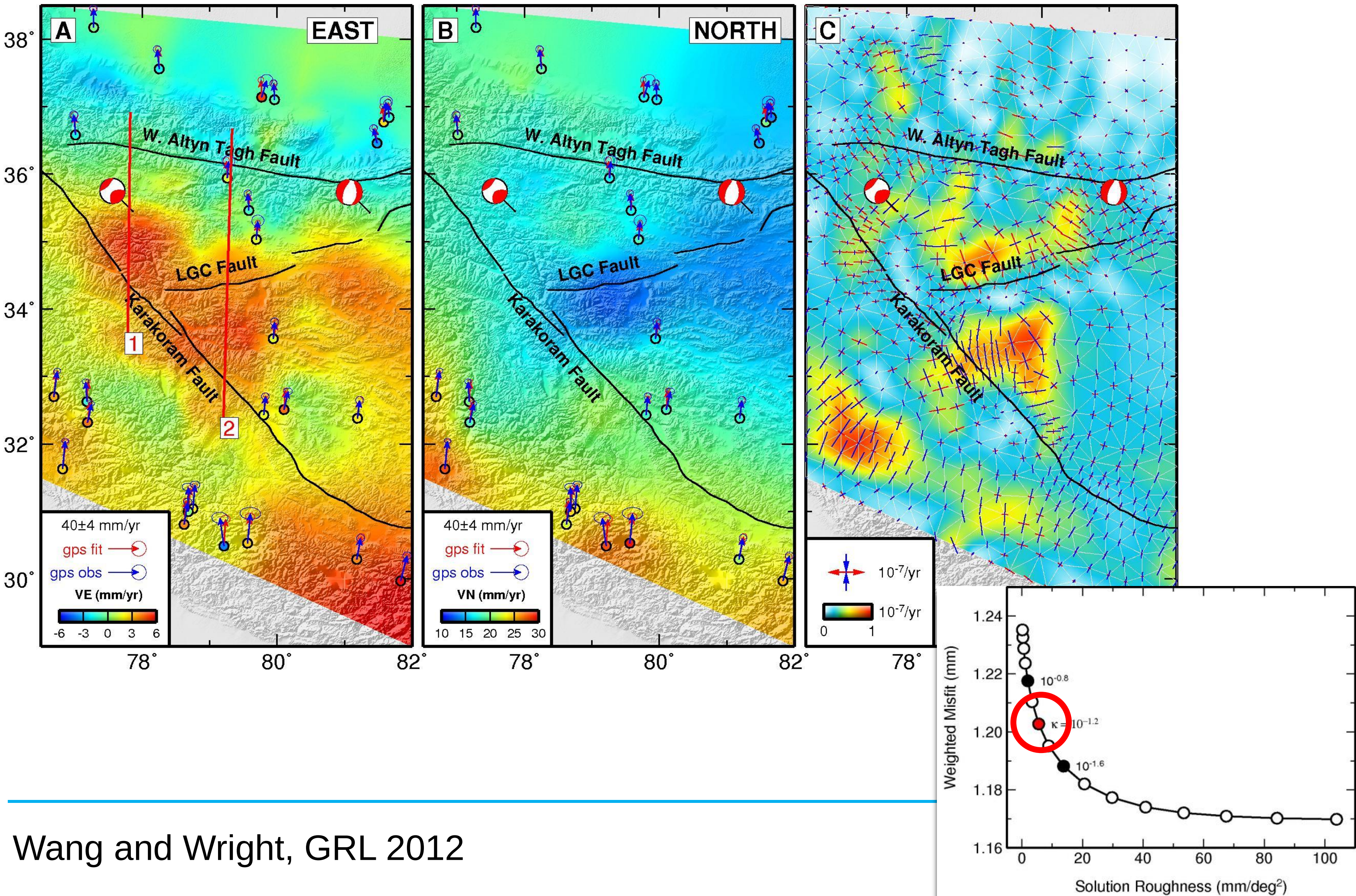

Wang and Wright, GRL 2012

Velocity & Strain Rate Field from GPS only

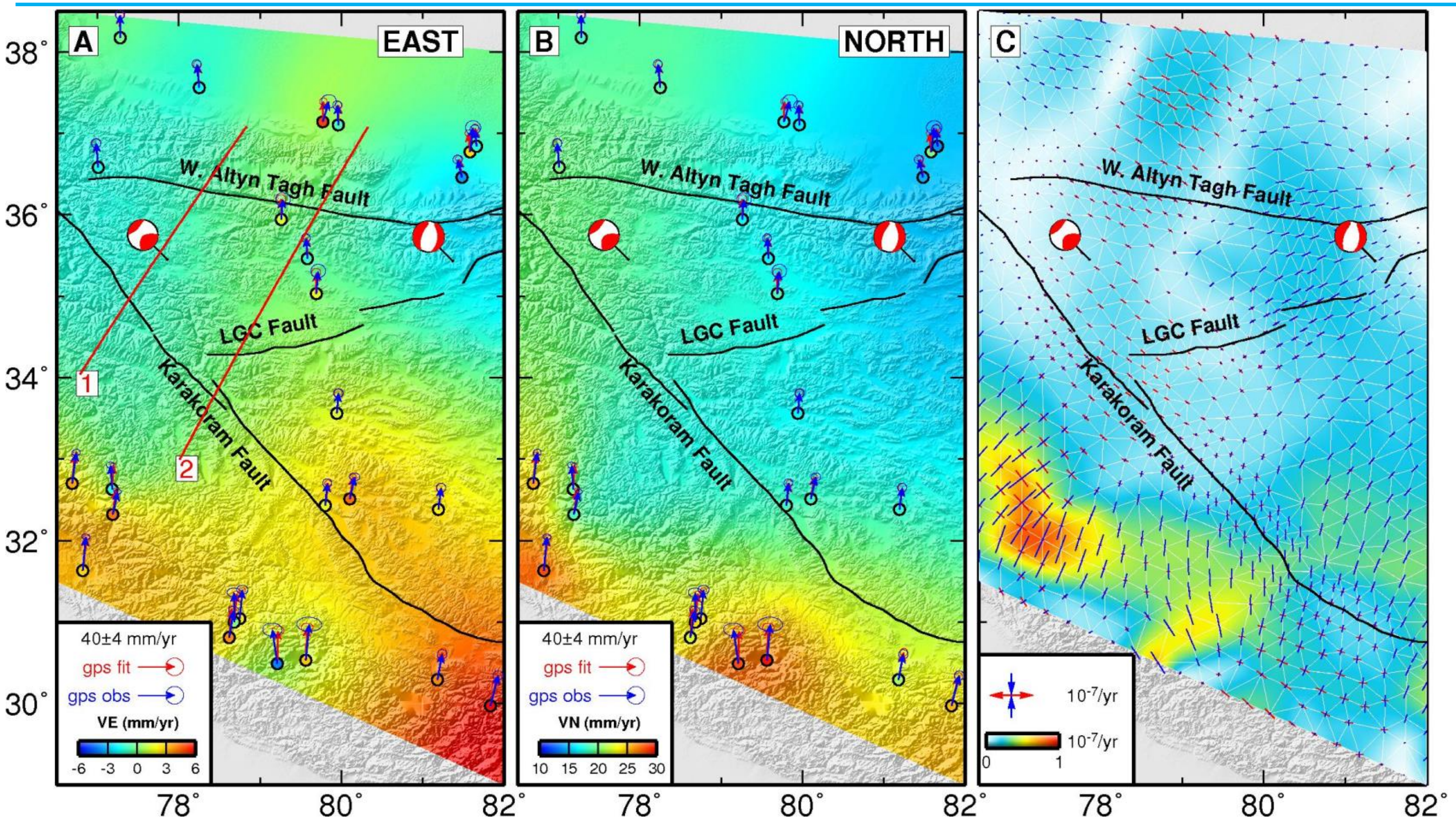

Wang and Wright, GRL 2012

Velocity & Strain Rate Field from GPS & InSAR

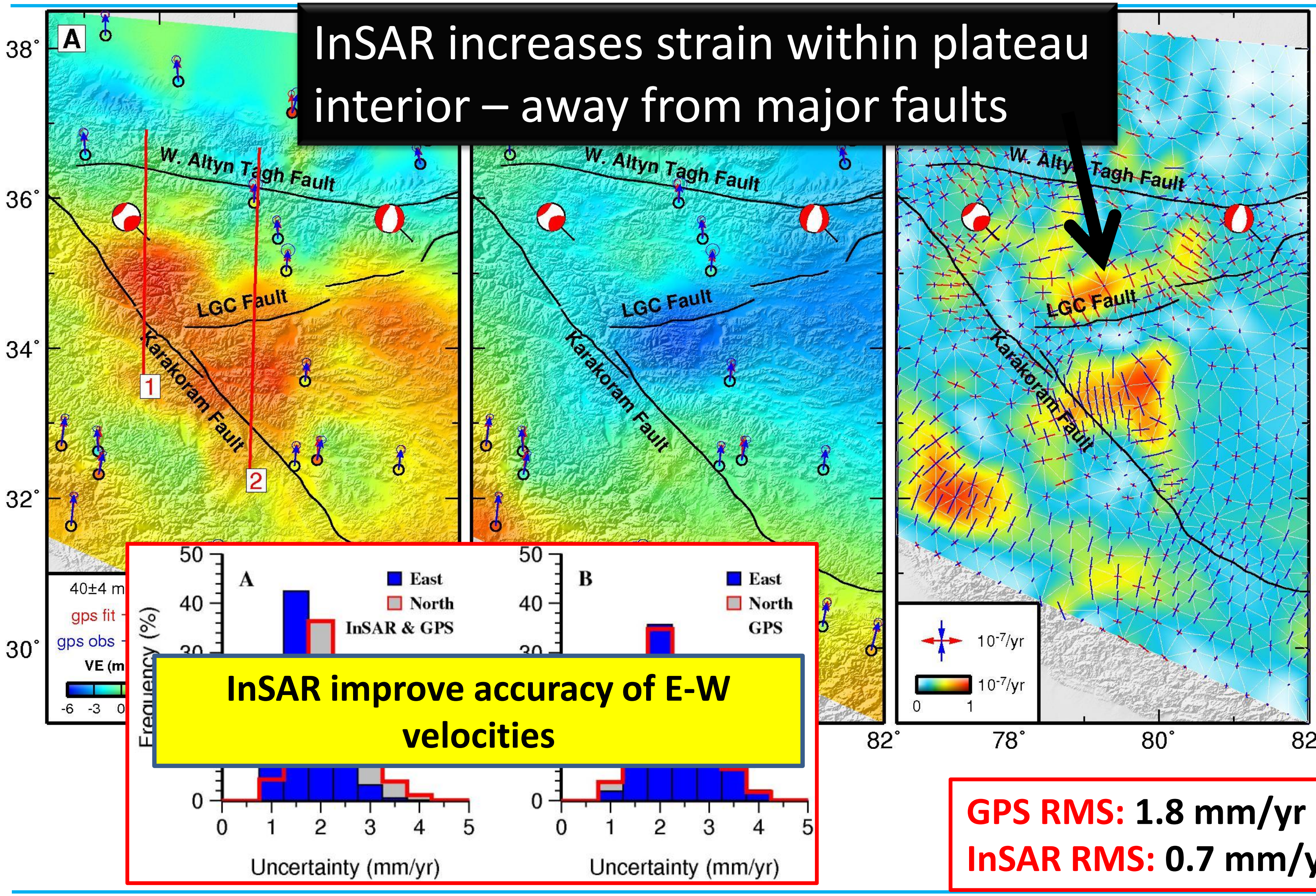

GPS RMS: 1.8 mm/yr
InSAR RMS: 0.7 mm/yr

Wang and Wright, GRL 2012

Slip Rates Along the Karakoram Fault

- Right-lateral slip along the entire fault
- Variable slip rate along the fault (0-6 mm/yr)
- Rule out present-day slip rates of >10 mm/yr
- No significant focused strain

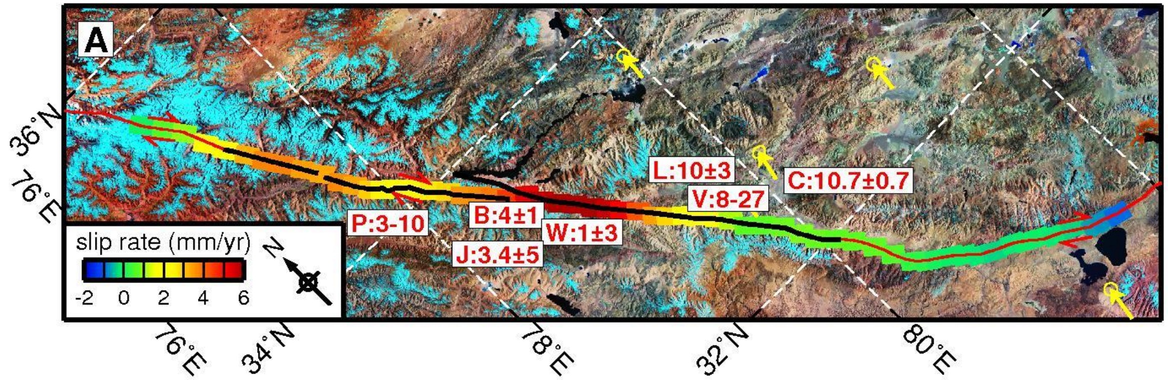

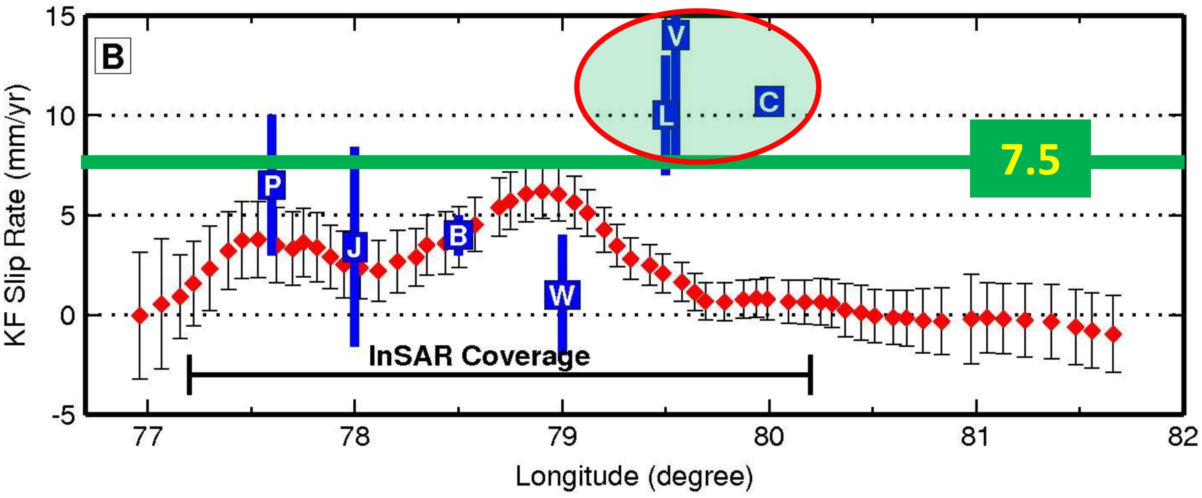

Limitation: Turbulent Atmosphere

Ground-based water vapour measurement

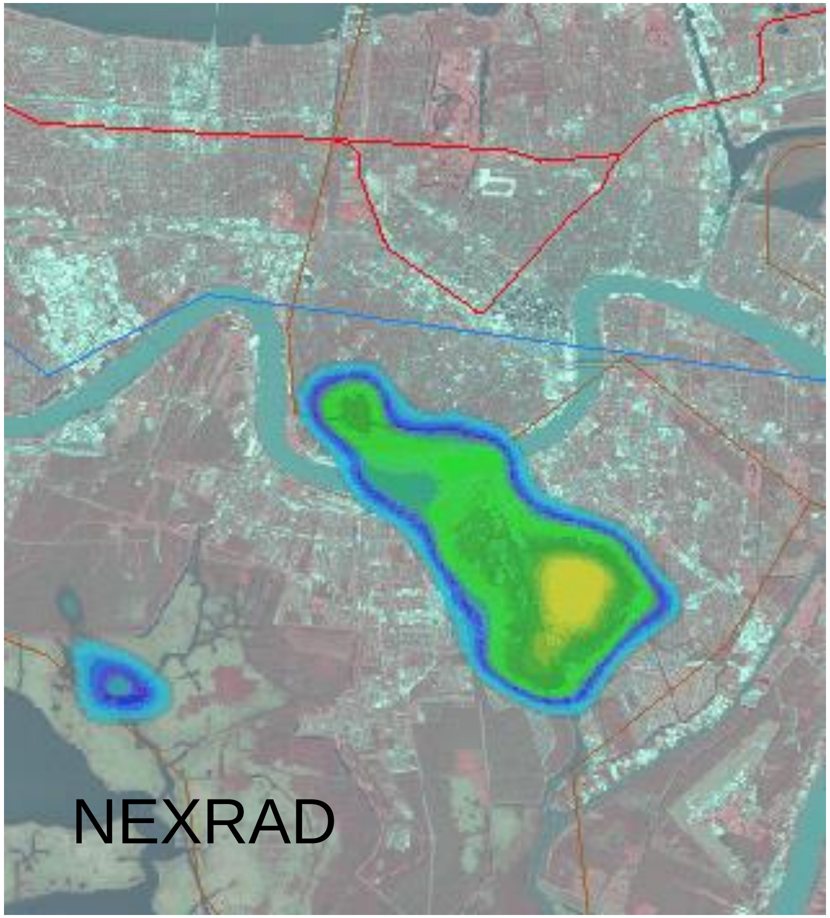

Interferogram

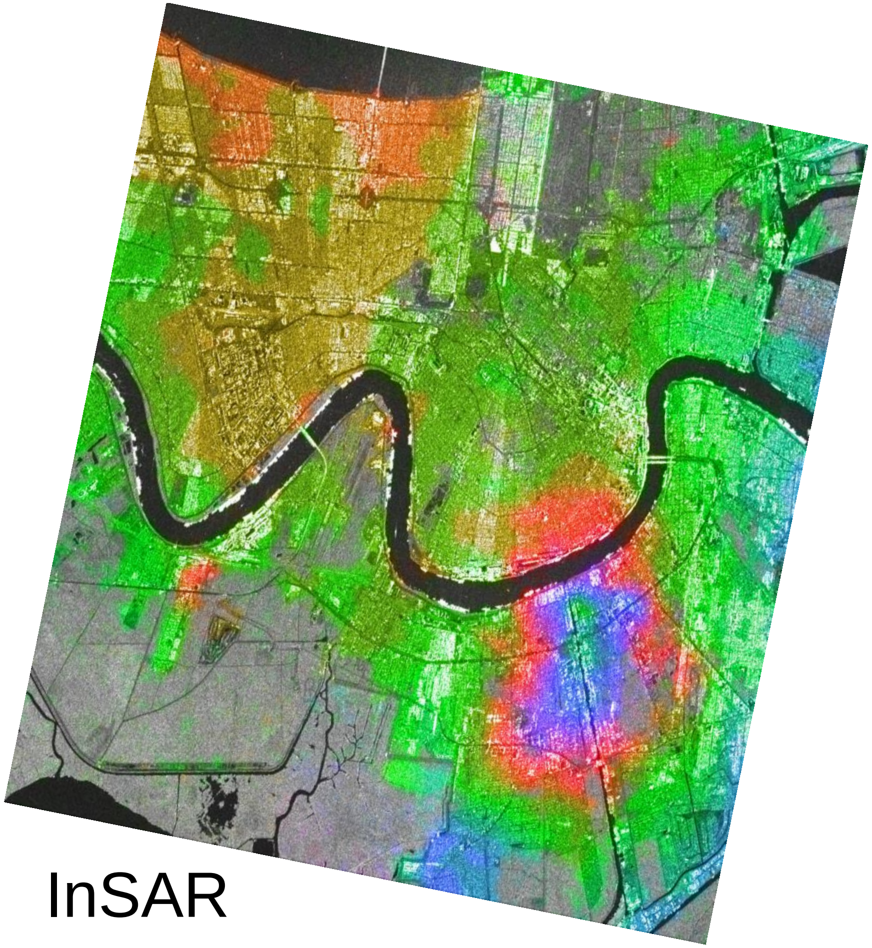

InSAR

Limitation: Stratified Atmosphere

Mt Etna, Italy.

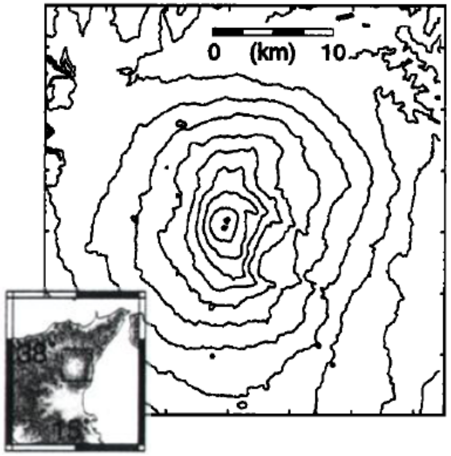

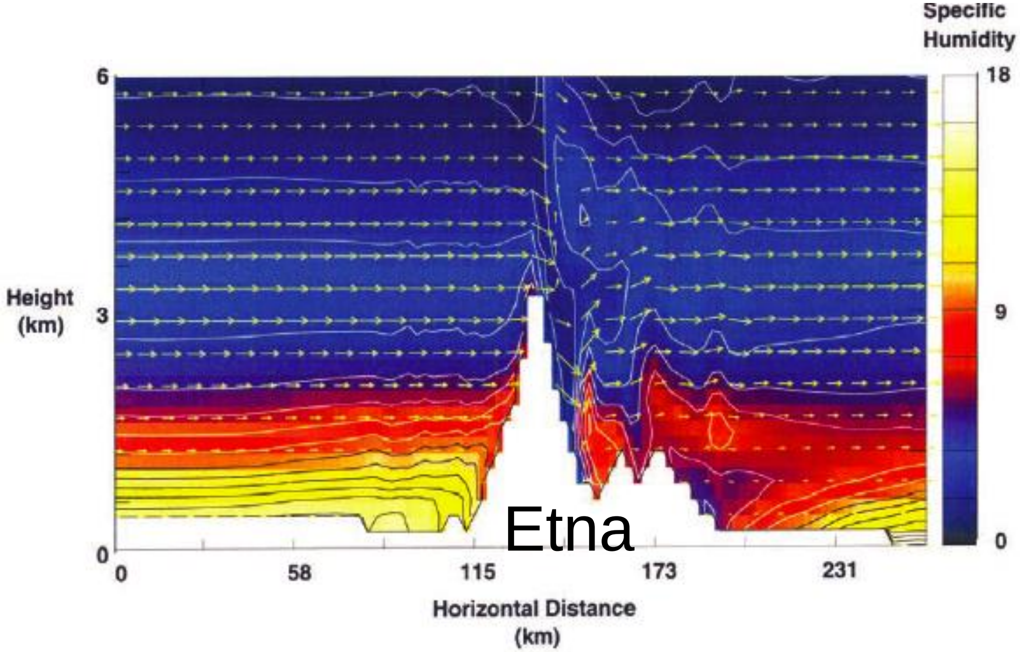

NH3D Model, Wadge 2002.

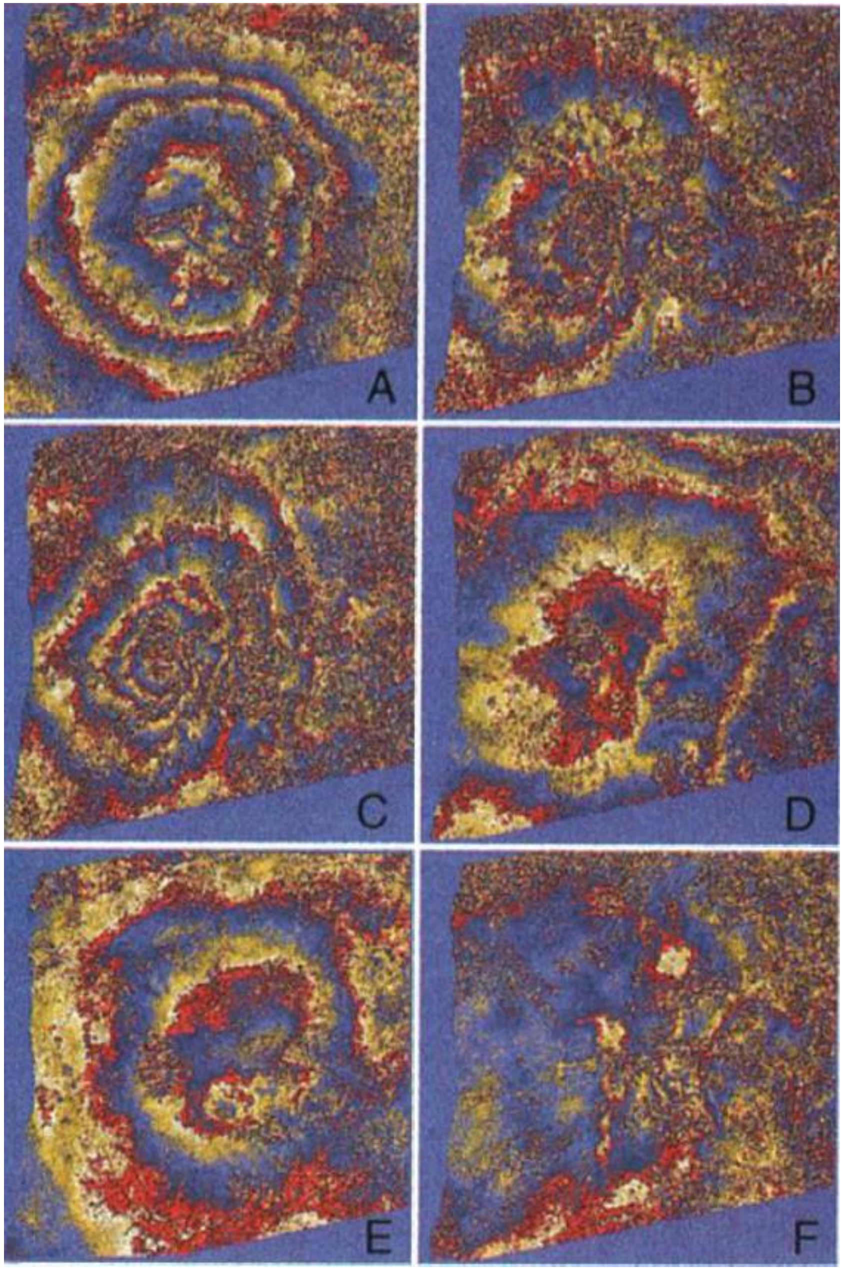

Limitation: Seasonal Atmosphere

Elliot, Fringe 07

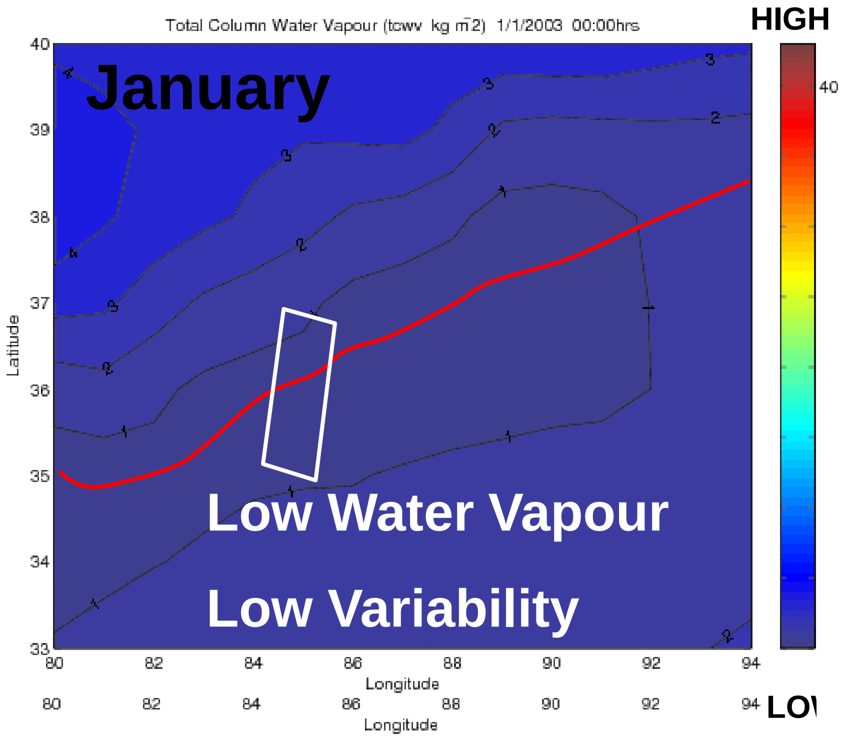

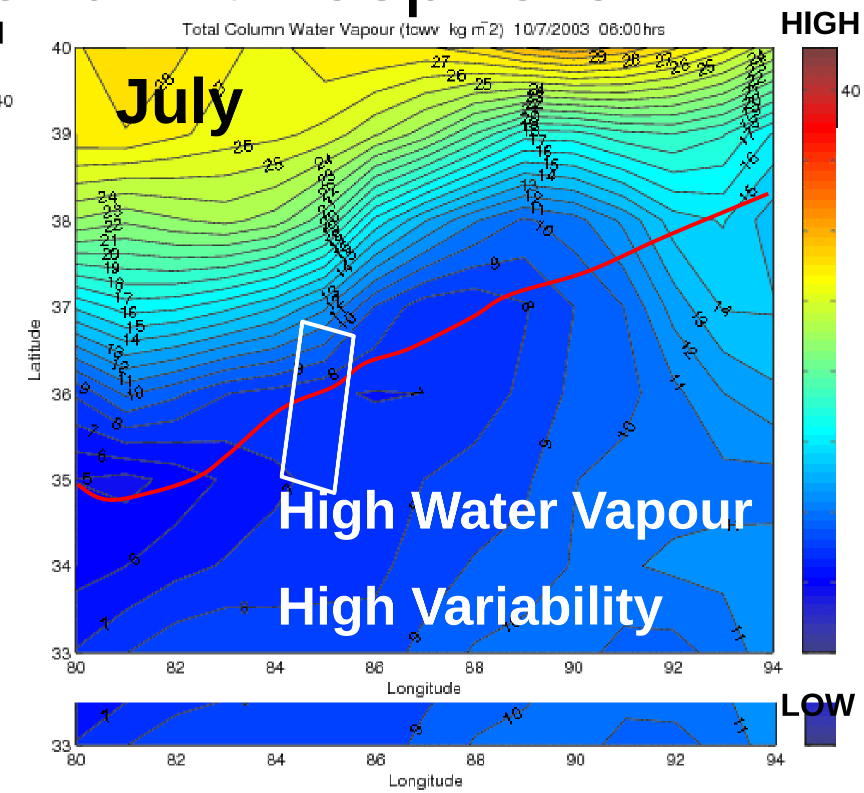

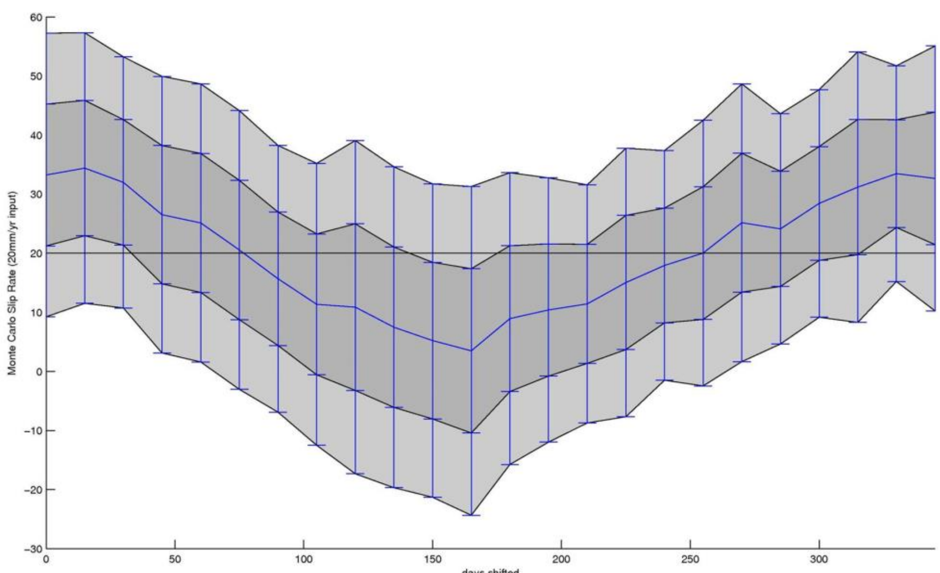

Synthetic Test of Rate Bias

Input Rate: 20 mm/yr

Recovered Rate: 5-35 mm/yr

Corrections 1: Linear/Smooth Velocity Assumption

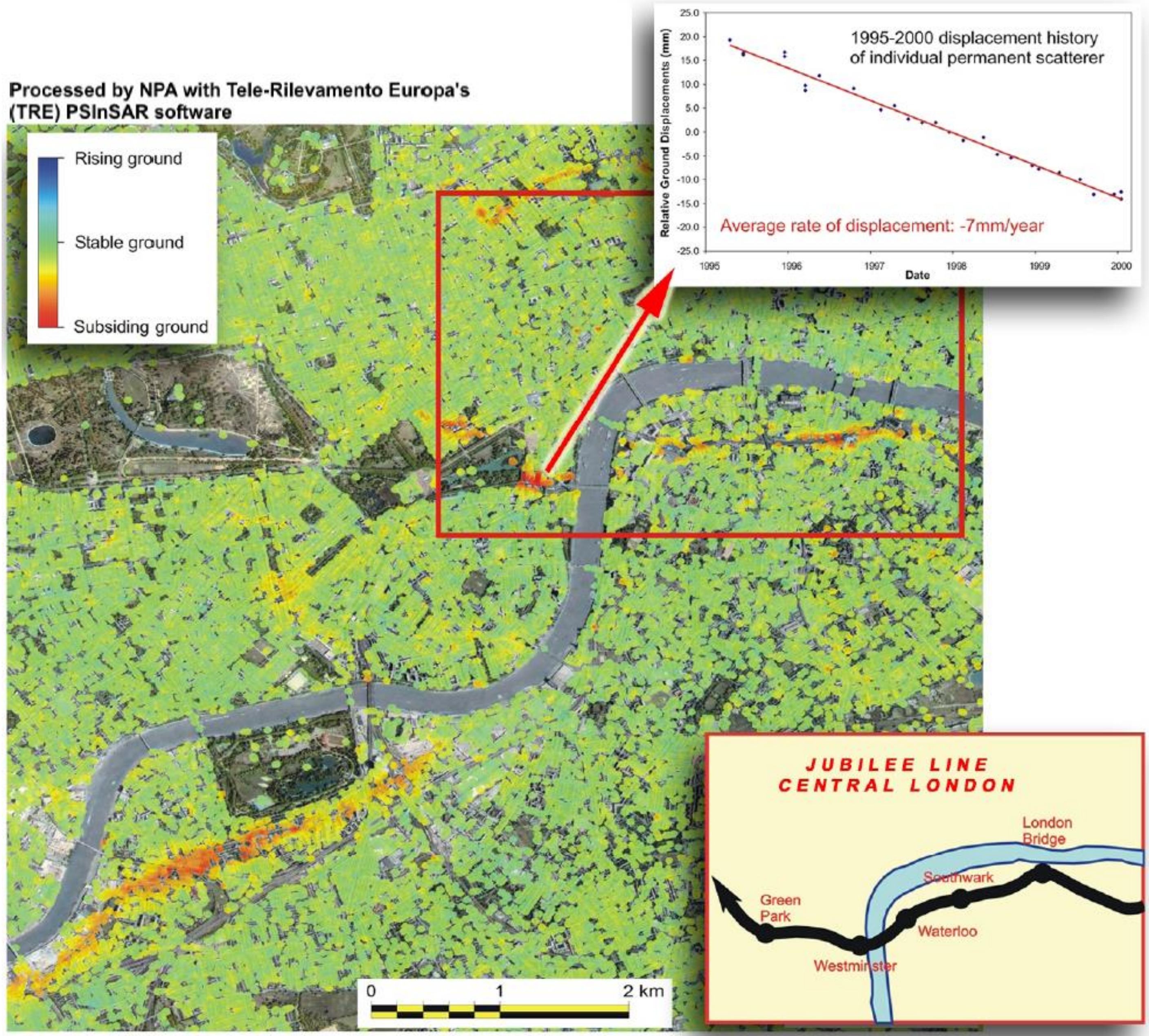

Correction 2: GPS

Requires dense GPS network

Li et al, 2006

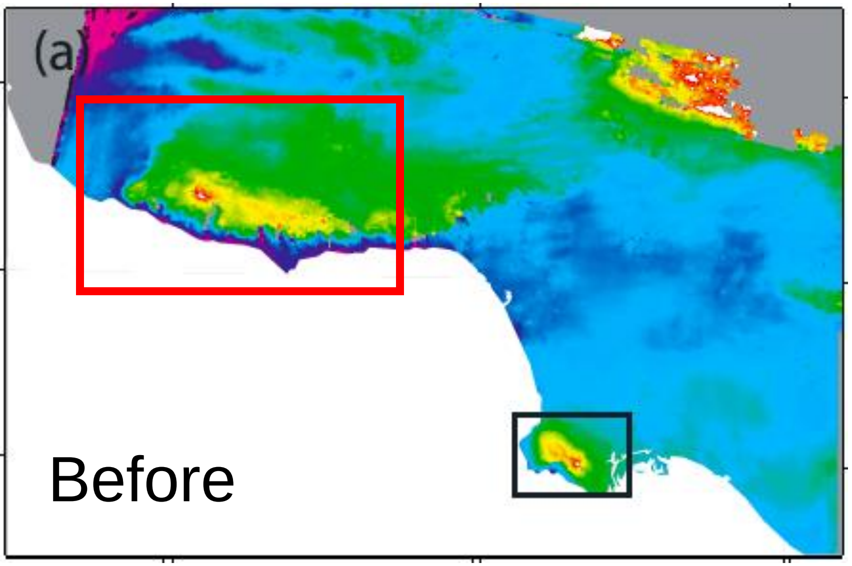

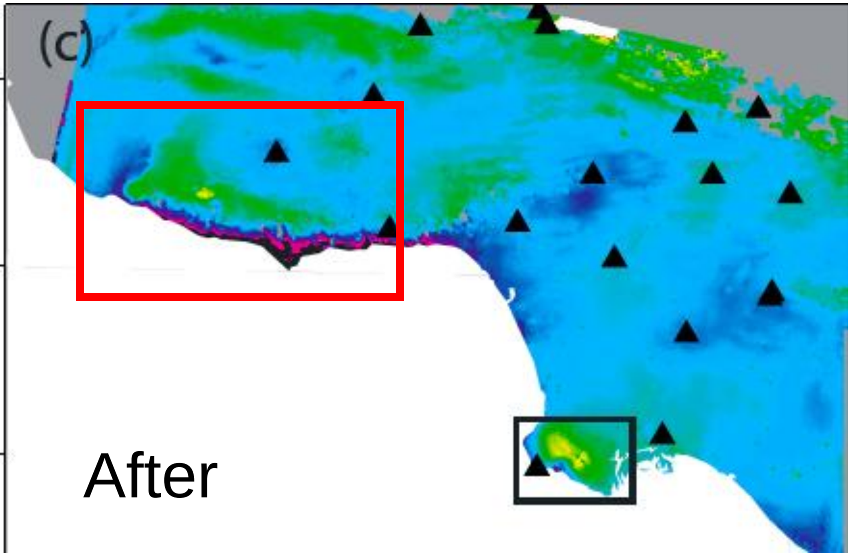

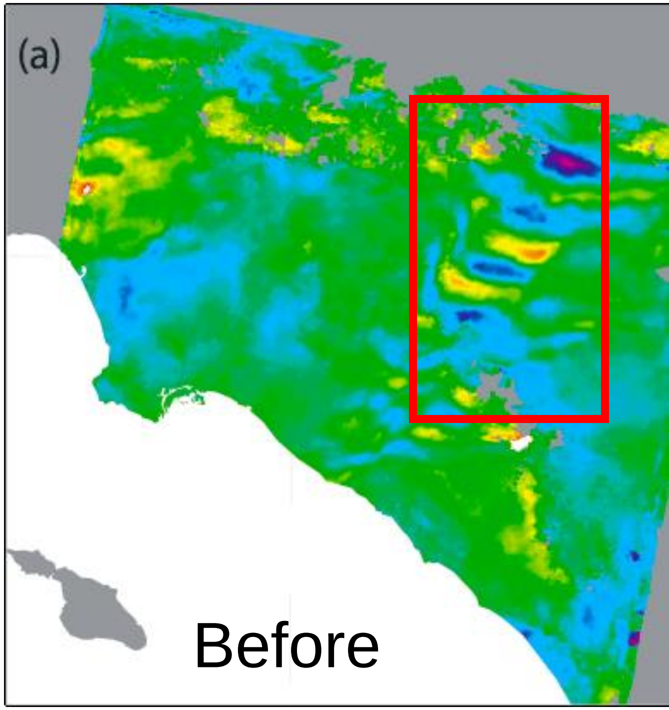

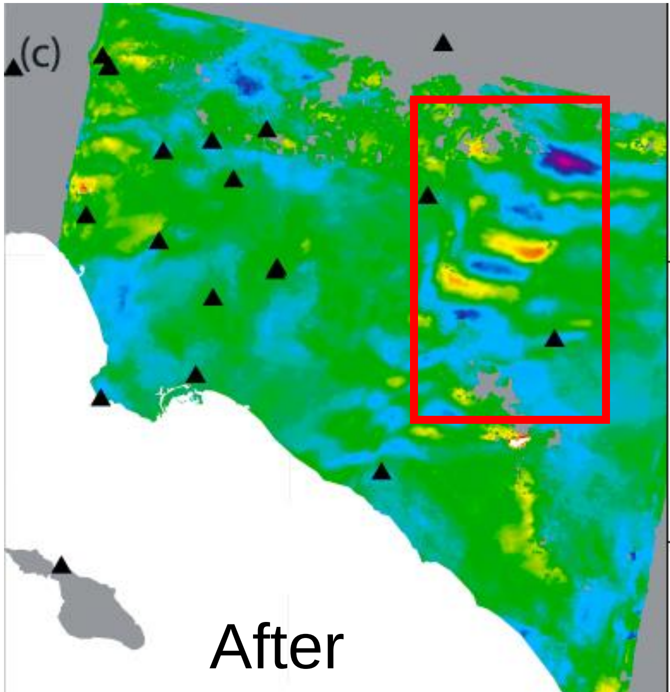

Correction 3: MERIS (or MODIS)

Passive Optical/IR sensor on Envisat

Raw Interferogram

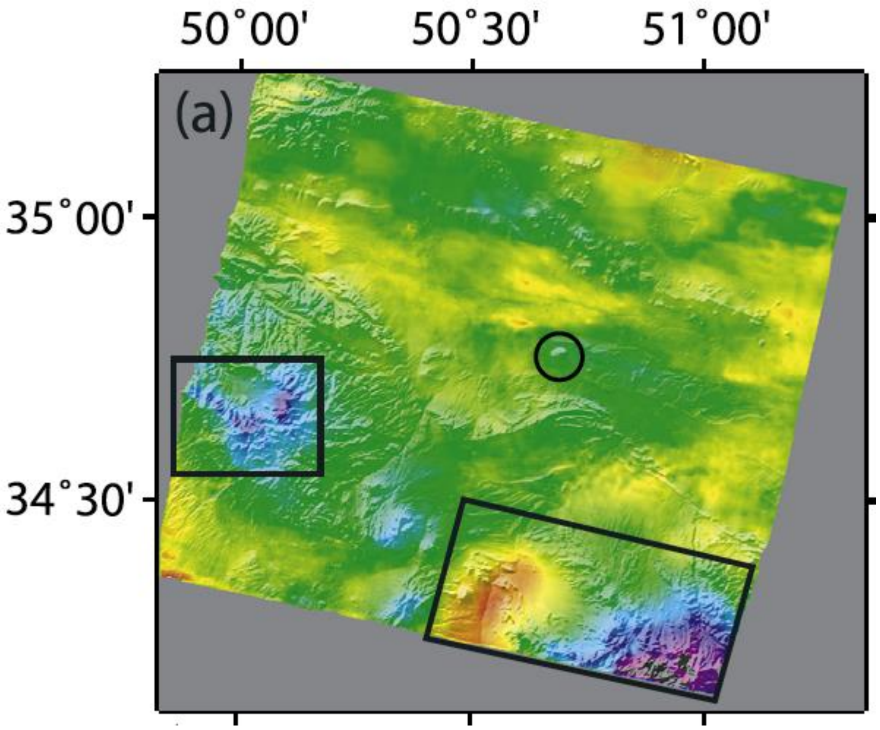

Corrected

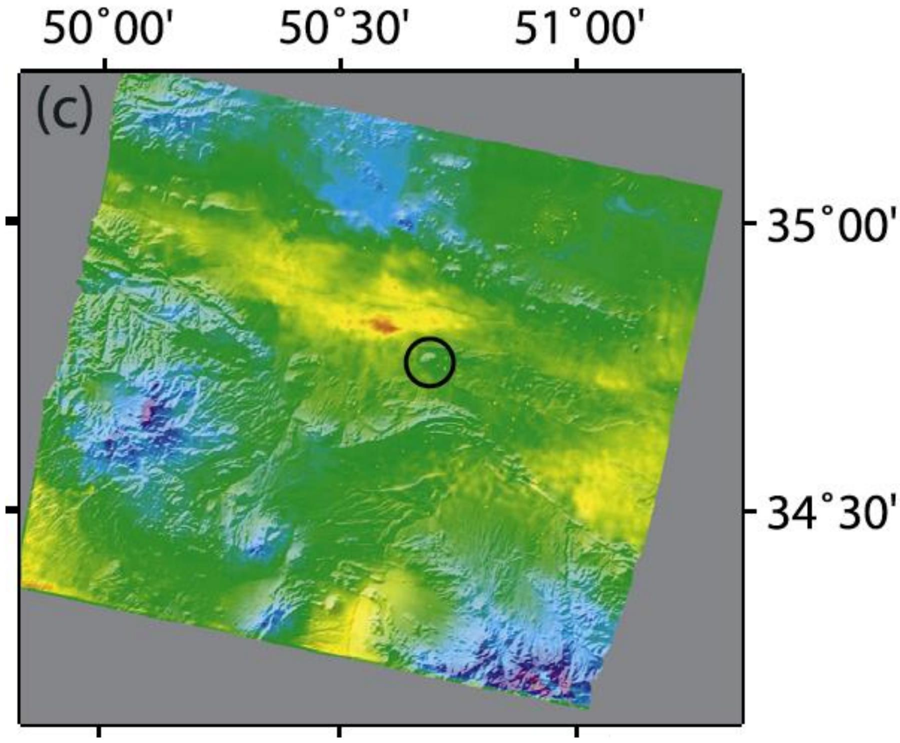

Requires: descending orbit , daytime and cloud free conditions.

Li et al, 2006

Atmospheric Correction 4: Weather Model.

3 km resolution

Reduces long-wavelength (>30 km) effects but not smaller scale features.

Foster et al, 2006

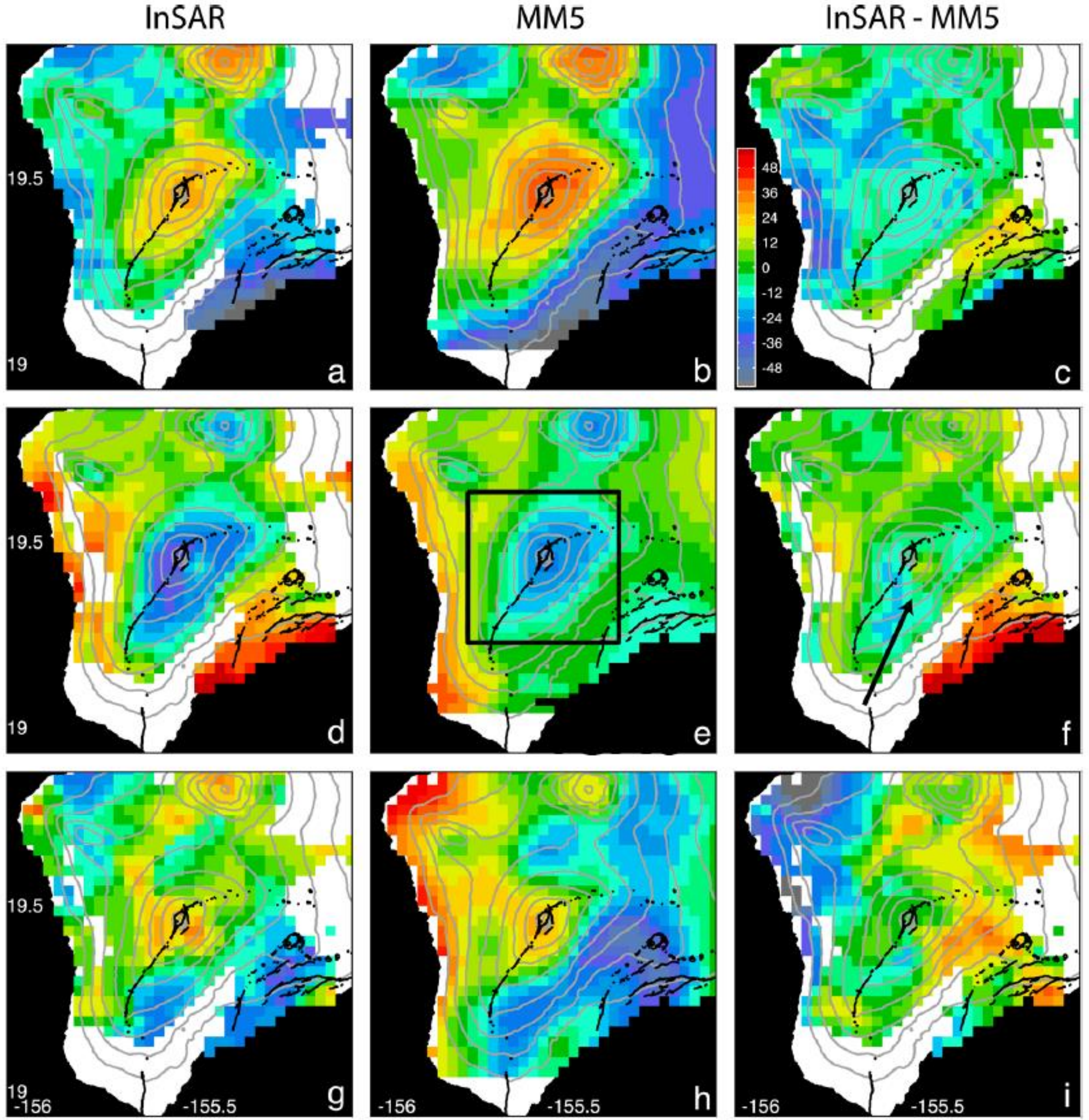

Atmospheric Correction 4: Weather Model (2)

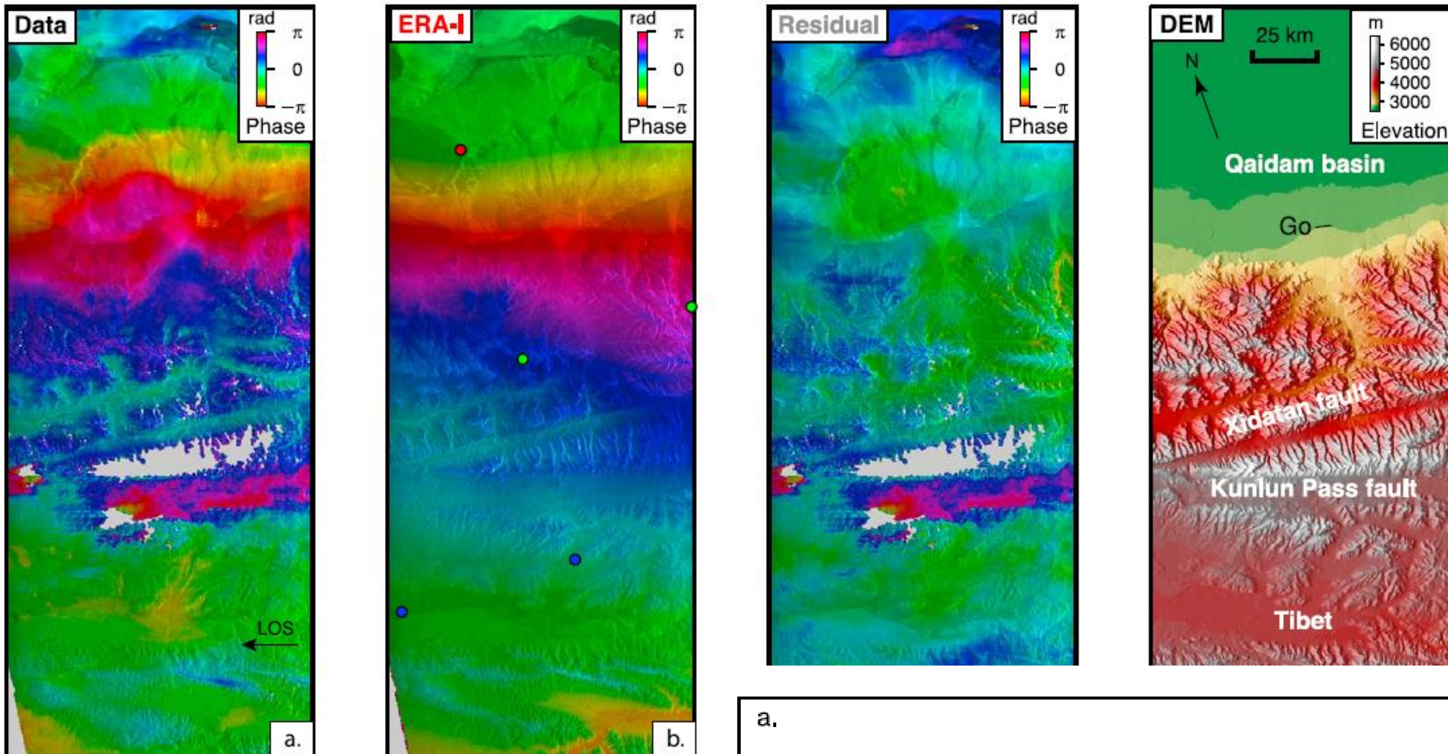

Jolivet et al., 2011

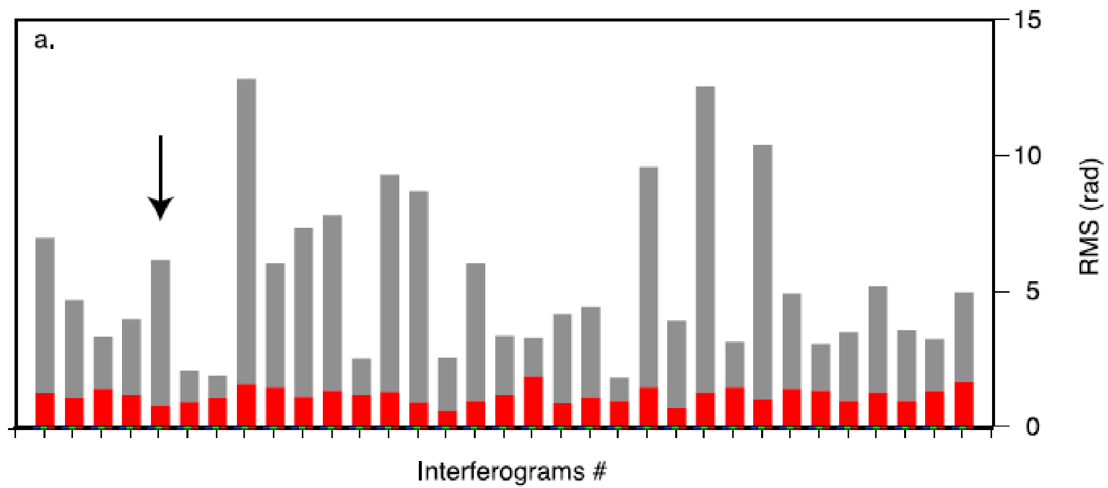

Earthquakes

1. Coseismic Deformation

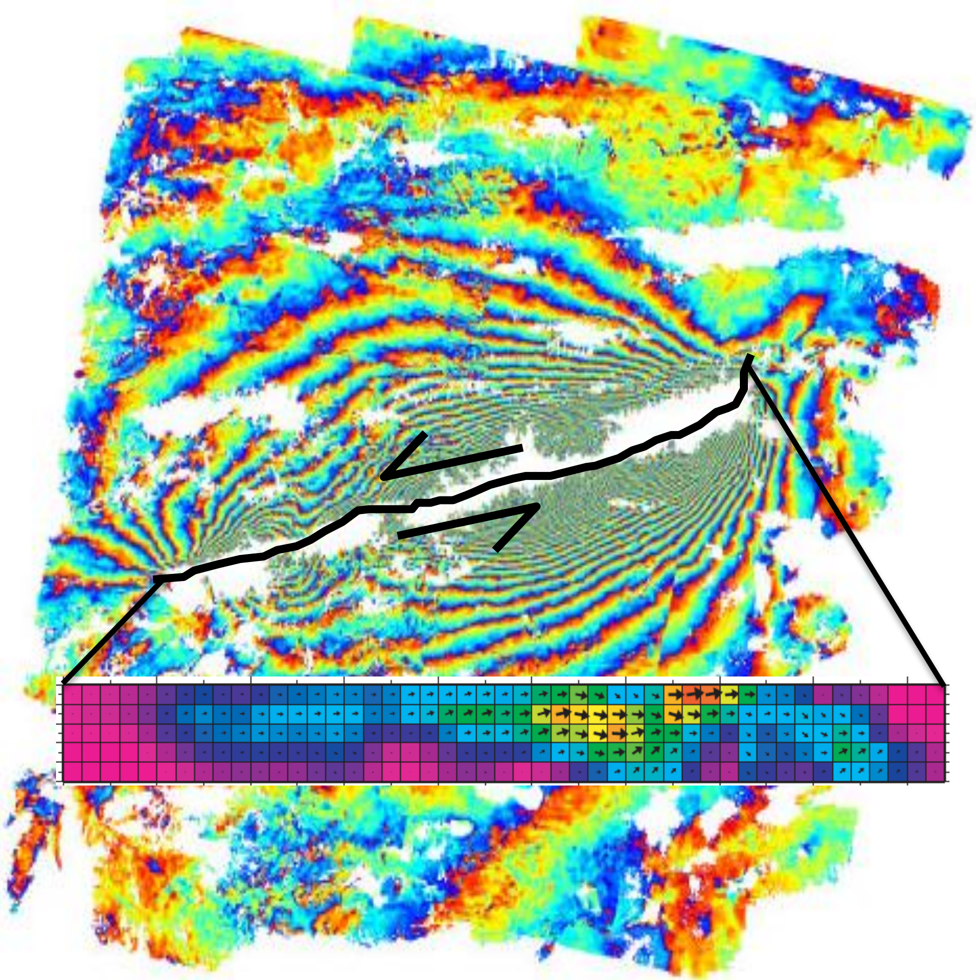

Current Capability

• Map deformation fields for most damaging earthquakes.
• Identify responsible faults
• Estimate slip models.
• Assess impact on future hazard .

What could be done?

• Routine analysis of **ALL** damaging earthquakes, c.f. Harvard CMT.
• Real-time assessment of causative fault and likely damage area.
• Near-real time assessment of future hazard (aftershocks + triggered quakes).

Why are we not doing this already?

• Data.
• Method Development.
• Manpower.

Earthquakes

2. Interseismic Strain

Current Capability

• Measure interseismic strain rates on suitable, targeted faults.

• Use these to constrain slip rate and hence assess future hazard.

What could be done?

• Routine measurement of strain across whole regions.

• Assessment of slip rates and relative hazard of multiple faults (including unidentified faults).

Why are we not doing this already?

• Data.

• Method Development.

• Manpower.

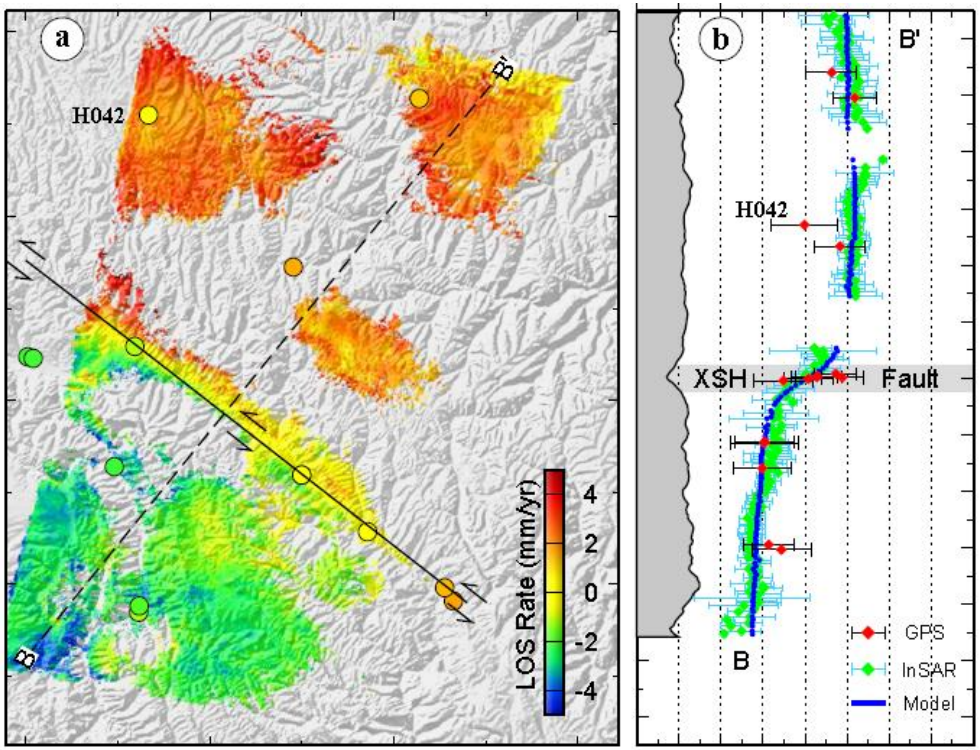

Wang, Wright and Biggs., GRL 2009

Volcanoes

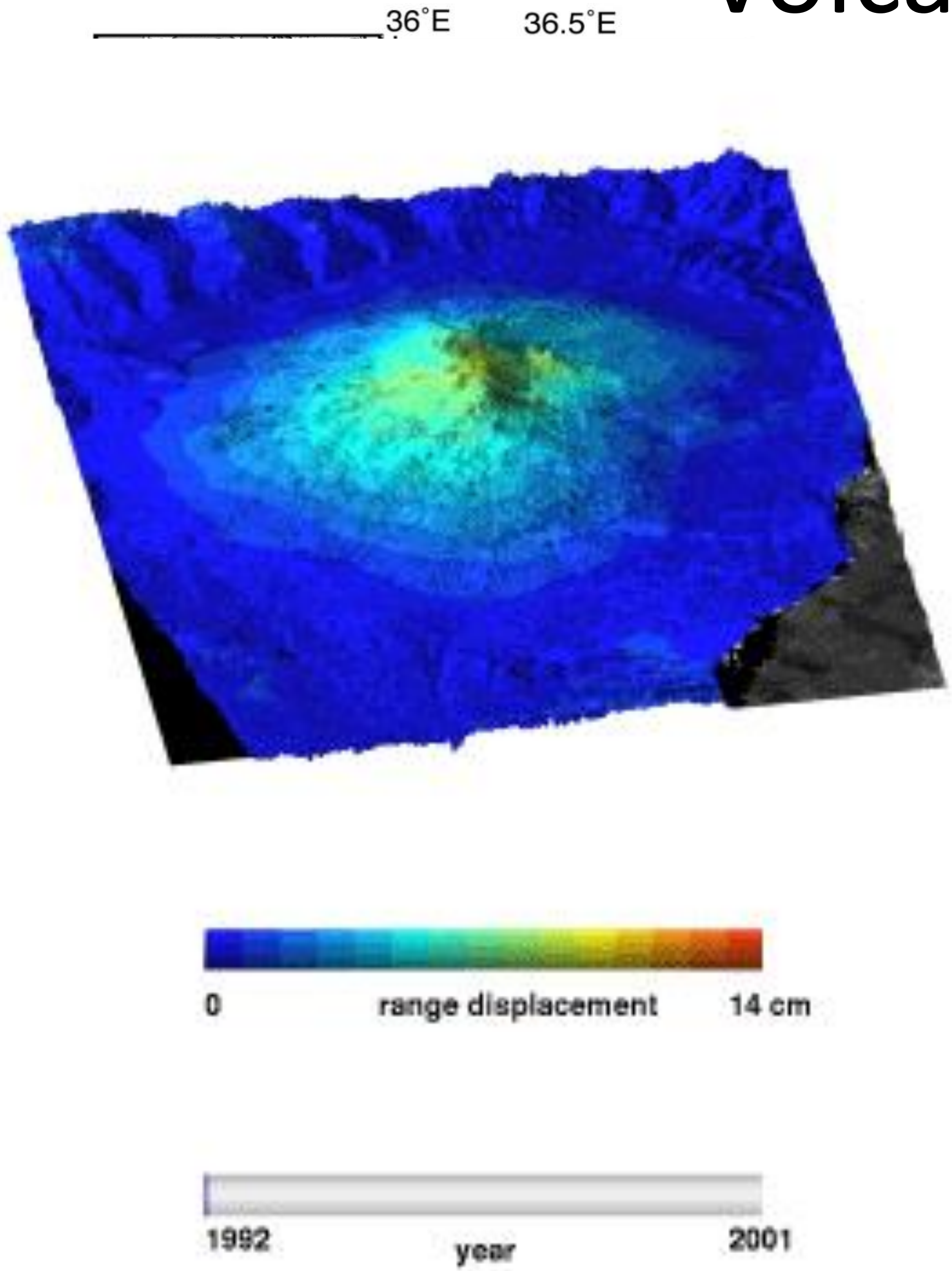

Current Capability

- Time-series analysis for suitable, targeted volcanoes .
- Snapshot regional surveys.
- Integration with other data sets.

What could be done?

- Routine monitoring of ALL volcanoes worldwide (or in a region).
- Target application of ground monitoring in countries where resources are limited.

Why are we not doing this already?

- Data.
- Method Development.
- Manpower.

Radar Missions

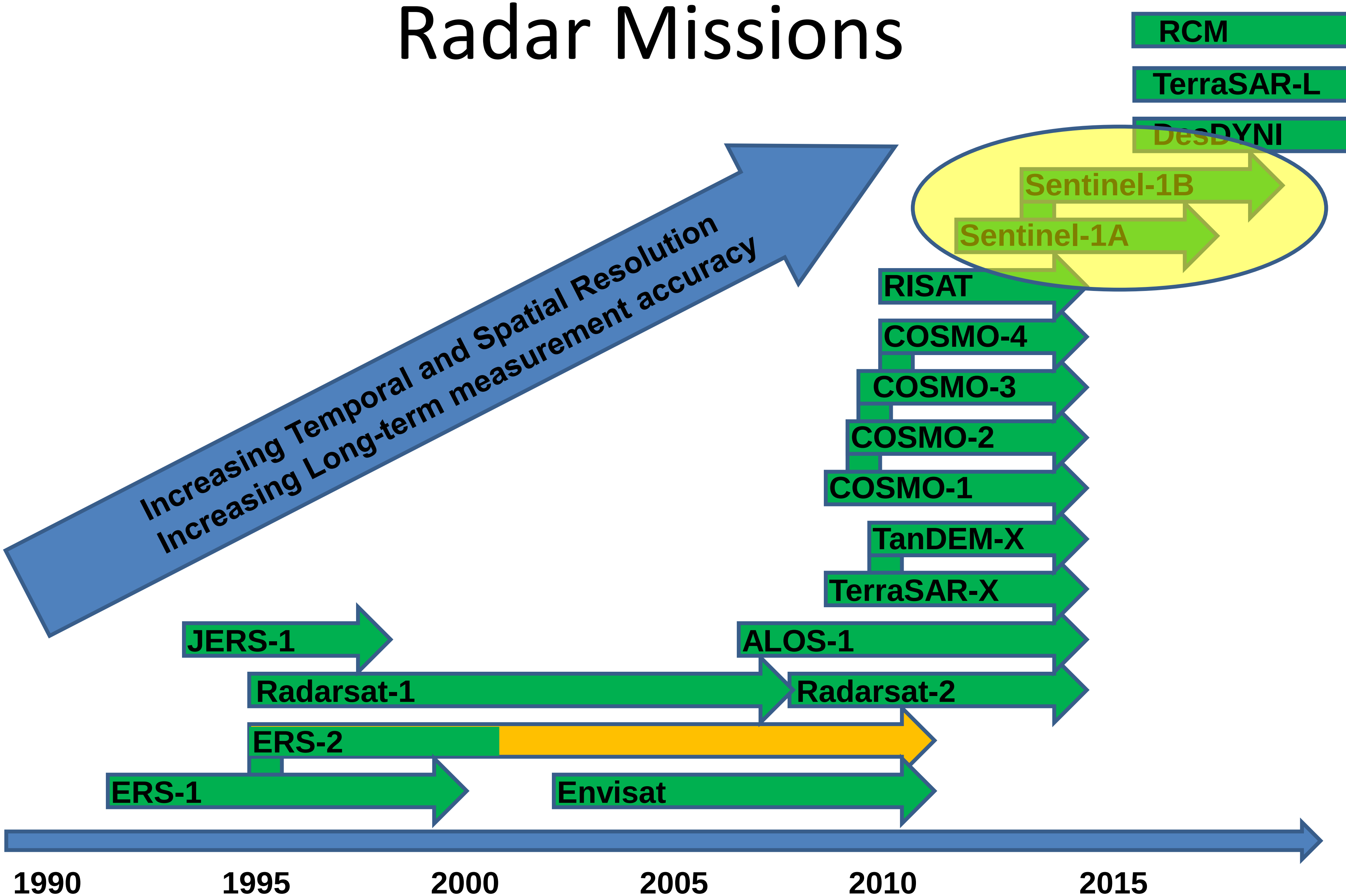

The Future

Sentinel-1 (ESA, GMES)

- “Operational” C-band InSAR
- 12 day repeat, 2 satellites ⇨ 3 day revisit
- Funded for 20 years, Launch early 2014

Conclusions

- InSAR is a powerful, low-cost tool for monitoring Earth deformation
- Capability improving continuously (smaller rates, bigger areas…)
- Future missions and method development will ensure InSAR is a standard technique


SUPERVOLCANO
bbc.co.uk/supervolcano